The Role of Ultrasound in Finger Flexor Tendon Shear

Ultrasound Assessment of Finger Flexor Tendon Shear:

Implications for Carpal Tunnel Syndrome

By

Jimmy Tat, B.Sc.

A Thesis Submitted to the School of Graduate Studies in

Partial Fulfillment of the Requirements for the Degree

Master of Science

McMaster University

MASTER OF SCIENCE (2014) McMaster University

(Kinesiology) Hamilton, Ontario

TITLE: Ultrasound Assessment of Finger Flexor Tendon Shear: Implications for Carpal Tunnel Syndrome

AUTHOR: Jimmy Tat, B.Sc. (McMaster University)

SUPERVISOR: Dr. Peter J. Keir

NUMBER OF PAGES: xxiii, 146

THESIS ABSTRACT

The purpose of this thesis was to understand the implications of ultrasound in the assessment of flexor tendon shear to establish its role in carpal tunnel syndrome. An *in vitro* and *in vivo* approach was used to examine ultrasound "shear" between the tendon and adjacent tenosynovium. Ultrasound shear is defined by the relative displacement between the tendon and tenosynovium, and has been considered a surrogate measure of tendon shear. However, the mechanical implications of relative displacement are not well understood. In Chapters 2 and 3, an *in vitro* approach was used to compare ultrasound to direct measurements of tendon displacement and tendon shear. Chapter 2 demonstrated the validity of colour Doppler ultrasonography in the evaluation of tendon displacement. Chapter 3 assessed the relationship between ultrasound shear and mechanical tendon shear using frictional work. We dispelled the notion that ultrasound shear represents tendon shear by showing it only captures the viscoelastic stretch of the tenosynovium in tendon shear; missing surface friction from neighbouring anatomical structures in the carpal tunnel. However, measuring viscoelastic resistance in tendon motion is important for the development of pathological fibrosis and thickening of the tenosynovium, a characteristic finding in carpal tunnel syndrome. In Chapter 4 we further established the clinical utility of ultrasound *in vivo* by showing ultrasound shear discriminated carpal tunnel syndrome symptomatic individuals from the healthy population. Ultrasound measures progressed with symptoms suggesting an etiological progression of fibrosis and thickening with carpal tunnel syndrome.

This thesis concluded that ultrasound only partially represents tendon shear with the viscoelastic component, but underscored the clinical implications. Ultrasound provides a non-invasive assessment of viscoelastic resistance that will be highly valuable for our understanding of the role of wrist and hand motion in the etiology of injury with potential applications in the diagnosis of carpal tunnel syndrome.

Keywords: carpal tunnel syndrome, tendon, tenosynovium, ultrasound, shear

ACKNOWLEDGEMENTS

I would like to thank Dr. Peter Keir for his mentorship. He gave me the opportunity to work through my problems, but also knew when to provide support. Thank you for challenging me to be a better researcher.

I am also thankful for my collaboration with Aaron Kociolek, PhD candidate and Katherine Wilson, MSc. My time in the anatomy lab with Aaron was exciting, humbling, and stressful, and we became great problem solvers. Katherine was amazing in our work with patients and I truly enjoyed working together to learn the ultrasound system. I am glad to have shared the experience with you.

Lastly, I am grateful for all the love and support I received from my family throughout my academic career. Thank you to my mother, for inspiring me to pursue carpal tunnel syndrome research; my father, for teaching me patience and a strong work ethic; and my sisters, for keeping me grounded through this process.

THESIS FORMAT AND ORGANIZATION

This thesis contains material from my (Jimmy Tat) Master's research and has been prepared in a "sandwich" format as outlined in the McMaster University School of Graduate Studies' Guide for the Preparation of Thesis. This thesis begins with the general introduction to the research area (Chapter 1), followed by 2 studies that have been prepared as 3 manuscripts and individual thesis chapters (2-4). The thesis ends with a concluding chapter (Chapter 5) that provides discussion of the findings and recommendations for future research in the area.

Chapter 2 provided a detailed validation of colour Doppler ultrasonography in measurement of tendon displacement in the human carpal tunnel. Chapter 2 has been accepted for publication in the *Journal of Ultrasound in Medicine*.

Chapter 3 served as the first mechanical evaluation of ultrasound-based kinematic tendon shear and examined the effect of biomechanical risk factors. Chapter 3 has been prepared for submission to the *Journal of Orthopaedic Research*.

Chapter 4 investigated the application of ultrasound for the clinical assessment of carpal tunnel syndrome severity. Chapter 4 has been prepared for submission to *Clinical Biomechanics*.

CONTRIBUTIONS TO PAPERS WITH MULTIPLE AUTHORS

Chapter 2

Tat, J., Kociolek, A.M.K., and Keir, P.J. Validation of colour Doppler ultrasonography for evaluating relative displacement between flexor tendon and subsynovial connective tissue. Accepted to the *Journal of Ultrasound in Medicine on* July 22, 2014.

Chapter 3

Tat, J., Kociolek, A.M.K., and Keir, P.J. Relative tendon-SSCT displacement using ultrasound and mechanical tendon shear capture different phenomena. Prepared for submission to *Journal of Orthopaedic Research*.

Contributions

Chapter 2 has been prepared for the *Journal of Ultrasound in Medicine* and Chapter 3 for the *Journal of Orthopaedic Research*. All co-authors have contributed to these manuscripts.

The methodology, collection, analysis, interpretation, and manuscript preparation was performed by Jimmy Tat with input from Aaron Kociolek. Chapter 2 and 3 used cadaver specimens that required the same methodology from Aaron Kociolek's PhD thesis, which evaluated the effect of biomechanical risk factors on tendon frictional work. Therefore, collection occurred concurrently for both research projects using the same specimens. My contributions focused on ultrasound, specifically the relationship between ultrasound

shear and mechanical tendon shear and the effect of biomechanical risk factors on ultrasound shear. The work by Aaron Kociolek helped to establish the validity of our testing paradigm and further substantiated my ultrasound findings. Dr. Peter Keir oversaw the project from conception to preparation of the manuscripts and provided funding for the research study.

Chapter 4

Tat, J., Wilson, K.E., and Keir, P.J. Pathological changes in the subsynovial connective tissue increases with severity of carpal tunnel syndrome symptoms. Prepared for submission to *Clinical Biomechanics.*

Contributions

All co-authors have contributed substantially to this chapter. The study conception, methodology, data collection, analysis, and manuscript preparation was performed by Jimmy Tat. Katherine Wilson was vital to data collection including the recruitment of CTS symptomatic participants and administering clinical questionnaires. Dr. Peter Keir contributed to the study including funding.

TABLE OF CONTENTS

LIST OF TABLES

CHAPTER 2

CHAPTER 3

CHAPTER 4

LIST OF FIGURES

CHAPTER 1

CHAPTER 2

CHAPTER 4

LIST OF ABBREVIATIONS

CTS:	Carpal tunnel syndrome
SSCT:	Subsynovial connective tissue
PS:	Parietal synovium
VS:	Visceral synovium
SSI:	Shear strain index
FDS:	Flexor digitorum superficialis
FDP:	Flexor digitorum profundus
PIP:	Proximal interphalengeal
MCP:	Metacarpal phalengeal
D_{FDS}:	Displacement flexor digitorum superficialis tendon
D_{SSCT}:	Displacement subsynovial connective tissue
η_p^2:	Partial eta squared
ANOVA:	Analysis of variance
TCL:	Transverse carpal ligament
BCTQ:	Boston carpal tunnel questionnaire
CB:	Carpal bones

LIST OF APPENDICES

CHAPTER 1 INTRODUCTION

1.1 Introduction

Musculoskeletal disorders of the wrist and hand are common in the workplace and result in greater work disability than other body regions (Barr et al. 2004). Occupations in textiles, machining, and transportation are at high risk of developing these disorders due to work operations that involve highly repetitive hand motion (Zakaria et al. 2004). Repetitive trauma injuries of the distal upper limb include flexor tendinitis, tenosynovitis, tendinosis, and peripheral neuropathies such as carpal tunnel syndrome (Tanaka et al. 2001). Of these occupational-related disorders, carpal tunnel syndrome is the most frequently reported, and particularly debilitating, with many cases requiring surgical intervention (Manktelow et al. 2004; Feuerstein et al. 1999).

Carpal tunnel syndrome (CTS) is characterized by compression of the median nerve that can result in motor weakness, pain, tingling, and numbness in the fingers innervated by the median nerve (the thumb, index finger, middle finger, and half of the ring finger). In 1997, the incidence of CTS was estimated to be 37.2 women and 23.2 men per 100,000 workers in Ontario (Zakaria et al. 2004). The Workplace Safety Insurance Board of Ontario reported an average cost of $13,700 per worker and a total of $13,200,000 per year in 1996 (Manktelow et al. 2004). These costs can include prolonged lost work time and expensive interventions such as carpal tunnel release surgeries. A better understanding of the pathophysiology and occupational risk factors associated with CTS can help ameliorate these problems.

Occupational epidemiology studies have shown strong relationships between posture, force, and repetition and the development or incidence of carpal tunnel syndrome (Bernard, 1997). There is also evidence that the combination of multiple work factors poses even greater injury risk than any one factor alone (Schoenmarklin et al. 1994; Chiang et al. 1993; Silverstein et al. 1987). While the etiology has been extensively studied, the exact pathomechanics remain elusive. A major clinical finding in CTS patients is non-inflammatory fibrosis and thickening of the tenosynovium, also termed subsynovial connective tissue (SSCT) in the literature (Ettema et al. 2006; Jinrok et al. 2004). Thus, the structure and function of the SSCT has received greater attention in recent years.

The SSCT is a microvacuolar system that facilitates gliding in the carpal tunnel by reducing friction between flexor tendons and the median nerve (Guimberteau et al. 2010). The SSCT consists of a microvacuole framework with multiple layers of collagen bundles that are interconnected by perpendicular (vertical) collagen fibrils. The fibrils also tether the SSCT to tendons and nerve, such that tendon or nerve excursions move layers of the SSCT. Tendon excursions transfer force to SSCT layers by stretching fibrils in the direction of motion (Figure 1.1). This occurs in an organized manner, so layers closest to the tendon move first and recruitment extends to the outer most layers at the visceral synovium (Ettema et al. 2006) (Figure 1.2). The sequential stretch and recruitment causes the SSCT to move with the tendon, but with a delay. Excessive differential motion between the tendon and SSCT can result in stretching fibrils beyond elastic limits, leading to tissue failure and "shear injury" (Vanhees et al. 2012; Ettema et al. 2006). In cadaveric

specimens without a history of CTS, maximum shear stress occurs at 30% shear strain (equivalent to 13.5 mm of shearing motion) which suggests tissue damage incurred from tendon motion is within physiological ranges (Osamura et al. 2007). These findings are also consistent with the severity of fibrosis most apparent at layers near the tendon and SSCT border (Ettema et al. 2006).

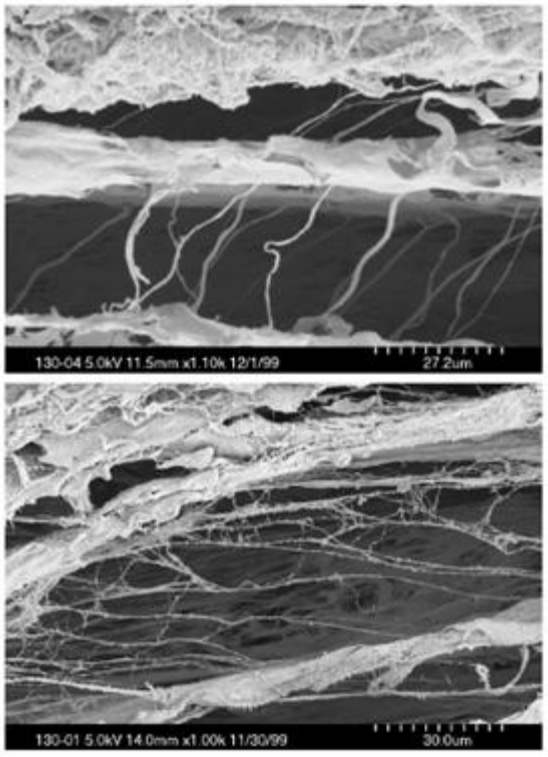

Figure 1.1 Scanning electron microscopic image of the SSCT structure. *(Above)* Vertical fibrils interconnect adjacent layers of the SSCT. *(Below)* Fibres become stretched during tendon motion. From Ettema et al. 2006.

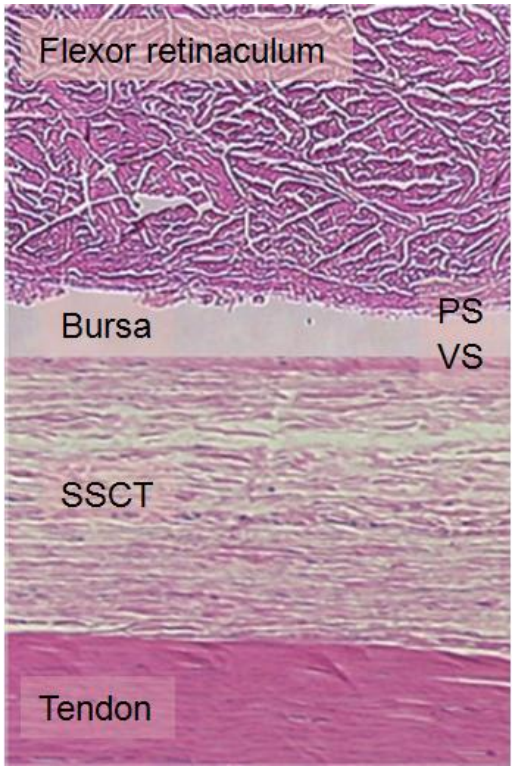

Figure 1.2 Layers of the carpal tunnel. The bursa is surrounded above by the parietal synovium (PS) and below with the visceral synovium (VS). Adapted from Ettema et al. 2006

Recent advances in ultrasound technology, such as improved imaging resolution, have allowed researchers to measure relative motion between the tendon and SSCT *in vivo* (Tat et al. 2013; van Doesburg et al. 2012; Yoshii et al. 2009). Traditional Doppler-based techniques calculate tissue velocities based on Doppler shift frequency ($f = 2 \cdot v \cdot f_o \cdot cos\theta / c$), which uses the relationship between the transducer frequency (f_o), velocity of sound in the medium (c), and the insonation angle (θ) between the transducer beam and moving tissue, to determine the velocity of the moving tissue (v). While a number of studies have employed Doppler methods to track tendon motion, including pulse-wave Doppler and colour Doppler applications (Oh et al. 2007; Soeters et al. 2004; Holland et al. 1999; Buyruk et al. 1998; Cigali et al. 1996); the angle dependency is typically regarded as a limitation contributing to measurement error (Yoshii et al. 2009). However, potential errors can be reduced by maintaining appropriate insonation angles (of approximately 60^o) (Liu et al. 2005).

As an alternative to Doppler methods, speckle tracking is angle independent, employing an image-based approach to quantify tendon displacement. Speckle tracking uses custom-made two-dimensional block-matching algorithms to track heterogeneities in musculoskeletal tissue (speckle patterns) through a sequence of ultrasound B-mode images. While the use of speckle tracking has increased in popularity, the technique is still novel for tendon motion and not without limitations. Yoshii et al. (2009) compared Doppler and speckle tracking to *in vivo* tendon excursion estimated from a geometric model (An et al. 1983) and found that speckle tracking had improved relationships with the geometric model, but largely underestimated the magnitude. While Doppler provided

better mean absolute measurement error for tendon displacement. Doppler techniques (specifically colour Doppler) also allow for simultaneous tracking of the tendon and adjacent SSCT. This cannot always be achieved with speckle tracking due to difficulties in tracking small and hyperehoic (bright) tissue, such as the SSCT. Colour Doppler ultrasound appears to be a viable tool and deserves further investigation for the measurement of relative motion between structures in the carpal tunnel.

Relative longitudinal motion between the tendon and SSCT, termed ultrasound shear, has been used to quantify the risk of shear injury. Relative motion is commonly represented using the shear strain index (SSI). The SSI is calculated as the difference in longitudinal displacement between the tendon and SSCT, expressed as a percentage of tendon excursion (tendon excursion – SSCT excursion) / tendon excursion x 100% (Yoshii et al. 2008). It represents the potential for shear over an entire finger movement range with greater ultrasound shear indicating an increased risk for shear injury. There is evidence that relative motion is mediated by biomechanical risk factors including wrist posture, repetition, duration and independent finger movements (Tat et al. 2013; Yoshii et al. 2011; Yoshii et al. 2009; Yoshii et al. 2008).

Shear injury is implicated in the development of pathological fibrosis and thickening of the SSCT associated with CTS (Figure 1.3). These pathological changes can affect the functional properties of the SSCT (Ettema et al. 2008). For example, CTS patients present with increased differential motion (van Doesburg et al. 2012; Ettema et al. 2008) in which the tenosynovium moves more independently of the tendon. Ettema et al. (2008) found this "dissociated" movement pattern in patients with a direct

measurement of relative displacement during carpal tunnel release surgery (Ettema et al. 2008). Fewer interconnections between SSCT layers could account for disrupted gliding function (Figure 1.4). In fact, Korsanje et al. (2012) explored the use of SSCT mechanics in the clinical diagnosis of CTS and found SSCT displacement predicted the most affected hand in CTS patients with 87% accuracy (most affected hands had smaller displacements). This suggests ultrasound-based measurements of carpal tunnel motion could be useful in the clinical assessment of CTS. Currently, the diagnostic protocol for CTS is not standardized and still prone to false negatives (Jablecki et al. 2002). The protocol can include any combination of physical examination, patient history for signs and symptoms, and/or electrodiagnostic tests (nerve conduction studies or needle electromyography). Clinicians frequently use electrodiagnostic tests due to the direct quantification of median nerve pathophysiology (median nerve conduction velocity is impaired by compression). However, these tests can have low and variable sensitivity (49-84%) and should not be used for diagnosis alone (Jordan et al. 2002). Ultrasound has value in diagnosing false negative electrodiagnostic cases (Koyuncuoglu et al. 2005) and therefore has potential to augment current CTS diagnostic protocols. More research is necessary to fully understand the clinical utility of ultrasound.

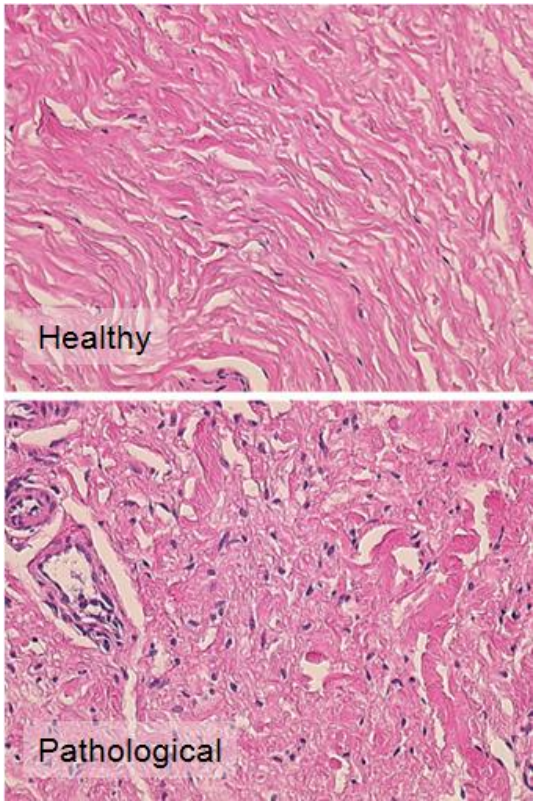

Figure 1.3 Pathological fibrosis of the SSCT include a number of histological changes such as increased fibroblast frequency (purple nuclei) and reorganization of collagen fibres. From Ettema et al. 2006.

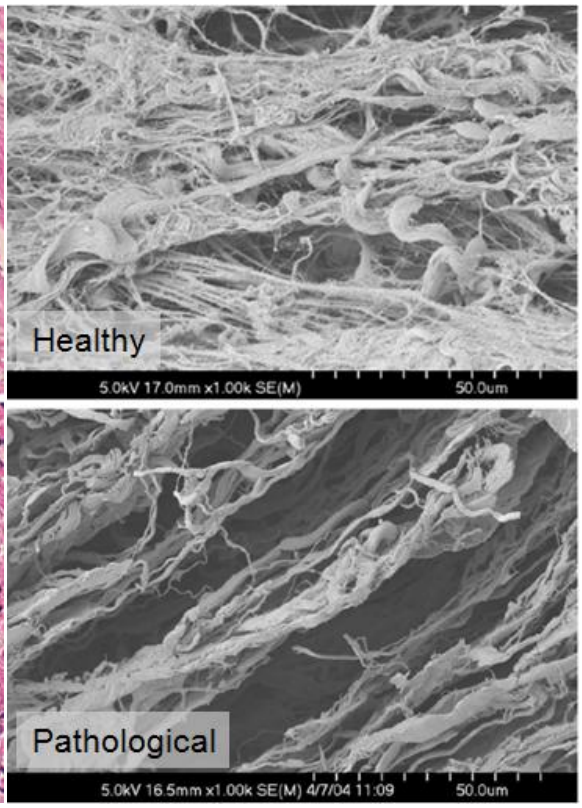

Figure 1.4 Normal interconnections between layers of the SSCT are disrupted and indicate pathological fibrosis. From Ettema et al. 2006.

The testing paradigm, for tendon shear studies using ultrasound, suggest increased differential motion between the tendon and SSCT is associated with greater shear forces in the SSCT, thereby predisposing to shear damage. However, the significance of ultrasound shear has yet to be investigated, and there is a need for comparison to a direct measurement of mechanical tendon shear. Mechanical tendon shear (work done by tendon on surrounding tissue) has been quantified using a two-dimensional belt-pulley model of the wrist (Moore et al. 1991). Tendon gliding in the wrist was represented as a

belt wrapping around a pulley (e.g. the pulley consists of the transverse carpal ligament in wrist flexion and carpal bones in wrist extension). The force exerted on the pulley was related to the belt tension, radius of curvature, frictional coefficient, and belt-pulley contact angle. Moore et al. (1991) used this relationship to calculate tendon frictional work and found it to be the most predictive of carpal tunnel syndrome in the workplace compared to any other physical measure, such as tendon loading and wrist or hand kinematics.

A similar paradigm was used to test gliding characteristics of the flexor tendon in the human carpal tunnel with cadaveric hands and wrists (Zhao et al. 2007). Two force transducers measured tendon force proximal and distal to the carpal tunnel, with the difference being friction (friction force = proximal tendon force – distal tendon force). Zhao et al. (2007) reported increased tendon friction in a flexed wrist posture consistent with increased contact stress against the transverse carpal ligament represented in biomechanical models (Moore et al. 1991; Armstrong and Chaffin, 1978). Though the paradigm is useful for measuring overall tendon shear, unique contributions to friction cannot be quantified. In the carpal tunnel, frictional sources may include surface friction between adjacent structures (bursa, SSCT layers, transverse carpal ligament, carpal bones) and viscoelastic resistance from the SSCT (stretch of the interconnecting collagen fibrils between SSCT layers). This thesis used a cadaver model to directly measure tendon shear while moving the tendon with a combination of different wrist postures, forces, and velocities. Examining multiple risk factors will help tease out the effect of different sources of friction. We chose to use fresh frozen specimens to avoid chemical

preservation (such as with embalming) that could affect the fidelity of the model. The process of freezing and storing specimens is expected to have a minimal effect on tendon mechanical properties (Wren et al. 2001). Tendon shear will be quantified with frictional work using direct measurements of force with transducers proximal and distal to the carpal tunnel and with ultrasound using relative tendon-SSCT displacement. The comparison of ultrasound with frictional work will provide important insight into the utility of ultrasound as it relates to injury.

1.2 Purpose and Hypotheses

The global purpose of the thesis was to evaluate the use of ultrasound in the assessment of flexor tendon shear to understand its role in carpal tunnel syndrome. Excessive shear in the carpal tunnel has been implicated in the etiology of fibrosis and thickening of the flexor tenosynovium, the most common pathological findings in CTS patients. Ultrasound has been used to quantify shear injury risk with relative longitudinal displacement between the tendon and tenosynovium. However, the relationship between relative motion and shear is not well understood. The thesis investigates the mechanical and clinical implications of ultrasound shear to understand its function in examining the pathomechanics of CTS. The conception of this thesis was inspired by work during my undergraduate thesis to investigate tenosynovium phenomenon (See Pilot Work Appendix D).

The specific purposes and hypotheses for each chapter are outlined below:

Chapter 2

In my thesis proposal we intended to evaluate multiple ultrasound techniques (colour Doppler and speckle tracking) for the measurement of tendon displacement, however this thesis only used colour Doppler. Recent communications highlight the usefulness of speckle tracking and led to extensive pilot work to try and utilize this technique (See Pilot Work Appendix D). However, we experienced difficulty with speckle tracking (due to large motion artifacts) that made tracking impractical; while we found colour Doppler gave a more robust measure of tendon and SSCT motion. The study addressed the need to reappraise the colour Doppler method for relative tendon displacement studies.

Purpose: To evaluate the use of colour Doppler ultrasonography in the measurement of tendon displacement with 3 tendon velocities (5, 10, 15 cm/s) using a cadaver model.

Hypothesis: Tendon displacement measured by colour Doppler ultrasound will demonstrate high accuracy compared to displacement measured on the tendon line (potentiometer). Measurement error will be influenced by tendon velocity and tendon displacement.

Chapter 3

This study followed the validation of colour Doppler ultrasound in Chapter 2, which showed it can be used to quantify relative displacement in the carpal tunnel. The current study used colour Doppler to measure relative displacement between the tendon-SSCT in fresh frozen cadaveric specimens.

Purpose: To investigate the meaning of ultrasound shear by assessing the relationship between relative tendon motion and a direct mechanical measurement of tendon forces to calculate tendon frictional work. Also, the effect of biomechanical risk factors on relative motion will be evaluated including wrist posture (neutral, 30^{o} flexion), force (10, 20, 30 N), and velocity (5, 10, 15 cm/s).

Hypothesis: Relative tendon motion will increase in accordance with frictional work. We anticipate an interaction effect between the 3 variables (posture, force, and velocity) for both experimental measurements of shear (ultrasound and frictional work). Tendon shear will increase with a flexed wrist posture, higher forces, and faster velocities.

Chapter 4

This study was a follow-up to Chapter 3. Ultrasound "shear" only partially represented tendon shear with the viscoelastic stretch of the tenosynovium. This study explored the clinical implications of measuring viscoelastic resistance *in vivo* with ultrasound.

Purpose: To examine the relationship between the tenosynovium (morphological and functional properties measured by ultrasound) and CTS severity assessed with clinical symptoms questionnaires. We will use a CTS symptomatic population scored based on severity from the Boston Carpal Tunnel Questionnaire and Katz Hand Diagram.

Hypothesis: CTS symptomatics will demonstrate pathological changes in the tenosynovium inferred by greater SSCT thickness (morphological) and

increased differential motion between the tendon-SSCT (functional) compared to healthy participants. The altered morphology and functionality of the tenosynovium assessed with ultrasound will be positively associated with the clinical symptoms questionnaires.

CHAPTER 2

VALIDATION OF COLOUR DOPPLER ULTRASONOGRAPHY FOR EVALUATING RELATIVE DISPLACEMENT BETWEEN FLEXOR TENDON AND SUBSYNOVIAL CONNECTIVE TISSUE

Jimmy Tat, BSc, Aaron M. Kociolek, MSc, Peter J. Keir, PhD*

Occupational Biomechanics Laboratory, Department of Kinesiology, McMaster University, Hamilton, ON, Canada, L8S 4K1

*Corresponding Author:

Peter J. Keir, PhD
McMaster University
Department of Kinesiology
Ivor Wynne Centre, room 212
1280 Main Street West
Hamilton, ON, Canada, L8S4K1
Telephone: 905-525-9140 ext. 23543
Email: pjkeir@mcmaster.ca

Short running title: Validation of colour Doppler for relative tendon-SSCT motion

Accepted to: *Journal of Ultrasound in Medicine*

Type: Original Research

2.1 Abstract

Objective. A common pathological finding in carpal tunnel syndrome is fibrosis and thickening of the subsynovial connective tissue (SSCT). This suggests an etiology of excessive shear forces that have been quantified using ultrasound with relative longitudinal displacement between the flexor tendon and adjacent SSCT. **Methods.** Eight unmatched fresh frozen cadaver arms were used to evaluate colour Doppler ultrasound in the measurement of tendon displacement. The middle flexor digitorum superficialis tendon was moved through a physiological excursion of 20 mm at 3 different tendon velocities (50, 100, 150 mm/s). **Results.** We found colour Doppler provided accurate measurement of tendon displacement, with absolute errors of -0.05 mm (50 mm/s), -1.24 mm (100 mm/s) and -2.36 mm (150 mm/s) on average throughout the tendon excursion range. Evaluating relative displacement between the tendon-SSCT during finger flexion-extension movements also offered insight into the gliding mechanism of the SSCT. During flexion, we observed a curvilinear increase in relative displacement, with greater differential motion at the end range of displacement, likely due to the sequential stretch of the fibrils between successive layers of the SSCT. In extension, there was a linear return in relative displacement, suggesting a different unloading mechanism characterized by uniform relaxation of fibrils. **Conclusions.** We demonstrated the validity of colour Doppler displacement for use in the evaluation of relative motion. Colour Doppler ultrasound is useful in our understanding of the behaviour of the SSCT during tendon excursion that may elucidate the role of finger motion in the etiology of shear injury.

Keywords: ultrasound, colour Doppler, tendon, subsynovial connective tissue, shear, viscoelastic

2.2 Introduction

Carpal tunnel syndrome (CTS) is the most common peripheral compression neuropathy. Although workplace CTS has been well investigated using epidemiological studies, the exact etiology remains elusive and is most likely multi-factorial. However, there is evidence that repetitive hand and finger motions can increase the risk of CTS in the workplace.[1,2] During finger motions, flexor tendon gliding is facilitated by a paratenon and bursa within the carpal tunnel. These structures reduce tendon gliding friction, but can be damaged with excessive shear forces between tendons.[3] Pathological changes in the paratenon, including fibrosis and thickening, are common characteristics of CTS.[4,5] As a consequence, the structure and function of the paratenon have been well investigated in recent years.

In the carpal tunnel, the paratenon, termed subsynovial connective tissue (SSCT), is described as a microvacuolar system consisting of multiple layers of collagen bundles interconnected by vertical fibrils.[6] These fibrils also tether the SSCT to the flexor tendons and the median nerve, such that tendon or nerve excursions move layers of the SSCT. During tendon motion, tendon force is transferred to the SSCT layers by stretching the fibrils in the direction of tendon motion. This is thought to occur in an organized manner, with layers closest to the tendon moving first, followed by successive layers extending to the visceral synovium. Excessive differential motion between the tendon and SSCT can result in stretching fibrils beyond viscoelastic limits, leading to tissue failure and shear injury.[5,7] These findings are consistent with the greatest severity of fibrosis most apparent within layers in close proximity to the tendon.[5]

Relative longitudinal displacements between the tendon and adjacent SSCT have been used to quantify shear injury.[8] Greater relative motion suggests an increased risk of shear injury.[5,7] Osamura et al[9] found this could occur during finger motions in a physiological range. There is also evidence that differential motion is mediated by occupational risk factors including wrist posture, repetition, duration, and independent finger movements.[8,10-12] These findings highlight the utility of differential motion in understanding the etiology of CTS.

Recent advances in ultrasound technology, such as improved image resolution, have allowed researchers to measure relative motion between the tendon and SSCT.[4,8,10,13] Traditional Doppler-based techniques calculate tissue velocities based on Doppler shift frequencies ($f = 2 \cdot v \cdot f_o \cdot cos\theta / c$), which use the relationship between the transducer frequency (f_o), velocity of sound in the medium (c), and the insonation angle (θ) between the transducer beam and moving tissue, to determine the velocity of the moving tissue (v). While a number of studies have employed Doppler methods to track tendon motion, including pulse-wave Doppler and colour Doppler techniques,[13-17] the angle dependency is typically regarded as a limitation contributing to measurement error[8] especially considering the orientation of carpal tunnel anatomy can produce less than optimal insonation angles. However, maintaining an angle of insonation of less than 60^o can help to reduce potential errors.[18]

As an alternative to Doppler methods, speckle tracking ultrasound uses block-matching algorithms to track musculoskeletal tissue heterogeneities (speckle patterns) in a sequence of grey-scale images.[19] While speckle tracking is often considered an "angle

independent" approach, block-matching schemes inherently require some angle dependency in acquiring images to orient the tissue for tracking rectilinear regions of interest. Yoshii et al[8] found that speckle tracking was more highly correlated than pulse-wave Doppler to tendon excursion estimated with a geometric model.[20] While the same study found speckle tracking underestimated the magnitude of excursion by nearly one third, these findings have detracted from the use of Doppler techniques. There is evidence that limitations of pulse-wave Doppler do not apply to colour Doppler as the functions differ in ability to measure tissue motion due to the specific methods used to quantify Doppler shifts.[21] Colour Doppler ultrasound also provides the advantage of simultaneously measuring adjacent tissue from a single ultrasound collection that is not limited to measuring small structures. Tracking small structures, such as the SSCT, poses a challenge for speckle tracking due to the limited speckle patterns and hyperechogenicity. This is highly relevant for current testing paradigms that evaluate relative motion between the tendon and adjacent SSCT.

In early validation studies, colour Doppler only localized tendon position, while pulse-wave Doppler was used to quantify tendon velocities.[14-17] However, this may be inadequate for the measurement of relative motion between tendon and SSCT. More recently, Oh et al[13] used colour Doppler ultrasound for tracking tendon and SSCT velocities in a cadaver model. Colour Doppler demonstrated high accuracy in the range of 2.5 cm/s to 10 cm/s velocities and detected differential motion between the tendon and SSCT. However, only peak tendon velocities from ultrasound were compared to a direct velocity measurement. Thus, there is a need for a comprehensive evaluation of colour

Doppler in the measurement of tendon displacement. Only by evaluating the progression of tissue displacements over time, will we obtain an understanding of the way structures in the carpal tunnel move as a system, which will help elucidate the role of finger motion in the etiology of shear injury.

The purpose of this study was to validate colour Doppler ultrasonography in the measurement of tendon displacement over time. This was tested in a cadaver model using 3 tendon velocities within a physiological range of tendon excursion and force. Error was examined at multiple increments of tendon excursion. The time-history of relative displacements between the tendon and SSCT will improve our understanding of the gliding mechanism in the carpal tunnel.

2.3 Methods

2.3.1 Cadaveric specimens

Eight unmatched fresh frozen cadaver arms with a mean age (± standard deviation) of 56.9 ± 16.1 years were amputated proximal to the elbow. The exclusion criteria consisted of a known history of CTS, peripheral nerve disease, or wrist tendinopathy. The arms were slowly thawed at 5°C for 12 – 15 hours prior to dissection. The four flexor digitorum superficialis (FDS) and profundus (FDP) tendons, the flexor pollicus longus tendon, and median nerve were identified at the proximal level of the carpal tunnel using passive finger movements. All tendons were excised from their proximal and distal attachments to connect to our testing apparatus. Otherwise, the carpal tunnel was left undisturbed and the ulna and radius remained intact to maintain fidelity of

the wrist complex. The study protocol was approved by the Hamilton Integrated Research Ethics Board.

2.3.2 Experimental procedure

A specimen is shown in our testing apparatus (Figure 2.1). The proximal aspect of the forearm was fixed with a metal clamp. The distal forearm, third metacarpal, and third finger distal phalanx were tightly secured to the apparatus with plastic ties. The middle FDS tendon (FDS3) was attached to a pulley system to permit motion in the proximal (representing finger flexion) and distal (finger extension) directions. The remaining 7 flexor tendons (index, ring, and little finger), middle finger flexor digitorum profundus, flexor pollicus longus tendon and median nerve all remained under passive physiological tension of 250 g.[22] The lines of action were best maintained as they would exit the carpal tunnel to represent the interface between the tendon and SSCT *in vivo*.

Testing was performed with the wrist fixed in a neutral posture. A mechanical actuator (ERC3, IAI America Inc., Torrance, CA) moved the middle FDS tendon at 3 velocities (50, 100, 150 mm/s) against the resistance of a 20 N constant force spring (N-Series, Vulcon Spring Co., Telford, PA). The tendon was displaced 30 mm in the proximal and distal directions to simulate finger flexion and extension, respectively. Tendon force and tendon velocities were selected to represent *in vivo* conditions. Active, unresisted finger motion, such as performing keystrokes, can produce tendon forces in the range of 8 - 30 N.[22,23] We previously found tendon velocities reached up to 150 mm/s in a dynamic full finger flexion-extension movement task.[10]

The motor excursion end ranges were subject to high accelerations to achieve our constant velocities; thus, the first and last 5 mm intervals were not included in the analysis. We analyzed the tendon excursion from 5-25 mm for a total range of 20 mm, which is representative of full finger motion consisting of complete flexion of the MCP and PIP finger joints.[24] A high-precision rotary potentiometer (6370 Series, State Electronics Corp., East Hanover, NJ) was positioned on the tendon line to obtain motor displacements. Prior to collection, each specimen was preconditioned with 24 flexion-extension cycles. Subsequent trials consisted of 4 continuous flexion-extension movements.

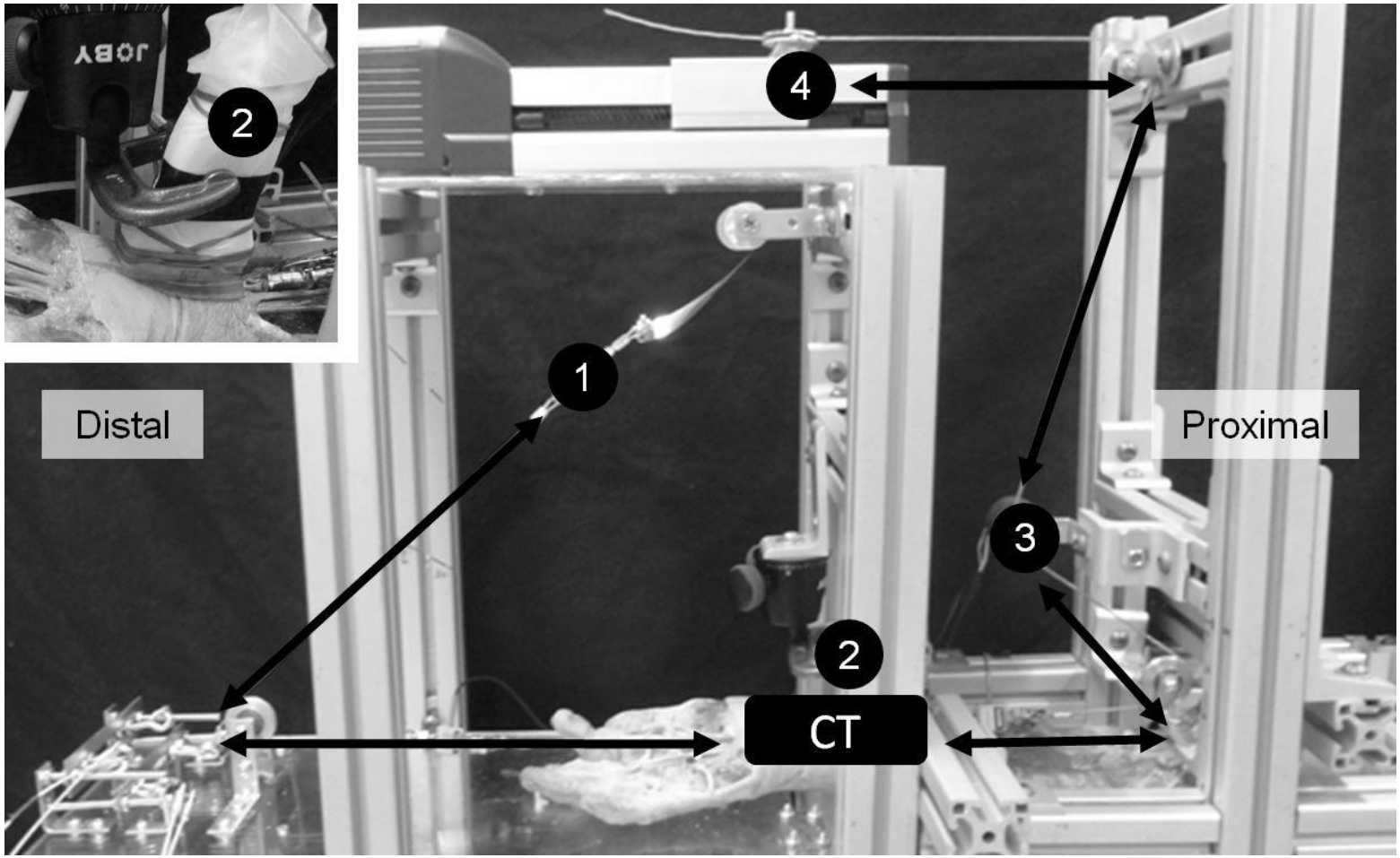

Figure 2.1 A cadaver forearm in the testing apparatus. The tendon line moves only the middle FDS tendon in the proximal-distal directions as indicated by the arrows. The tendon line consists of a (1) constant force spring, (2) ultrasound probe, (3) rotary potentiometer, and (4) mechanical actuator. (*Above left*) Close up of the probe positioned above the carpal tunnel (CT) using a gel wedge as a coupling medium.

2.3.3 Sonographic Measurements

A Vivid q BT10 (GE Healthcare, Milwaukee, WI) console with a linear array transducer (12LRS) imaged the carpal tunnel during tendon motion. A clamp fixed the transducer at the proximal wrist crease of the specimen such that it was longitudinally in line with the middle finger FDS tendon. The colour Doppler method was used to quantify tissue velocity information and included a B-mode image of the tissue of interest and overlaying colour maps for the quantification of velocity. The tendon and SSCT structures were identified in B-mode. The tendon appeared as distinct fibrillar striations traversing the length of the carpal tunnel. The bordering SSCT was a thin, parallel, bright layer (on each side of the tendon). Colour maps were used to isolate the position of the middle FDS tendon. The tendon was moved proximally (flexion) and distally (extension) to highlight structures with blue and red colour maps, respectively. The colour intensity represented velocity magnitude, with brighter colours indicating faster velocities.

The transducer was set to a depth of 3.0 cm with a single focal point located at the depth of the tendon. To optimize the angle of insonation, we used an ultrasound beam steer angle (20^{o}) and a custom gel wedge (Aquaflex Gel Pad, Cone Instruments, Solon, OH). The angle of insonation (θ) was the incident angle between the Doppler beam and moving tissue. The angle was measured by positioning the sample volume cursor over the tendon and adjusting the green line until it was parallel to the tendon motion direction (Figure 2). This was important for calculating tissue velocities and we maintained a mean ($\pm$ standard deviation) angle of 62.9 ± 1.9^{o}. Other sonographic settings included a scale $\pm$ 11.0 cm/s for detecting tissue velocities (prior to adjusting for insonation angle), a low

velocity reject (12.7 mm/s) and transducer frequency of 13 MHz. Tendon motion trials were recorded with cineloops at 29.5 frames per second.

Cineloops (containing B-mode images of the tendon and SSCT and overlaying colour maps) were exported for offline analyses using dedicated Q-analysis software (Echopac, GE Healthcare, Milwaukee, WI). Colour maps allowed for simultaneous evaluation of flexor tendon and SSCT in the same video clip. Three circular markers (0.5 mm diameter) were placed longitudinally along the FDS tendon (Figure 2.2). The markers represented left, middle, and right regions on the colour map.[10] Multiple markers were used to limit potential errors associated with tracking a single point (out of plane motion, local artifacts, tissue deformation), which might be susceptible to weak ultrasound echoes in any one region of the colour map window. Three additional circular markers were placed adjacent to each FDS tendon marker to represent velocities of the adjoining SSCT. All markers remained stationary throughout the video clip and were visually inspected to remain over the tissue of interest. Each marker returned a unique tissue velocity profile. The mean tissue velocity of the 3 FDS markers and 3 SSCT markers were calculated, low-pass filtered at 6.0 Hz and corrected for the angle of insonation (factor of $cos\theta$). The mean FDS and mean SSCT velocities were integrated to determine displacements.

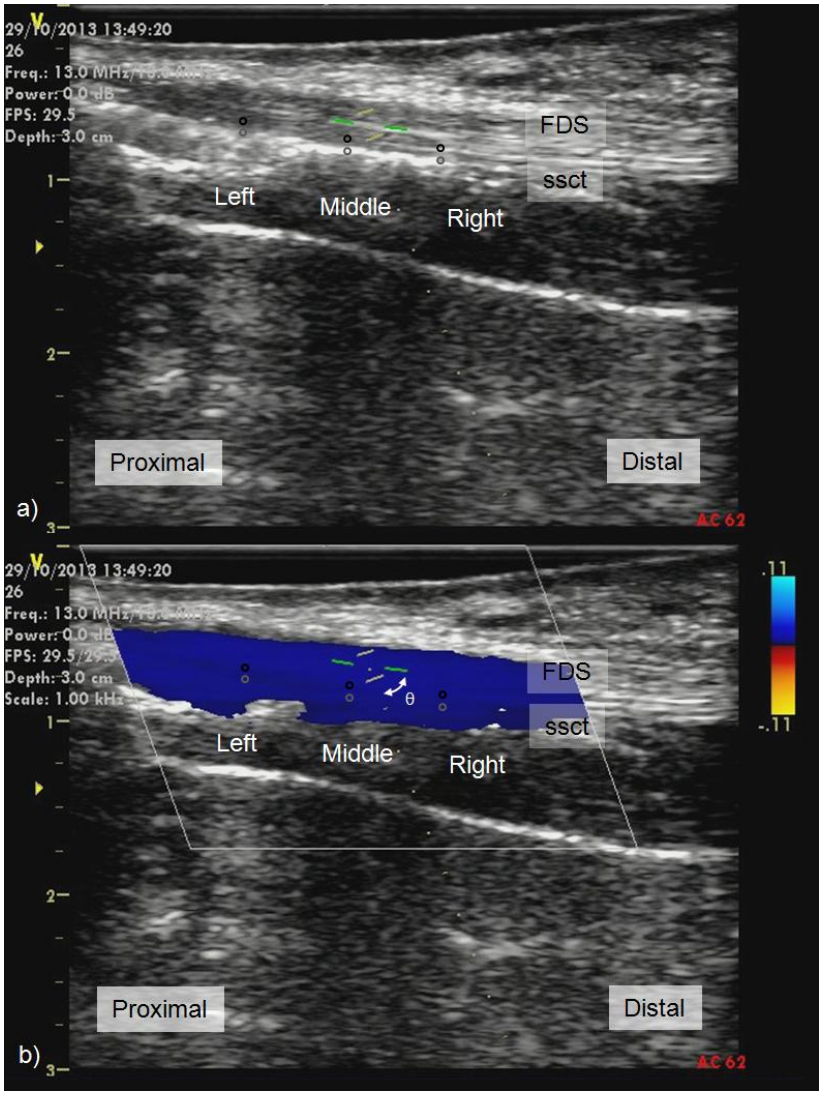

Figure 2.2 Colour Doppler ultrasound provided a simultaneous (a) grayscale echogram and (b) colour map. The grayscale image was used to identify the flexor digitorum superficialis (FDS) tendon, shown as a hypoechoic fibrillar band and the subsynovial connective tissue (SSCT), a thin hyperechoic layer bordering the tendon. The sample volume cursor was used to measure the angle of insonation ($\theta = 62^{o}$ in this case) for post-processing angle corrections. The angle was measured between the Doppler beam (dotted line) and tendon movement direction (green lines at sample volume). In the colour Doppler window, pairs of markers were positioned in the left, middle, and right region of the colour map. The top marker of each pair represented the tendon (black marker) and the bottom was the subjacent SSCT (gray marker). Each marker was angle corrected and integrated to obtain tissue displacements. Note: the sample volume was not used for pulse-wave Doppler or M-mode measurements.

2.3.4 Data analysis

Motor displacements and ultrasound displacements were collected simultaneously throughout tendon excursion for each trial. The potentiometer measured motor displacements at 120 Hz (LabView 8.5, National Instruments Corp., Austin, TX) which were then low-pass filtered at 6.0 Hz. Typical ultrasound displacement histories for the tendon, SSCT and relative tendon-SSCT are shown in Figure 2.3. Relative motion between the tendon and SSCT was defined as tendon displacement - SSCT displacement,[25] calculated on a point-by-point basis to show the progression of relative differences throughout tendon excursion.

Measurement error was defined by the absolute difference between colour Doppler tendon displacement and motor tendon displacement at 4 intervals of motor displacement (5, 10, 15, 20 mm) for both flexion and extension directions. For each direction, we also calculated the maximum relative displacement between the tendon and SSCT using a shear strain index, SSI = (tendon displacement – SSCT displacement) / tendon displacement × 100%.[12] The maximum tendon and SSCT displacement at 20 mm of motor excursion was used for the shear strain calculation. Mean SSI were calculated for the 3 tendon velocities in flexion and extension. All calculations were performed in Matlab 7.6 (MathWorks, Inc., Natick, MA).

2.3.5 Statistical Analysis

A one-way repeated measures analysis of variance model was used to test the effect of tendon velocity (50, 100, 150 mm/s) on SSI in both flexion and extension (SPSS v.13.0, SPSS Inc, Chicago, IL). All significant findings were further analysed with

Tukey's honestly significant difference test. Significance was set to $p<0.05$ and all values are presented as means (± standard deviations).

2.4 Results

Absolute measurement error for colour Doppler tendon displacements were evaluated in flexion and extension at 3 tendon velocities (50, 100, 150 mm/s). In both movement directions, faster tendon velocities had greater absolute measurement error (Table 2.1). The mean absolute error in the flexion direction was -0.05 ± 0.79 mm at 50 mm/s, -1.24 ± 1.24 mm at 100 mm/s, and -2.36 ± 1.56 mm at 150 mm/s. During extension movements, the mean absolute measurement error was -0.53 ± 0.97 mm at 50 mm/s, -1.84 ± 1.65 mm at 100 mm/s, and -2.8 ± 1.78 mm at 150 mm/s. Absolute error also increased incrementally with tendon displacement for both movement directions. Colour Doppler underestimated tendon displacements, but the magnitude of measurement error was dependent on both tendon excursion and tendon velocity.

Figure 2.3 shows the mean displacement profile for the tendon and SSCT at each velocity. The profiles indicate that the tendon and SSCT move in parallel, but with a delay in the SSCT. Differential motion between the tendon-SSCT increased with tendon excursion and reached a maximum at the end of the 20 mm of flexion excursion range. This was evaluated using the shear strain index and we found velocity-dependent differences for both flexion and extension finger movement directions (Figure 2.4). In flexion, SSI increased significantly from 50 to 150 mm/s by 95.7 % ($p < 0.05$) while a significant increase of 87.7 % occurred between 50 and 150 mm/s in extension ($p < 0.05$).

Table 2.1

Absolute measurement error (mm) presented at 4 motor excursion levels (5, 10, 15, 20 mm) for 3 tendon velocities. Values are represented as mean (± standard deviation).

Motor		Ultrasound			
		Flexion		Extension	
Velocity	Displacement	Displacement (mm)	Absolute error (mm)	Displacement (mm)	Absolute error (mm)
50 mm/s	5 mm	5.00 (0.45)	0.00 (0.45)	4.71 (0.46)	-0.29 (0.46)
	10 mm	9.96 (0.62)	-0.04 (0.62)	9.53 (0.77)	-0.47 (0.77)
	15 mm	14.91 (0.91)	-0.09 (0.91)	14.33 (1.14)	-0.67 (1.14)
	20 mm	19.92 (1.18)	-0.08 (1.18)	19.33 (1.41)	-0.67 (1.41)
100 mm/s	5 mm	3.87 (0.41)	-1.13 (0.41)	3.79 (0.60)	-1.21 (0.60)
	10 mm	8.65 (0.87)	-1.35 (0.87)	8.24 (1.25)	-1.76 (1.25)
	15 mm	13.83 (1.45)	-1.17 (1.45)	13.03 (1.81)	-1.97 (1.81)
	20 mm	18.69 (1.92)	-1.31 (1.92)	17.57 (2.43)	-2.43 (2.43)
150 mm/s	5 mm	3.16 (0.77)	-1.84 (0.77)	3.27 (0.80)	-1.73 (0.80)
	10 mm	7.52 (1.32)	-2.48 (1.32)	7.31 (1.51)	-2.69 (1.51)
	15 mm	12.50 (1.76)	-2.50 (1.76)	11.88 (1.92)	-3.12 (1.92)
	20 mm	17.38 (2.22)	-2.62 (2.22)	16.32 (2.25)	-3.68 (2.25)

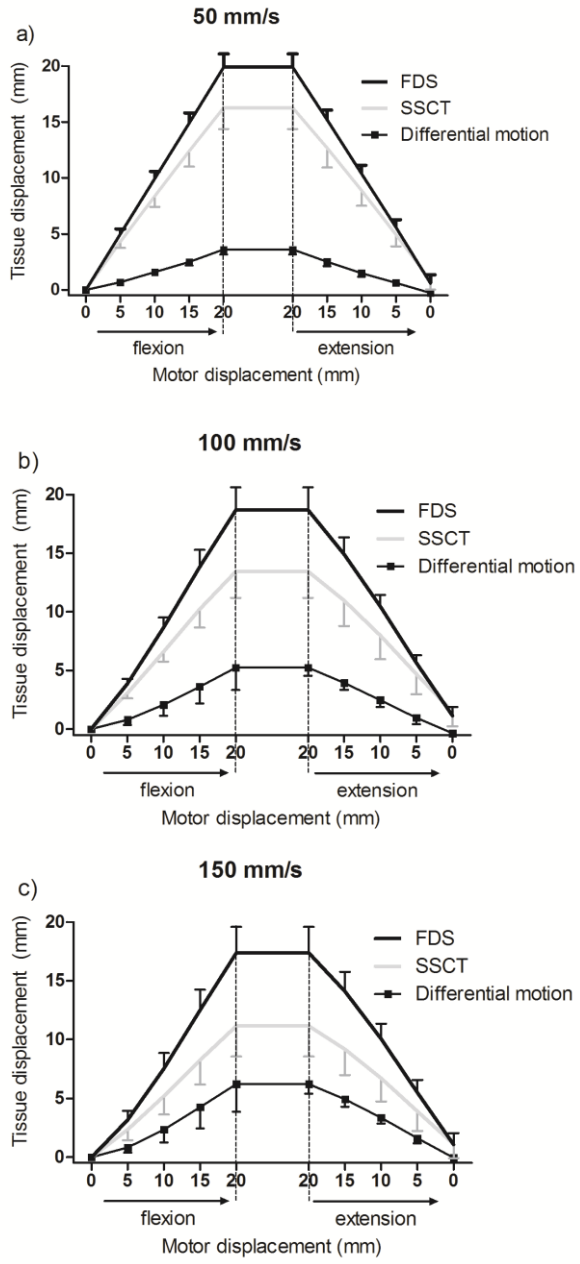

Figure 2.3 The average ultrasound displacement profile for 20 mm of motor excursion in flexion (proximal) and extension (distal) directions (N=8). The motor was moved at 3 constant velocities, a) 50 mm/s b) 100 mm/s c) 150 mm/s. FDS represents the flexor digitorum superficialis and SSCT indicates the subsynovial connective tissue. Differential motion was calculated as (tendon displacement – SSCT displacement). Error bars represent one standard deviation.

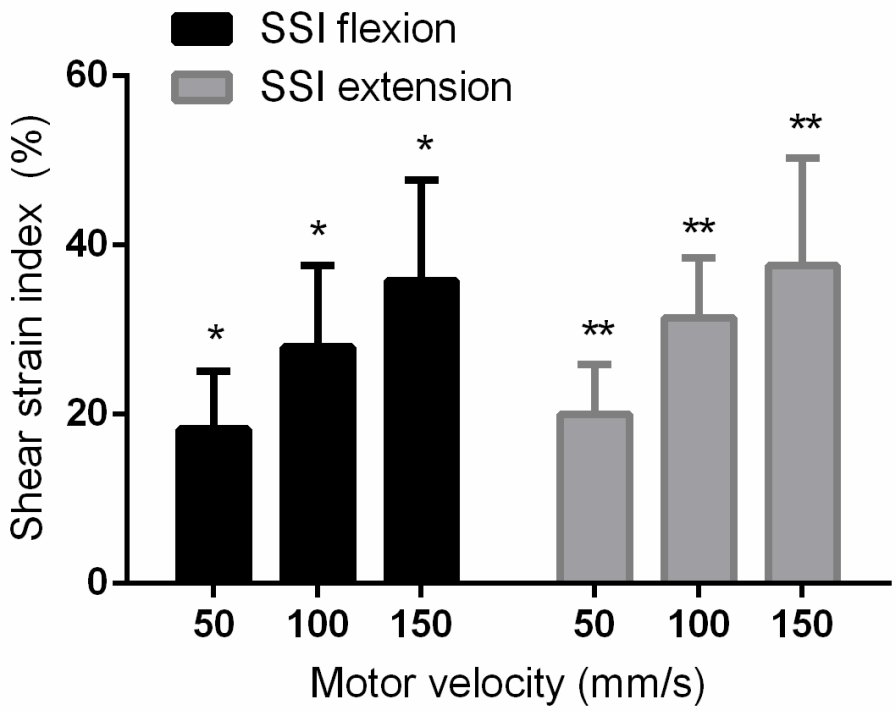

Figure 2.4 Mean shear strain index (SSI) in flexion and extension for 3 tendon velocities (N=8). SSI, $(D_{FDS}-D_{SSCT})/D_{FDS}$, was the maximum relative motion calculated from the maximum displacement after 20 mm of motor excursion. *denotes significant difference across all velocities ($p < 0.05$). **denotes significance between 50 mm/s vs. 100 mm/s and 50 mm/s vs. 150 mm/s. Error bars indicate one standard deviation.

2.5 Discussion

We evaluated the colour Doppler technique using physiological tendon velocities and found that absolute measurement error for tracking tendon displacements was influenced by both the magnitude of excursion and velocity. However, the relative error at each tendon velocity was similar across all tendon excursions, and underestimated tendon displacement. These findings suggest that the systematic differences associated with tendon velocity and excursion can be adjusted to improve *in vivo* estimates of tendon displacement.

Previously, pulse-wave Doppler measurements of tendon displacement showed poor relationships with estimates of tendon excursion from a geometric model.[8] We did not find this limitation in colour Doppler as we demonstrated that tendon excursion was accurately represented throughout the time-history of tendon motion. Moreover, colour Doppler provided measurement error similar to a previous *in vitro* validation of tendon displacement using an angle independent approach with speckle tracking.[19] For similar testing parameters (velocity and excursion), we found similar absolute (< 0.1 mm) and relative (< 1%) errors. By optimizing the angle of insonation (approximately 60^{o}),[18] using a 20^{o} beam steer angle and gel wedge, we effectively attenuated the presumed limitation of angle dependency. Colour Doppler thus provides an accurate measurement of the magnitude of tendon displacement on a point-by-point basis.

The validation of colour Doppler for tracking tissue displacement gives insight into important aspects of the carpal tunnel system. We interpreted the relative displacement profile between the tendon and SSCT to speculate about the gliding

mechanism of the SSCT. We found that high tendon velocities produced large peak differential motion (SSI) between the tendon and SSCT, suggesting a viscous component with the SSCT. In the SSCT, the viscous properties are suggested to be largely due to the gel-like interfibrillar matrix (protegolycans) that surround the collagen fibrils and layers.[6] The interfibrillar matrix likely causes motion of the layers to be strain-rate dependent. Therefore, faster tendon velocities moved successive layers at a slower rate due to viscous shear, leading to smaller SSCT excursions and greater differential motion. We observed smaller SSCT excursions in fast versus slow tendon velocities at all excursion levels (Figure 2.3).

The elastic response in the SSCT is also apparent with the displacement histories for the tendon and SSCT. We found a nonlinear increase in differential motion throughout the tendon displacement in flexion (Figure 2.5). Ettema et al[5] found that SSCT fibrils were stretched further with greater differential motion between the tendon-SSCT using an electron microscope. As the tendon moves further in the flexion direction, fibrils become progressively stretched, with layers closest to the tendon experiencing the most stretch, producing a nonlinear increase in resistance. This would decrease SSCT motion relative to the tendon at greater tendon excursions. Interestingly, this is consistent with an *in vitro* assessment of gliding resistance force on the tendon, showing nonlinear increases in flexion direction excursions that may indicate contributions from the viscoelastic stretch of SSCT fibrils.[26] We propose that differential motion may reflect viscoelastic shear forces; however, the relationship between differential motion and shear

stress has yet to be investigated. We intend on further investigating the meaning of ultrasound-based differential motion and its mechanical implications in future studies.

In our testing paradigm, flexion excursions (proximal motion of the tendon) resulted in tendon "loading" that stretched the SSCT, while extension excursions involved "unloading" the tendon to relax the SSCT. We found differential motion returned more linearly during extension than flexion, suggesting a different gliding mechanism for loading versus unloading the SSCT (Figure 2.5). In flexion excursions, we attributed the nonlinearity, which was most apparent with the fastest velocity (150 mm/s), to the viscous nature of the sequential and progressive strain of the interconnecting fibrils. We would expect a similar shape if the fibrils were unloaded in a sequential manner. Rather, we found a consistent linear return, suggesting the entire SSCT system picked up the slack, such that layers of the SSCT moved by uniform relaxation of fibrils. Motion facilitated by passive fibril relaxation could account for slower SSCT excursions during tendon unloading (during extension motion). An understanding of the gliding mechanism can provide insight into how tendon force is transferred to the SSCT during loading and unloading, which may be relevant in elucidating conditions that approach the viscoelastic injury threshold.

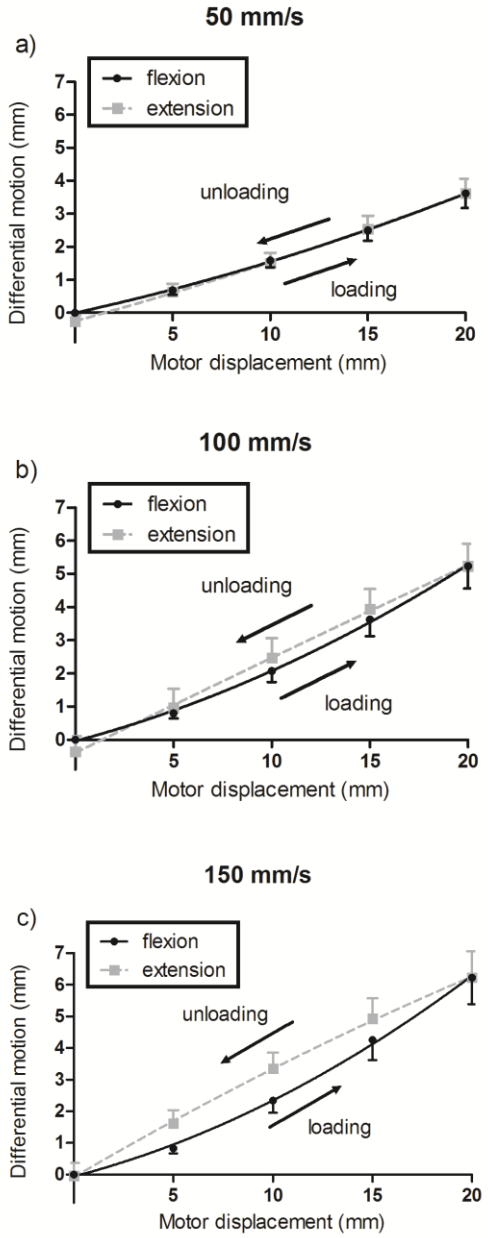

Figure 2.5 The mean differential motion profile for flexion-extension movement cycles at a) 50 mm/s b) 100 mm/s c) 150 mm/s tendon velocities (N=8). Flexion (proximal) direction excursions represented "loading" SSCT fibrils (stretch in direction tendon motion) and extension (distal) movements involved "unloading" SSCT fibrils (relaxation). The x-axis is motor displacement (mm) relative to the position at the start of flexion excursion. The y-axis is differential motion (tendon displacement – SSCT displacement). Error bars represent one standard error of mean.

Recent communications suggest that measurement error with *in vitro* speckle tracking[19] is small, in low magnitude motions and excursions that are not necessarily representative of *in vivo* motions. Yoshii et al[8] showed speckle tracking largely underestimated the magnitude of tendon excursion *in vivo*, which is a common problem associated with speckle decorrelation (motion artifacts).[27] The current study supports previous work by showing colour Doppler provides better estimates of tendon excursion with smaller mean absolute error.[8] Colour Doppler offers the additional advantage of tracking small tissue (i.e. marker diameter of 0.5 mm) with robust outcomes. This is difficult with speckle tracking due to a lack of heterogeneous speckle patterns, particularly with the hyperechoic nature of the SSCT, making tracking very laborious and in some cases even impractical. These factors make colour Doppler a good tool for quantifying relative displacement between the tendon and SSCT in the carpal tunnel.

There were a few limitations to the study. We moved the tendon 30 mm in the flexion and extension direction, but disregarded the first and last 5 mm to avoid end range accelerations and maintained constant velocities. Oh et al[13] also found colour Doppler to have difficulty detecting velocities below than 2.5 cm/s which would have occurred at the start of tendon motion. Second, a cadaver model does not entirely represent the *in vivo* system which could limit the interpretation of our findings. However, our data was comparable to our previous *in vivo* study (Tat et al. 2013), despite not representing the small lateral and palmodorsal tendon motions that occur during *in vivo* tendon excursion. While out of plane motion can limit the accuracy of longitudinal displacements using colour Doppler, it would be consistent for the tendon and adjacent SSCT. In these cases,

it is important to align the probe parallel to the longitudinal tendon direction for optimal longitudinal measurements. We also used fresh frozen specimens and took precautions to avoid dehydrating the tissue to preserve the properties of the tendon sheath. Finally, we did not measure displacement of individual SSCT layers, but interpreted the relationship of the relative tendon-SSCT displacement to infer the gliding mechanism. To our knowledge there is no technique currently available to measure motion of individual layers during dynamic tendon excursions. However, our ultrasound system provided the resolution to track the SSCT complex surrounding the tendon which has an approximate thickness 0.5 mm in healthy individuals.[4] For this study, the gliding mechanism of the SSCT was determined based on relative motion between the tendon and SSCT, since tendon loads are transferred via interconnecting fibrils to move layers of the SSCT.

In conclusion, this study showed that colour Doppler ultrasound provides an accurate and precise measurement of tendon displacement that will be useful for tendon shear strain testing paradigms. We also inferred the gliding mechanism of the SSCT based on the relative displacement profiles which suggested viscous and elastic properties. The viscous effect was seen by velocity-dependent increases in relative displacement. In tendon loading, the sequential stretch of fibrils between successive SSCT layers produced a nonlinear increase in relative motion between the tendon and SSCT. However, tendon unloading followed a more linear return which suggests passive and uniform relaxation of the fibrils and the individual layers of the SSCT.

2.6 Acknowledgements

This study was supported by funding from the Natural Sciences and Engineering Research Council Discovery Grant (# 217382-09). We also thank Bruce Wainman, Glen Oomen, and the entire staff of the Education Program in Anatomy for their assistance in the preparation of cadaver specimens prior to dissection.

2.7 References

1. Moore A, Wells R, Ranney D. Quantifying exposure in occupational manual tasks with cumulative trauma disorder potential. Ergonomics 1991, 34: 1433-1453.
2. Silverstein BA, Fine LJ, Armstrong TJ, Occupational factors and the carpal tunnel syndrome. Am J Ind Med 1987, 11: 343-358.
3. Barr AE, Barbe MF, Clark BD. Work-related musculoskeletal disorders of the hand and wrist: Epidemiology, pathophysiology, and sensorimotor changes. J Orthop Sports Phys Ther 2004, 34: 610-27.
4. van Doesburg MHW, van der Molen AM, Henderson J, Cha SS, An KN, Amadio PC. Sonographic measurements of subsynovial connective tissue thickness in patients with carpal tunnel syndrome. J Ultrasound Med 2012, 31: 31-36.
5. Ettema AM., Amadio PC, Zhao C, Wold LE, O'Byrne MM, Moran SL, An KA. Changes in the functional structure of the tenosynovium in idiopathic carpal tunnel syndrome: A scanning electron microscope study. Plast and Reconstr Surg 2006, 118: 1413-1422.
6. Guimberteau JC, Delage JP, McGrouther DA, Wong JKF. The microvacuolar system: how connective tissue sliding works. J Hand Surg 2010, 35: 614-622.
7. Vanhees M, Morizaki Y, Thoreson AR, Larson D, Zhao C, An KA, et al. The effect of displacement on the mechanical properties of human cadaver subsynovial connective tissue. J Orthop Res 2012, 30: 1732-1737.

8. Yoshii Y, Zhao C, Henderson J, Zhao KD, An KN, Amadio PC, Shear strain and motion of the subsynovial connective tissue and median nerve during single digit motion. J Hand Surg 2009, 34: 65-79.

9. Osamura, N, Zhao C, Zobitz ME, An KN, Amadio PC. Evaluation of the material properties of the subsynovial connective tissue in carpal tunnel syndrome. Clin Biomech 2007, 22: 999-1003.

10. Tat J, Kociolek AM, Keir PJ. Repetitive differential motion increases shear strain between the flexor tendon and subsynovial connective tissue. J Orthop Res 2013, 31: 1533-1539.

11. Yoshii Y, Zhao C, Henderson J, Zhao KD, An KN, Amadio PC. Velocity dependent changes in the relative motion of the subsynovial connective tissue in the human carpal tunnel. J Orthop Res 2011, 29: 62-66.

12. Yoshii Y, Zhao C, Zhao KD, Zobitz ME, An KN, Amadio PC. The effect of wrist position on the relative motion of tendon, nerve, and subsynovial connective tissue within the carpal tunnel in a human cadaver model. J Orthop Res 2008, 26: 1153-1158.

13. Oh S, Belohlavek M, Zhao C, Osamura N, Zobitz ME, An K. Detection of differential gliding characteristics of the flexor digitorum superficialis tendon and subsynovial connective tissue using color Doppler sonographic imaging. J Ultrasound Med 2007, 26: 149-155.

14. Soeters JNM, Roebroeck ME, Holland WPJ, Hovius SER, Stam, HJ. Non-invasive measurement of tendon excursion with a colour Doppler imaging system:

a reliability study in healthy subjects. Scand J Plast Reconstr Surg Hand Surg 2004, 38: 356-360.

15. Holland WPJ, Buyruk HM, Hoorn E, Stam HJ. Tendon displacement assessment by pulsed Doppler tissue imaging: Validation with a reciprocating string test target. Ultrasound Med Biol 1999, 25: 1229-1239.

16. Buyruk HM, Holland WPJ, Snijders CJ, Laméris JS, Hoorn E, Stoeckart R, et al. Tendon excursion measurements with color Doppler imaging. J Hand Surg Br 1998, 23: 350-353.

17. Cigali BS, Buyruk HM, Snijders CJ, Laméris JS, Holland WPJ, Mesut R et al. Measurement of tendon excursion velocity with colour doppler imaging: A preliminary study on flexor pollicis longus muscle. Eur J Radiol 1996, 23: 217-221.

18. Liu EY, Steinman AH, Cobbold RS, Johnston KW. Human factors as a source of error in peak Doppler velocity measurement. J Vasc Surg 2005, 42: 972-979

19. Korstanje JWH, Selles RW, Stam HJ, Hovius SER, Bosch JG. Development and validation of ultrasound speckle tracking to quantify tendon displacement. Journal of Biomech 2010, 43: 1373-1379.

20. An KN, Ueba Y, Chao W, Cooney WP, Linscheid RL. Tendon excursion and moment arm of index finger muscles. J Biomech 1983, 16: 419-425.

21. Kukulski T, Voigt JU, Wilkenshoff UM, Strotmann JM, Wranne B, Halte L, et al. A comparison of regional myocardial velocity information derived by pulsed and

color Doppler techniques: an in vitro and in vivo study. Echocardiography 2003, 17: 639-651.

22. Schuind F, Garcia-Elias M, Cooney III, WP, An KN. Flexor tendon forces: in vivo measurements. J Hand Surg 1992, 17: 291- 298.

23. Dennerlein JT. Finger flexor tendon forces are a complex function of finger joint motions and fingertip forces. J Hand Ther 2005, 18: 120-127.

24. Brand, PW, Hollister A. Clinical Mechanics of the Hand, St. Louis: Mosby; 1993.

25. Hendersen J, Thoreson A, Yoshii Y, Zhao KD, Amadio PC, An KA. Finite element model of the subsynovial connective tissue deformation due to tendon excursion in the human carpal tunnel. J Biomech 2011, 44: 150-155.

26. Filius A, Thoreson AR, Yang TH, Vanhees M, An KA, Zhao C, et al. The effect of low- and high-velocity tendon excursion on mechanical properties of human cadaver subsynovial connective tissue. J Orthop Res 2014, 32: 123-128.

27. Yeung F, Levinson SF, Parker KJ. Multilevel and motion model-based ultrasonic speckle tracking algorithms. Ultrasound Med Biol 1998, 24: 427-441.

CHAPTER 3

RELATIVE TENDON-SSCT DISPLACEMENT USING ULTRASOUND AND MECHANICAL TENDON SHEAR CAPTURE DIFFERENT PHENOMENA

Jimmy Tat, BSc, Aaron M. Kociolek, MSc, Peter J. Keir, PhD*

Occupational Biomechanics Laboratory, Department of Kinesiology, McMaster University, Hamilton, ON, Canada, L8S 4K1

*Corresponding Author:

Peter J. Keir, PhD
McMaster University
Department of Kinesiology
Ivor Wynne Centre, room 212
1280 Main Street West
Hamilton, ON, Canada, L8S4K1
Telephone: 905-525-9140 ext. 23543
Email: pjkeir@mcmaster.ca

To be submitted to: *Journal of Orthopaedic Research*

Type: Original Article

3.1 Abstract

The most common finding in carpal tunnel syndrome is fibrosis and thickening of the subsynovial connective tissue (SSCT). The SSCT mediates gliding in the carpal tunnel and suggests excessive shear forces are involved in injury. Using ultrasound, relative motion between flexor tendon and SSCT has assessed "shear"; however, the implications of ultrasound shear are not understood. The middle flexor digitorum superficialis (FDS) tendon of 8 cadavers was moved in a combination of wrist postures (neutral, flexed), velocities (5, 10, 15 cm/s) and forces (10, 20, 30 N) to compare ultrasound shear with direct measurements of tendon frictional work. We found a significant posture × force interaction on tendon frictional work, likely due to greater surface friction against the transverse carpal ligament with a flexed wrist and high force ($p<0.05$). However, ultrasound shear increased independently with posture ($p<0.05$) and force ($p<0.05$), indicating ultrasound inadequately represented surface friction contributions. We found additive velocity effects in both measurements (ultrasound, $\eta_p^2=0.862$, $p<0.05$; frictional work, $\eta_p^2=0.937$, $p<0.05$) that suggest ultrasound only captures the viscoelastic component of tendon shear (stretch of SSCT). While ultrasound shear provides an incomplete measure of flexor tendon shear, measuring viscoelastic resistance can help elucidate the role of hand motion in SSCT pathology.

Keywords: carpal tunnel syndrome, ultrasound, tendon, shear, friction

3.2 Introduction

Musculoskeletal disorders of the wrist and hand are common in the workplace and result in greater work disability than other body regions.[1] Workers in textile, machining, and transportation industries are at high risk of developing these disorders due to work operations that involve highly repetitive hand motion.[2] Repetitive trauma injuries of the distal upper limb include flexor tendinitis, tenosynovitis, tendinosis, and peripheral neuropathies such as carpal tunnel syndrome.[3] Of these occupational-related disorders, carpal tunnel syndrome is the most frequently reported, and is particularly debilitating, with many cases requiring surgical intervention.[4-5]

Carpal tunnel syndrome (CTS) is a compression neuropathy of the median nerve. Epidemiology studies have shown relationships between CTS incidence and occupational risk factors including high repetition, awkward wrist postures and high force, especially when more than one is present.[6-9] Though the etiology has been extensively studied, the exact pathomechanics of CTS remains elusive, and is most likely multi-factorial. One major finding of CTS is non-inflammatory fibrosis and thickening of the subsynovial connective tissue (SSCT) surrounding the flexor tendons in the carpal tunnel.[10-11] These changes affect the function of the SSCT, and lead to impaired gliding of carpal tunnel structures.[12] Altered gliding mechanics may play a role in the link between repetitive hand motion and injury development.

The SSCT consists of collagen bundles that form layers around the flexor tendons and median nerve and is considered viscoelastic. Each layer of the SSCT is interconnected by small near perpendicular fibrils. During tendon motion, the layers are

sequentially recruited by the fibrils such that the SSCT moves in parallel with the tendon, but with a delay. With excessive differential motion, perpendicular fibrils of the SSCT may exceed elastic limits, and break, resulting in shear injury.[10,13] Chronic exposure to repetitive loading may give rise to a cycle of tissue degradation and reorganization that leads to fibrotic changes of the SSCT.[1] This is consistent with histological findings of fibrosis, which are most pronounced in the tenosynovial layers directly bordering the flexor tendons.[10]

Ultrasonography has been used to quantify the risk of shear injury by measuring relative longitudinal displacement between flexor tendon and adjacent SSCT. There is evidence that ultrasound shear is mediated by traditional biomechanical risk factors such as duration, posture, velocity, and independent finger motions.[14-17] Using ultrasound, greater differential motion between the tendon-SSCT is typically associated with larger shear forces and increased injury risk. However, the link between differential motion and mechanical shear force has yet to be investigated, and the clinical implications of ultrasound shear are not well understood.

The purpose of this study was to investigate ultrasound "shear" by evaluating relative tendon-SSCT motion alongside direct measurements of mechanical tendon shear using a frictional work approach. Frictional work is a well-established quantitative measure in musculoskeletal stress models.[18-19] Tendon frictional work is more predictive of injury than other physical measures of tendon loading and wrist/hand kinematics,[19] thus offers important insights into the nature tendon shear. A secondary objective was to examine the effects of biomechanical work-related disorder risk factors (posture, force,

and velocity) on ultrasound shear. To our knowledge, this represents the first evaluation of tendon force in ultrasound shear.

3.3 Methods

3.3.1 Cadaveric specimens

The study protocol was approved by the Hamilton Integrated Research Ethics Board. Eight unmatched fresh frozen cadaver arms with a mean age (± standard deviation) of 56.9 ± 16.1 years were amputated proximal to the elbow. Exclusion criteria consisted of a known history of CTS, peripheral nerve disease, and wrist tendinopathy. The arms were slowly thawed at 5°C for 12 – 15 hours prior to dissection. Passive finger movements identified all four flexor digitorum superficialis (FDS) and profundus (FDP) tendons, the flexor pollicus longus tendon, and median nerve, proximal to the carpal tunnel. The tendons were then excised from their proximal and distal attachments to connect with our testing apparatus. The carpal tunnel was otherwise left undisturbed and the ulna and radius remained intact to preserve the anatomic fidelity of the wrist complex.

3.3.2 Experimental procedure

The experimental procedure in detail may be found in Kociolek et al.[20]. In brief, the arm was secured to the testing apparatus at the proximal aspect of the forearm with an adjustable metal clamp. The wrist (proximal to the wrist crease), hand (at the 3rd metacarpal) and middle finger (at the distal phalanx) were tightly secured to our testing apparatus with plastic fasteners. The middle FDS tendon was attached to a pulley system to permit motion in both the proximal and distal directions representing finger flexion and

finger extension, respectively. The other remaining 7 flexor tendons of the index, ring, and little finger, as well as the flexor pollicus longus tendon and median nerve remained under passive physiological tension of 250 g via tension springs.[21] The lines of action of all structures (flexor tendons and median nerve) were best maintained as they would exit the carpal tunnel *in vivo*.

Movement of the FDS tendon in the proximal direction simulated finger flexion (Figure 3.1). This was achieved with a mechanical actuator (ERC3, IAI America Inc., Torrance, CA) connected to the proximal end of the tendon, while a constant force spring provided resistance distally (N-Series, Vulcon Spring Co., Telford, PA). Two light-weight miniature S-beam load cells (LCM-200, Futek Inc., Irvine, CA) were located in line with the tendon, immediately proximal and distal to the carpal tunnel. The load cells were used to measure tendon force and subsequently calculate gliding resistance in the tendon as the difference between the two load cells, $F_{Proximal} - F_{Distal}$.[22] A sonographic scanner (Vivid Q BT10, General Electric Healthcare, Milwaukee, WI) obtained tendon velocities inside the carpal tunnel using colour Doppler imaging. Motor displacements were also measured with a precision rotary potentiometer (6370 Series, State Electronics Corp., East Hanover, NJ) on the cable connecting the motor to the middle FDS tendon.

The tendon was moved using a combination of 2 wrist postures (0° neutral, 30^{o} flexion), 3 forces (10, 20, 30 N), and 3 velocities (5, 10, 15 cm/s). Each testing condition consisted of 4 simulated flexion excursions of 30 mm. This was meant to represent a full finger FDS excursion.[23-24] Trial order was block randomized by posture to minimize order effects. We selected tendon forces and velocities to represent *in vivo* loading,

similar to tendon forces during active finger motion such as performing keystrokes that can range from 8 – 30 N.[21,25] Tendon velocities were within the normal range for dynamic full finger flexion-extension movement (up to 15 cm/s).[14,16]

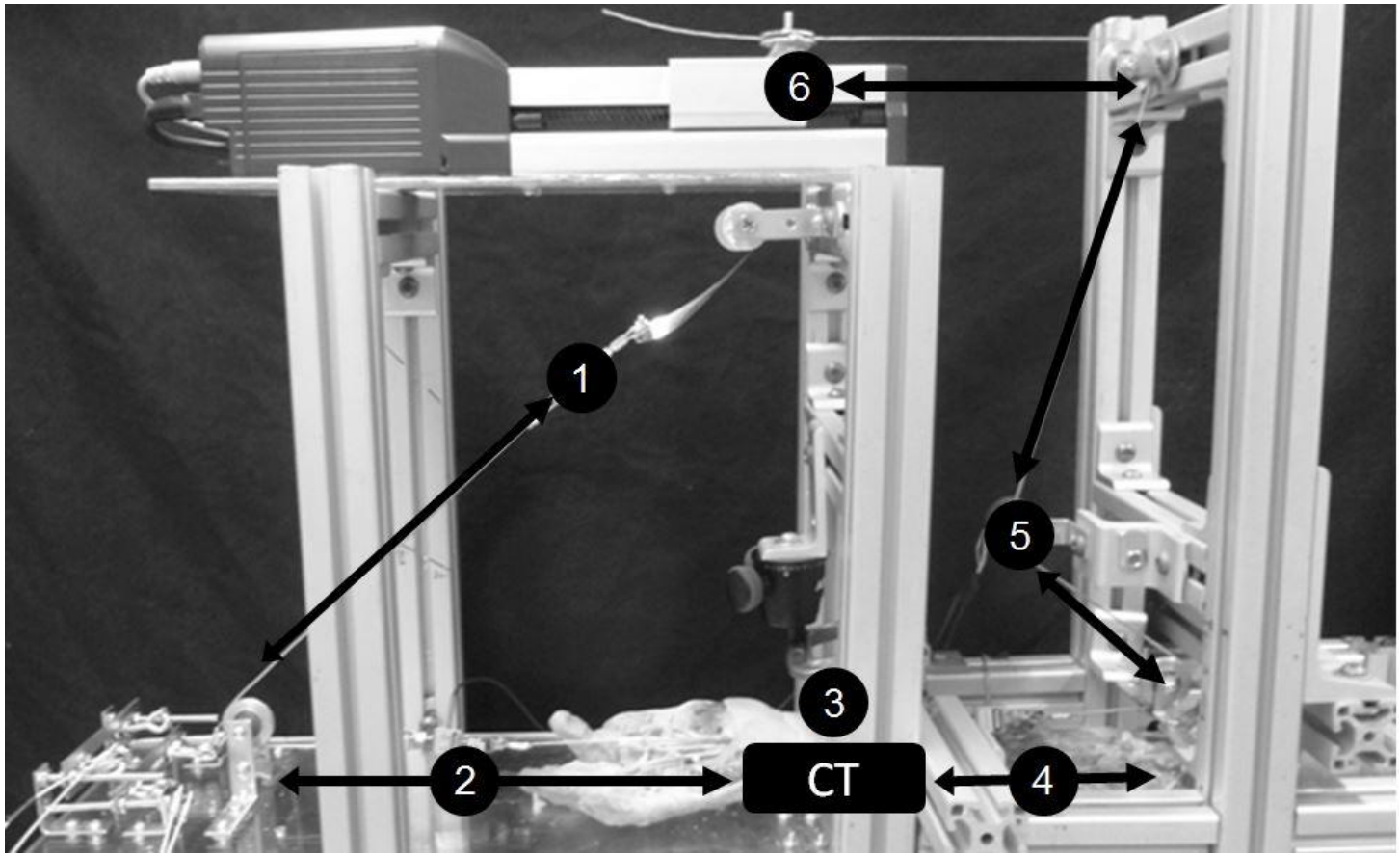

Figure 3.1 A cadaver forearm in the testing apparatus. The tendon line is connected to the middle FDS tendon and moves in the proximal-distal directions as indicated by the arrows. The tendon line consists of a (1) constant force spring, (2) distal force sensor, (3) ultrasound probe, (4) proximal force sensor, (5) potentiometer, (6) mechanical actuator. CT indicates the location of the carpal tunnel.

3.3.3 Sonographic measurement

A Vivid Q BT10 (GE Healthcare, Milwaukee, WI) console and a linear array transducer (12LRS) operating at a central frequency of 12 MHz imaged the carpal tunnel at the distal wrist crease. A clamp fixed the transducer at the proximal wrist crease of the cadaver, which was aligned longitudinally with the middle finger FDS tendon. We used colour Doppler imaging to obtain longitudinal velocities of the FDS tendon and SSCT (Figure 3.2). To identify the tendon, the motor was moved in both the proximal and distal directions to represent tendon motion with blue (flexion) and red (extension) colour maps. These colour maps indicated the direction as well as the velocity of tendon motion, with brighter colours representing higher velocities. Optimal tissue tracking was represented by saturated colour maps overlaying a distinct hypoechoic, fibrillar structure (FDS tendon) bordered by a thin, hyperechoic layer (SSCT).

The colour Doppler technique was previously validated for tendon motion using a cadaver model.[26,27] Similar sonographic settings were applied to optimize tissue tracking. The transducer was set to a depth of 3.0 cm with a focal point at the level of the tendon. The scale detected tissue velocities in the range of ± 11.0 cm/s (prior to adjusting for insonation angle). An ultrasound beam steering angle of 20º was further augmented with a custom gel wedge (Aquaflex Gel Pad, Cone Instruments, Solon, OH), thereby reducing the angle of insonation to approximately 60°. FDS tendon and SSCT velocities were recorded with 10-second video clips at 29.5 frames per second.

Raw images were post-processed using dedicated software (Echopac, GE Healthcare, Milwaukee, WI). Three circular markers (0.5 mm diameter) were placed

longitudinally along the FDS tendon (Figure 3.2). The markers represented left, middle, and right positions in the colour Doppler map.[14] Multiple markers were used to limit error associated with tracking a single point, which may be susceptible to weak ultrasound echoes. Three additional circular markers (0.5 mm diameter) were placed on the SSCT (adjacent to the FDS tendon markers). Each marker remained stationary throughout the ultrasound scan and returned a unique tissue velocity profile. The mean tissue velocity of the 3 FDS markers and 3 SSCT markers were calculated, low-pass filtered at 6.0 Hz, and corrected for the angle of insonation. FDS tendon and SSCT velocities were integrated to determine displacements.

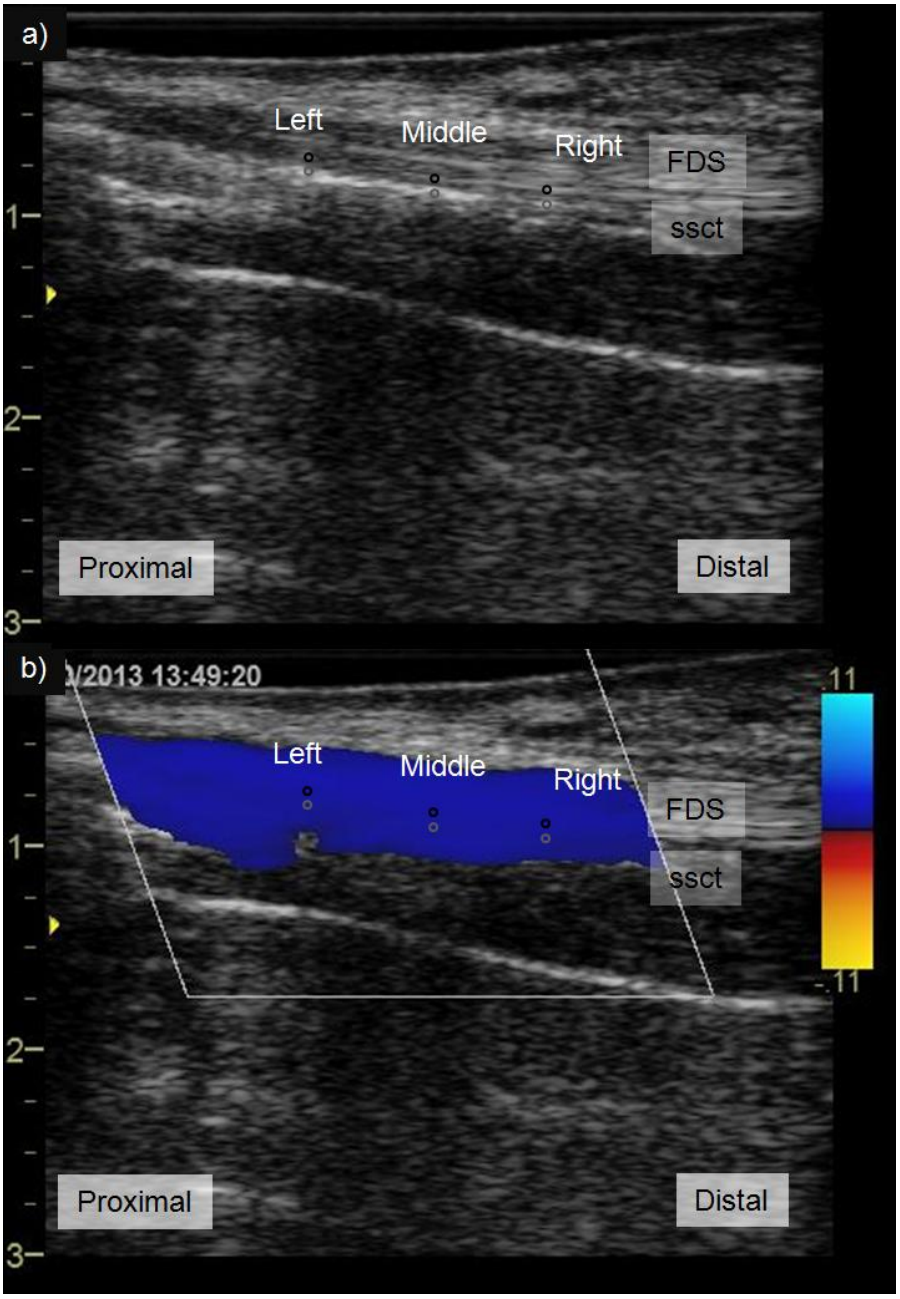

Figure 3.2 Ultrasound provided a simultaneous (a) grayscale echogram and (b) colour Doppler map of the middle tendon. The flexor digitorum superficialis (FDS) tendon is shown as a band of fibrillar striations bordered by a thin, bright subsynovial connective tissue (SSCT) layer. Pairs of markers were positioned at the left, middle, and right regions on the colour map. The top marker of each pair represented the tendon (black marker) and the bottom was the subjacent SSCT (gray marker). The blue colour map indicates flexion direction tissue movements.

3.3.4 Data analysis

Force and ultrasound data were simultaneously collected throughout tendon excursion for each condition. Proximal and distal flexor tendon forces were used to calculate tendon frictional work and represented mechanical shear, while ultrasound shear was quantified as the relative displacement between the tendon and SSCT. All calculations were performed in Matlab 7.6 (MathWorks, Inc., Natick, MA).

The two-load cells collected tendon force data at 120 Hz (LabView 8.5, National Instruments Corp., Austin, TX) and were subsequently low-pass filtered at 6.0 Hz. Tendon frictional work was calculated by integrating gliding resistance over motor excursion. This represented the total energy lost due to tendon shear during tendon motion, including surface friction with other carpal tunnel structures (bursa, SSCT layers, transverse carpal ligament), as well as viscoelastic stretch in the tendon-SSCT. Figure 3.3 depicts the average mechanical tendon shear profile across all experimental conditions.

Ultrasound shear was defined as relative displacement between the tendon and SSCT, calculated from the absolute difference between tendon and SSCT ($D_{FDS} - D_{SSCT}$).[28] Relative displacement provided a representation of ultrasound shear throughout the excursion range, similar to frictional work which is a cumulative measure. The average differential motion profile for all experimental test conditions is shown in Figure 3.3.

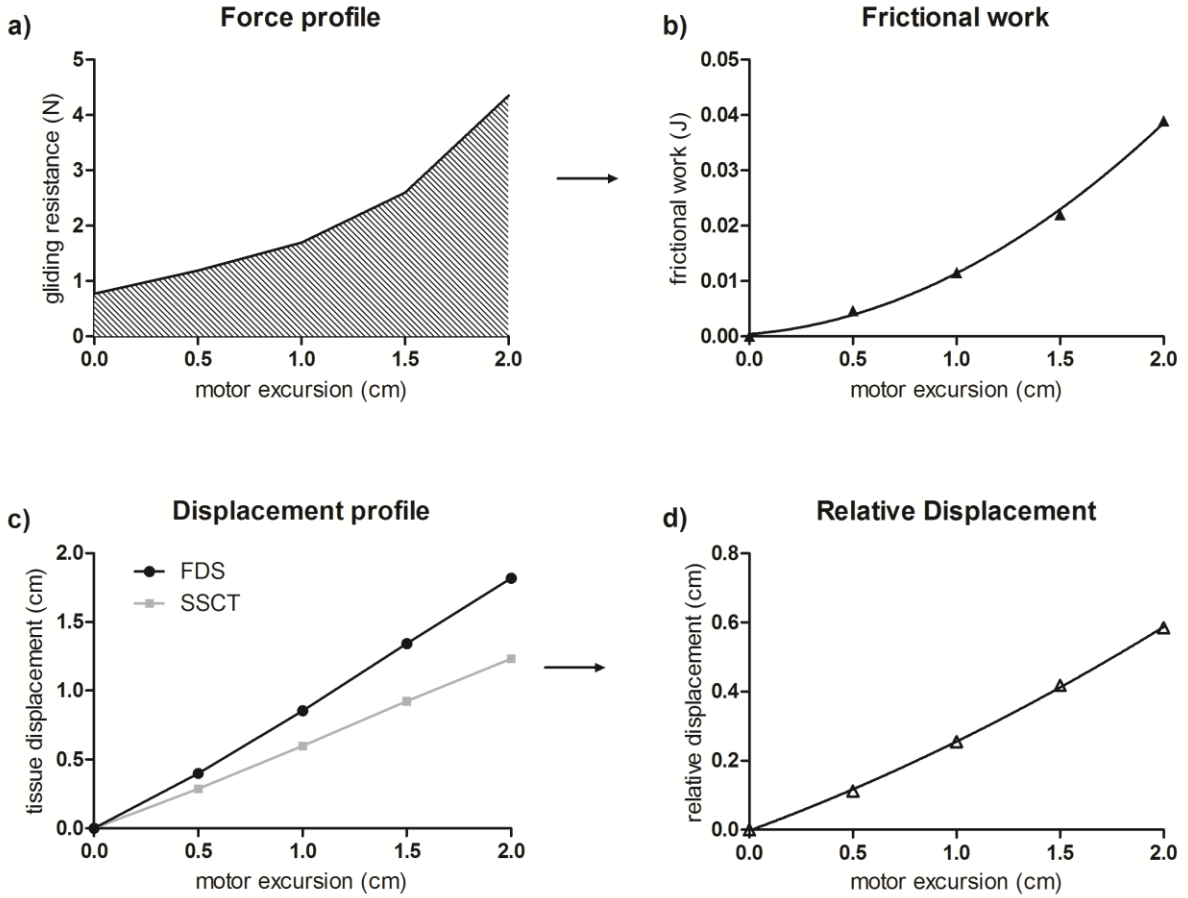

Figure 3.3 Average tendon shear profiles measured mechanically with force sensors and using ultrasound. Mechanical tendon shear was measured as the integral of (a) tendon gliding resistance over motor excursion to obtain (b) frictional work. For ultrasound, (c) relative displacement of the tendon and SSCT was calculated (d) as the absolute difference (D_{FDS}-D_{SSCT}). Both measurements increased nonlinearly with excursion.

3.3.5 Statistical Analysis

Two separate 3-way repeated measures analysis of variance models evaluated the effect of posture (0° neutral, 30° flexion), force (10, 20, 30 N), and velocity (5, 10, 15 cm/s) for tendon frictional work and relative displacement from ultrasound. Although we moved the motor 30 mm to simulate full finger flexion, the first and last 5 mm of tendon motion were disregarded to avoid confounding acceleration effects associated with the motor end ranges. Therefore, frictional work and relative displacement were calculated between 5-25 mm of motor excursion and corresponded to 20 mm of simulated flexion excursion. Significance was set to $p < 0.05$ and all significant findings were further analysed with Tukey's HSD. To directly compare our experimental treatments on both measures of shear (ultrasound versus mechanical), we evaluated the effect sizes (partial eta squared, η_p^2) of the modeled main effect and interaction terms.

3.4 Results

Frictional work and relative tendon displacement (from ultrasound) increased together with the prescribed tendon excursion. While both measurements increased non-linearly with tendon excursion, frictional work was more curvilinear (Figure 3.3). Additionally, for both measures, the curvilinear shape was more pronounced using higher tendon velocities. The peak frictional work and peak relative displacement occurred at the end of our analyzed range of simulated flexion excursion (20 mm of motion).

ANOVA results for frictional work and differential motion are presented in Table 3.1. A significant wrist posture × tendon force interaction was found for direct

measurement of frictional work ($p<0.05$, $\eta_p^2=0.55$). The magnitude of applied force significantly influenced flexor tendon frictional work in a flexed wrist posture, with a significant incremental increase at each force level ($p<0.05$). However, force had no significant effect in the neutral wrist posture (Figure 3.4). Using ultrasound, wrist posture and tendon force independently affected relative tendon-SSCT displacement as seen by significant main effects of wrist posture ($p<0.05$) and tendon force ($p<0.05$), without a coincident wrist posture × tendon force interaction. Relative displacement was greater with 30° of wrist flexion than a neutral wrist (0°). Tendon-SSCT relative motion was also significantly higher at 30 N than either 20 N or 10 N tendon forces ($p<0.05$). For this ultrasound measure, tendon force explained a relatively small proportion of variance ($\eta_p^2=0.377$) compared to wrist posture ($\eta_p^2=0.632$).

There was a significant main effect of tendon velocity on both frictional work and ultrasound. Higher tendon velocities increased frictional work ($p<0.05$) and relative displacement ($p<0.05$; Figure 3.5). Tendon velocity produced similar effect sizes for both measures of shear (frictional work, $\eta_p^2=0.937$; relative displacement, $\eta_p^2=0.862$), which were relatively large in comparison to the other independent variables (wrist posture and tendon force). These findings indicate that the two measures of shear had a similar response to tendon velocity.

Table 3.1 ANOVA summary for the effect of posture, force, and velocity on tendon shear measurements. Mechanical tendon shear is represented by frictional work (Work) and ultrasound shear (U/S) with relative displacement. * denotes significance ($p<0.05$).

Source	df		F ratio		p-value		η_p^2	
	U/S	Work	U/S	Work	U/S	Work	U/S	Work
Posture	(1,7)	(1,7)	11.99	6.90	0.010*	0.034*	0.632	0.496
Force	(2,14)	(2,14)	4.24	10.25	0.036*	0.002*	0.377	0.594
Velocity	(2,14)	(2,14)	43.83	104.97	0.000*	0.000*	0.862	0.937
Posture × Force	(2,14)	(2,14)	0.17	8.55	0.842	0.004*	0.024	0.550

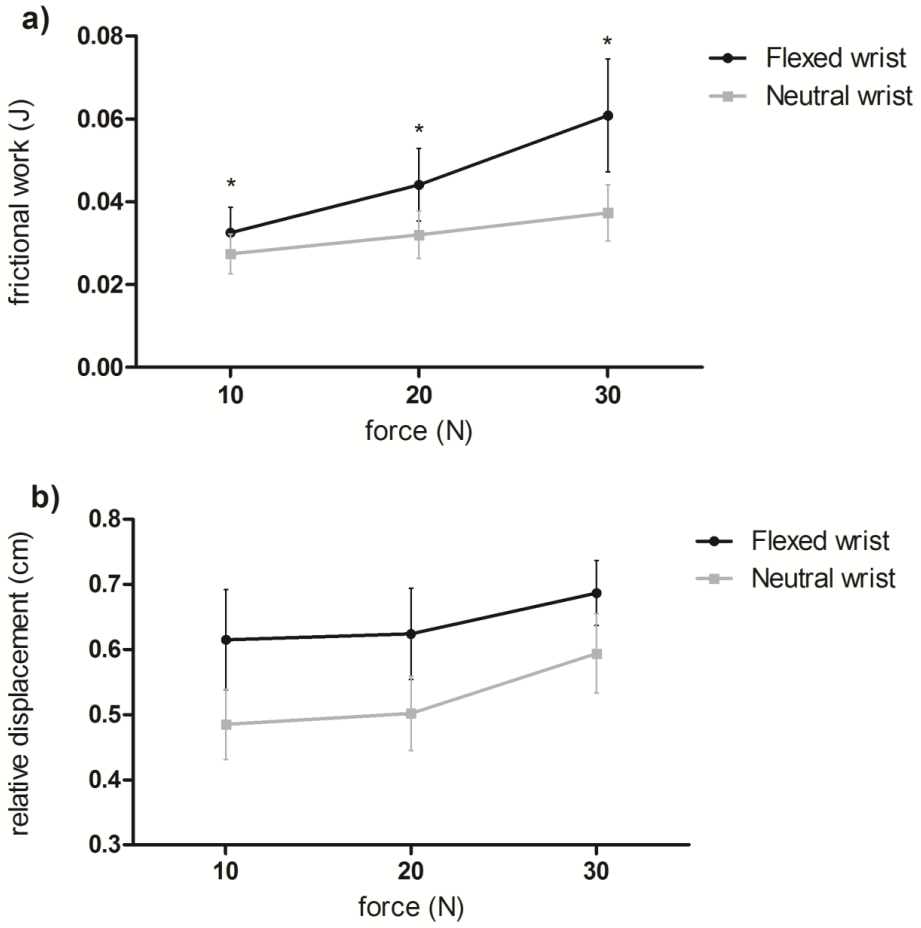

Figure 3.4 The posture and force relationship is multiplicative in (a) frictional work and independent in (b) relative displacement. The error bars represent one standard deviation. * denotes significant differences between all force levels ($p<0.05$).

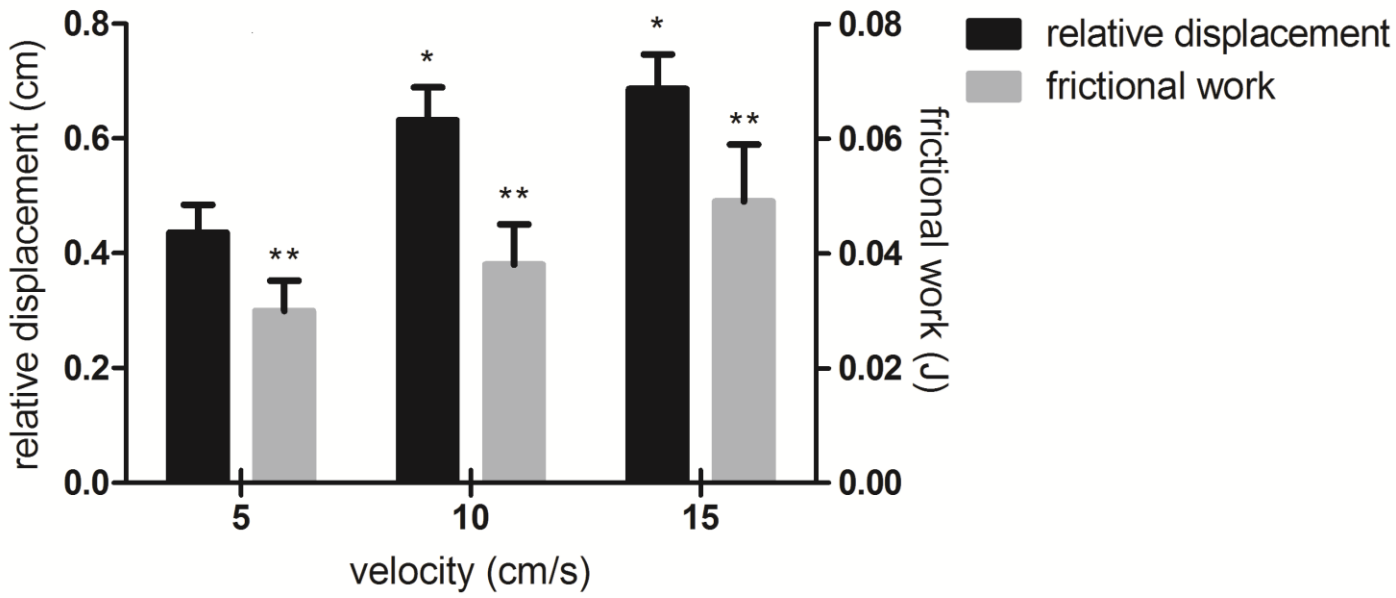

Figure 3.5 Velocity main effects for both mechanical shear and ultrasound shear. The error bars indicate one standard deviation. *denotes significantly different from 5 cm/s in relative displacement ($p<0.05$). ** represents significant difference between all velocities in frictional work ($p<0.05$).

3.5 Discussion

This study compared mechanical shear and what has been termed "ultrasound shear," with respect to the tendons in the carpal tunnel. We found that a mechanical assessment of frictional work using direct tendon force and displacement measurements in cadavers differed from "ultrasound shear" determined from relative motion of the flexor tendon and SSCT. A significant posture × force interaction was observed for frictional work that was not found for relative displacement. This phenomenon may be a result of the flexor tendons moving palmarly with wrist flexion, thus increasing contact stress against the transverse carpal ligament (TCL) and adjacent SSCT from neighbouring tendons.[29,30] Our study captured this effect with frictional work, and found higher tendon shear in a flexed wrist posture, especially with high tendon force. However, since wrist posture and tendon force had independent main effects with our ultrasound based measures, it appears that relative displacement (from ultrasonography) does not adequately represent shear from surface frictional sources (TCL or adjacent SSCT). Figure 3.6 shows the relationship between frictional work and ultrasound, and highlights the dissociation between the two measurements of shear in a flexed wrist owing to greater surface friction. However, we found that ultrasound did successfully capture the viscoelastic component of FDS tendon shear (stretch of the SSCT) due to independent velocity effects found in both ultrasound and direct mechanical tendon shear.

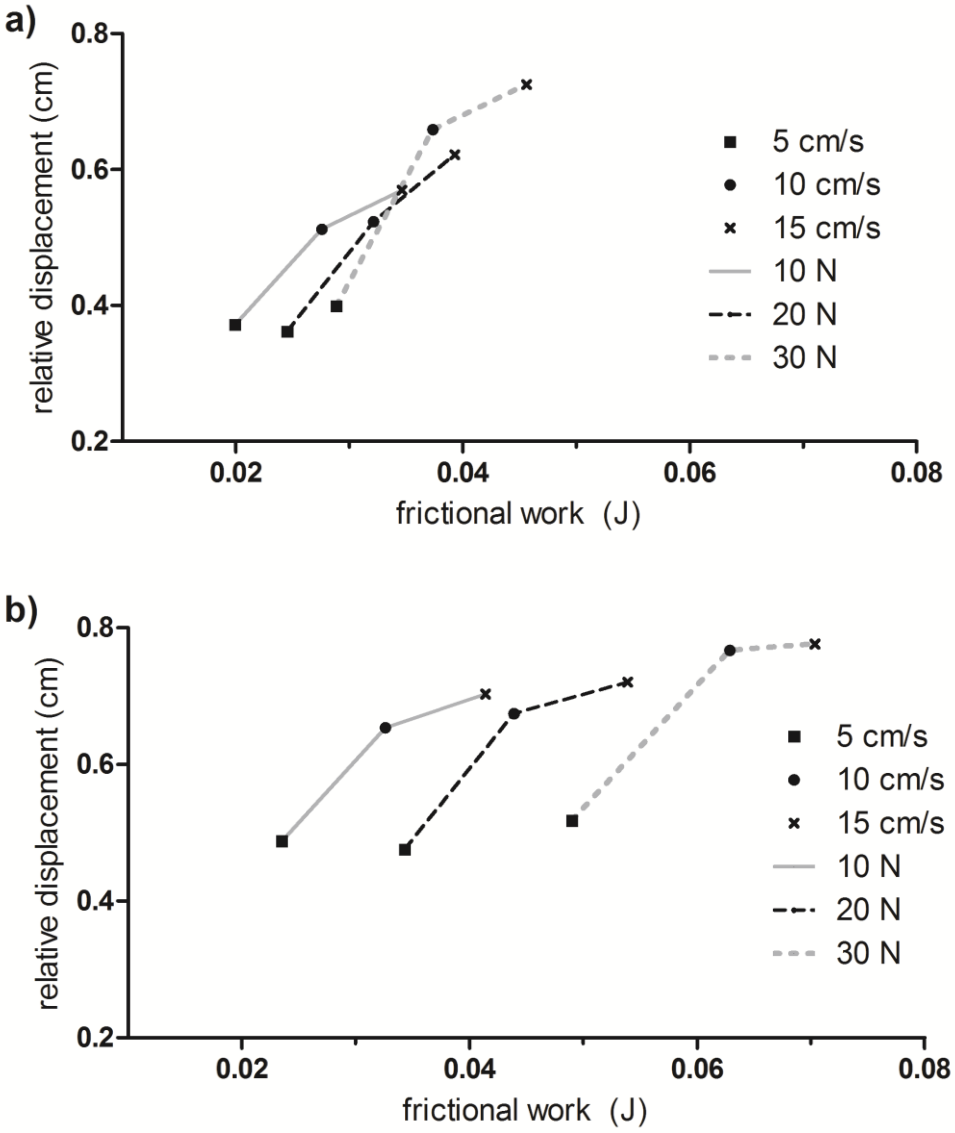

Figure 3.6 The relationship between ultrasound shear and frictional work was greatly affected by the posture and force interaction. A strong positive association was found in the (a) neutral wrist posture, where we expect the viscoelastic component of tendon shear to predominate. But in a (b) flexed wrist, there are also significant contributions from surface frictional sources resulting in a multiplicative force effect seen as 3 distinct force curves.

The unique gliding mechanism of the SSCT is well documented during tendon motion,[10,26,31] and includes the viscoelastic behaviour of the SSCT that was evident in our curvilinear motor excursion profiles (Figure 3.3). We used assessments of tendon velocity to further examine the viscoelastic resistance in tendon shear as strain rate in viscoelastic structures should be velocity-dependent and surface friction between two adjacent structures should be velocity-independent. Using ultrasound, we observed smaller longitudinal excursions of the SSCT at higher FDS tendon velocities that lead to increased relative displacement. These velocity-dependent increases were also found in tendon frictional work, producing similar effect sizes for frictional work (η_p^2=0.937) and relative displacement (η_p^2=0.862). Our findings indicate the two measurements of shear captured similar velocity effects that may reflect a viscous element invoked with stretching of the SSCT during tendon motion. Tendon velocity also accounted for the greatest proportion of variance of all the tested risk factors, which signifies that viscoelastic resistance is a large component of tendon shear.

This was the first study to evaluate the effect of tendon force on relative tendon displacement. While many studies have investigated the effect of force on tendon frictional work from a computational approach,[7,19,30] there is little research on the SSCT. Goldstein et al[32] tested deformation of the tendon using different loads by repetitively loading a cadaveric tendon. Larger forces were associated with greater tendon strain. We would expect even greater strain in the SSCT in response to force considering its viscoelastic properties.[33] At higher tendon forces, more force would be transferred to the SSCT, and we suggest this may increase elastic strain in the fibrils interconnecting layers

of the SSCT and increase viscoelastic resistance. This may explain our small, but consistent, decrease in SSCT displacement at 30 N.

Our frictional work findings are consistent with epidemiological studies that have shown a multiplicative increase in CTS risk with biomechanical risk factors.[7-9,34] The current significant wrist posture × tendon force interaction provides a mechanistic explanation for previous evidence that combined awkward wrist posture and high tendon force are strongly associated with workplace injury risk, while awkward wrist posture alone represents a lower risk. When evaluated using ultrasound, each risk factor had an independent and additive effect. This independent response to posture, velocity, and force may be explained by noting that ultrasound "shear" appears to reflect only viscoelastic effects and not the overall contributions of viscoelastic and surface (Newtonian) friction. This study highlights the positive relationship between relative displacement and viscoelastic shear strain, which may prove to be clinically useful in assessing the risk of shear injury.

In a previous study, we found that prolonged repetitive finger flexion-extension exhibited a dose-response relationship, with an increase in tendon-SSCT relative motion throughout the task, and even more so with single finger motion as was examined in the current study.[14] The current study further suggests that relative motion would increase at higher tendon velocities (high velocities are associated with highly repetitive tasks), thus increasing loading (and work done) on the surrounding SSCT, which may in turn lead to injury. The impact of these influencing factors underscores the role of task duration in

highly repetitive and forceful finger actions in the development of shear injury leading to pathological fibrosis.

The ability to non-invasively measure viscoelastic shear strain with ultrasound has important clinical applications. Assessment of relative displacement between the tendon, SSCT and surrounding tissues can provide insight into the health of the SSCT, which is relevant to the pathology of CTS. Large viscoelastic resistance during tendon motion may indicate pathological fibrosis, a disruption in SSCT interconnections, and/or impaired SSCT gliding function that all may be useful for the diagnosis of disease presence and severity. We intend to explore the diagnostic utility of ultrasound shear in a future study by assessing the progression of viscoelastic shear strain damage in patients with varying severity of CTS.

There were a few limitations to this study. Our findings suggest that ultrasound shear primarily reflects the viscoelastic component of tendon shear; however, we were unable to isolate contributions from surface friction between adjacent structures (e.g. bursa, SSCT layers, transverse carpal ligament) and viscoelastic stretch (SSCT fibrils). Thus, we used tendon velocity to infer the viscoelastic properties and operated in a tendon excursion range that has previously reported damage to the interconnections of the SSCT.[13,33] Since tissue damage was likely to occur with repetitive tendon loading in a cadaver, we controlled for order effects by block randomizing the test conditions and performed preconditioning movement cycles (30 flexion-extension cycles) prior to data collection.

Assessment of "shear" with ultrasound is a measure of relative displacement between the tendon and SSCT rather than mechanical flexor tendon shear. It captures the viscoelastic resistance associated with stretching the SSCT during tendon excursion and does not adequately represent surface friction with neighbouring anatomical structures in the carpal tunnel. We also found that relative tendon-SSCT motion responded independently to wrist posture, tendon velocity, and tendon force; unlike tendon frictional work that showed a multiplicative effect, specifically between wrist posture and tendon force. While ultrasound measures do not capture all aspects of mechanical shear, they do provide important mechanistic information with clinical implications in understanding the role of viscoelastic shear strain injury in the etiology of carpal tunnel syndrome.

3.6 Acknowledgements

This study was supported by funding from the Natural Sciences and Engineering Research Council Discovery Grant (# 217382-09). We would like to thank Bruce Wainman, Glen Oomen, and the Education Program in Anatomy at McMaster University for their assistance in the preparation of cadaver specimens.

3.7 References

1. Barr, A.E., Barbe, M.F., & Clark, B.D., 2004. Work-related musculoskeletal disorders of the hand and wrist: Epidemiology, pathophysiology, and sensorimotor changes. *Journal of Orthopaedic and Sports Physical Therapy*, 34 (10), 610-27.

2. Zakaria, D., Robertson, J., Koval, J., MacDermid, J., & Hartford, K., 2004. Rates of claims for cumulative trauma disorder of the upper extremity in Ontario workers during 1997. *Chronic Diseases in Canada*, 25 (1), 22-31.

3. Tanaka, S., Petersen, M., & Cameron, L., 2001. Prevelance and risk factors of tendinitis and related disorders of the distal upper extremity among US workers. *American Journal of Industrial Medicine*, 39 (3), 328-335.

4. Manktelow, R.T., Binhammer, P., Tomat, L.R., Bril, V., & Szalai, J.P., 2004. Carpal tunnel syndrome: Cross-sectional and outcome study in Ontario workers. *Journal of Hand Surgery*, 29A (2), 307-317.

5. Feuerstein, M., Burrell, L.M., Miller, V.I., Lincoln, A., Huang, G.D., & Berger, R., 1999. Clinical management of carpal tunnel syndrome: a 12-year review of outcomes. *American Journal of Industrial Medicine*, 35 (3), 232-245.

6. Bernard, B.P., 1997. *Musculoskeletal disorders and workplace factors: A critical review of epidemiologic evidence for work-related musculoskeletal disorders of the neck, upper extremity, and low back (Publication # 97-141).* Cincinnati, OH: National Institute for Occupational Safety and Health (Department of Health and Human Services).

7. Schoenmarklin, R.W., Marras, W.S., & Leurgans. S.E., 1994. Industrial wrist motions and incidence of hand/wrist cumulative trauma disorders. *Ergonomics*, 37 (9), 1449-1459.

8. Chiang, H.C., Ko, Y.C., Chen, S.S., & Yu, H.S., 1993. Prevalence of shoulder and upper-limb disorders among workers in the fish-processing industry. *Scandinavian Journal of Work and Environmental Health*, 19 (2), 126-131.

9. Silverstein, B.A., Fine, L.J., & Armstrong, T.J., 1987. Occupational factors and the carpal tunnel syndrome. *American Journal of Industrial Medicine*, 11 (3), 343-358.

10. Ettema, A.M., Amadio, P.C., Zhao, C., Wold, L. E., O'Byrne, M.M., Moran, S.L., An, K.A., 2006. Changes in the functional structure of the tenosynovium in idiopathic carpal tunnel syndrome: A scanning electron microscope study. *Plastic and Reconstructive Surgery*, 118 (6), 1413-1422.

11. Jinrok, O., Zhao, C., Amadio, P.C., An, K.N., Zobitz, M.E., Wold, L.E., 2004. Vascular pathological changes in the flexor tenosynovium (subsynovial connective tissue) in idiopathic carpal tunnel syndrome. *Journal of Orthopaedic Research*, 22 (6), 1310-1315.

12. Ettema, A.M., An, K.N., Zhao, C., O'Byrne, M.M., & Amadio, P.C., 2008. Flexor tendon and synovial gliding during simultaneous and single digit flexion in idiopathic carpal tunnel syndrome. *Journal of Biomechanics*, 41 (2), 292-298.

13. Vanhees, M., Morizaki, Y., Thoreson, A.R., Larson, D., Zhao, C., An, K.A., & Amadio, P.C., 2012. The effect of displacement on the mechanical properties of human cadaver subsynovial connective tissue. *Journal of Orthopaedic Research*, 30 (11), 1732-1737.

14. Tat, J., Kociolek, A.M., & Keir, P.J. 2013. Repetitive differential motion increases shear strain between the flexor tendon and subsynovial connective tissue. *Journal of Orthopaedic Research*, 31 (10), 1533-1539.

15. Yoshii, Y., Zhao, C., Henderson, J., Zhao, K.D., An, K.N., & Amadio, P.C., 2011. Velocity dependent changes in the relative motion of the subsynovial connective tissue in the human carpal tunnel. *Journal of Orthopaedic Research*, 29 (1), 62-66.

16. Yoshii, Y., Zhao, C., Henderson, J., Zhao, K.D., An, K.N., & Amadio, P.C.,2009. Shear strain and motion of the subsynovial connective tissue and median nerve during single digit motion. *Journal of Hand Surgery*, 34 (1), 65-79.

17. Yoshii, Y., Zhao, C., Zhao, K.D., Zobitz, M.E., An, K.N., & Amadio, P.C., 2008. The effect of wrist position on the relative motion of tendon, nerve, and subsynovial connective tissue within the carpal tunnel in a human cadaver model. *Journal of Orthopaedic Research*, 26 (8), 1153-1158.

18. Tanaka, S., & McGlothlin, J.D., 1993. A conceptual quantitative model for prevention of work-related carpal tunnel syndrome (CTS). *International Journal of Industrial Ergonomics*, 11 (3), 181-193.

19. Moore, A., Wells, R., & Ranney, D., 1991. Quantifying exposure in occupational manual tasks with cumulative trauma disorder potential. *Ergonomics*, 34 (12), 1433-1453.

20. Kociolek, A.M. Tat, J., & Keir, P.J. (July, 2014). Finger flexor tendon frictional work increases with tendon velocity and force. In proceedings of the 7th World Congress of Biomechanics, Boston, MA.

21. Schuind, F., Garcia-Elias, M., Cooney III, W.P., An, K.N. 1992. Flexor tendon forces: in vivo measurements. *Journal of Hand Surgery*, 17 (2), 291- 298.

22. Uchiyama, S., Coert, J.H., Berglund, L., Amadio, P.C., & An, K.N., 1995. Method for the measurement of friction between tendon and pulley. *Journal of Orthopaedic Research*, 13 (1), 83-89.

23. Brand, P. W., & Hollister, A. (1993). Clinical mechanics of the hand, Mosby Year Book.

24. An, K.N., Ueba, Y., Chao, W., Cooney, W.P., & Linscheid, R.L., 1983. Tendon excursion and moment arm of index finger muscles. *Journal of Biomechanics*, 16 (6), 419-425.

25. Dennerlein, J.T., 2005. Finger flexor tendon forces are a complex function of finger joint motions and fingertip forces. *Journal of Hand Therapy*, 18 (2), 120-127.

26. Tat, J., Kociolek, A.M., & Keir, P.J.. 2014. Validation of colour Doppler ultrasonography for evaluating relative displacement between flexor tendon and

subsynovial connective tissue. Accepted to the *Journal of Ultrasound in Medicine* on July 22, 2014.

27. Oh, S., Belohlavek, M., Zhao, C., Osamura, N., Zobitz, M.E., & An, K., 2007. Detection of differential gliding characteristics of the flexor digitorum superficialis tendon and subsynovial connective tissue using colour Doppler sonographic imaging. *Journal of Ultrasound Medicine*, 26 (2), 149-155.

28. Hendersen, J., Thoreson, A., Yoshii, Y., Zhao, K.D., Amadio, P.C., An, K.A., 2011. Finite element model of the subsynovial connective tissue deformation due to tendon excursion in the human carpal tunnel. *Journal of Biomechanics*, 44 (1), 150-155.

29. An, K.N., 2007. Tendon excursion and gliding: Clinical impacts from humble concepts. *Journal of biomechanics*, 40 (4), 713-718.

30. Armstrong, T.J., & Chaffin, D.B., 1978. An investigation of the relationship between displacements of the finger and wrist joints and the extrinsic finger flexor tendons. *Journal of Biomechanics*, 11 (3), 119-128.

31. Guimberteau, J.C., Delage, J.P., McGrouther, D.A., & Wong, J.K.F., 2010. The microvacuolar system: how connective tissue sliding works. *The Journal of Hand Surgery*, 35 (8), 614-622.

32. Goldstein, S.A., Armstrong, T.J., Chaffin, D.B., & Matthews, L.S., 1987. Analysis of cumulative strain in tendons and tendon sheaths. *Journal of Biomechanics*, 20 (1), 1-6.

33. Osamura, N., Zhao, C., Zobitz, M.E., An, K.N., & Amadio, P.C., 2007. Evaluation of the material properties of the subsynovial connective tissue in carpal tunnel syndrome. *Clinical Biomechanics*, 22 (9), 999-1003.

34. Hagberg, M., Morgenstern, H., & Kelsh, M., 1992. Impact of occupations and job tasks on the prevalence of carpal tunnel syndrome. *Scandinavian Journal of Work and Environmental Health*, 18 (6), 337-345.

CHAPTER 4

PATHOLOGICAL CHANGES IN THE SUBSYNOVIAL CONNECTIVE TISSUE INCREASES WITH SEVERITY OF CARPAL TUNNEL SYNDROME SYMPTOMS

Jimmy Tat, BSc, Katherine E. Wilson, MSc, Peter J. Keir, PhD*

Occupational Biomechanics Laboratory, Department of Kinesiology, McMaster University, Hamilton, ON, Canada, L8S 4K1

*Corresponding Author:

Peter J. Keir, PhD
McMaster University
Department of Kinesiology
Ivor Wynne Centre, Room 212
1280 Main Street West
Hamilton, ON, Canada, L8S 4K1
Telephone: 905-525-9140 ext. 23543
Email: pjkeir@mcmaster.ca

To be submitted to: *Clinical Biomechanics*

Type: Original Contribution

4.1 Abstract

Fibrosis and thickening of the subysnovial connective tissue (SSCT) are the most common pathological findings in carpal tunnel syndrome (CTS). The relationship between SSCT motion and CTS severity was assessed in CTS symptomatics (N=11) and healthy controls (N=11). Participants were categorized as symptomatic based on a positive score with the Boston Carpal Tunnel Questionnaire and Katz hand diagram, while controls indicated no symptoms. Using ultrasound, SSCT pathology was inferred from SSCT thickness (thickness ratio, SSCT thickness / tendon thickness) and fibrosis with altered gliding function (shear strain index, $(D_{tendon}-D_{SSCT}) / D_{tendon}$). To assess gliding function, participants performed 10 repeated flexion-extension cycles of the long finger at a rate of one cycle per second. CTS symptomatics had a 38.5% greater thickness ratio and 39.2% greater shear strain index compared to healthy participants ($p<0.05$). We found a positive association between SSCT pathology and clinical symptom severity (thickness ratio, $r=0.52$, $p<0.05$; shear strain index, $r=0.56$, $p<0.05$). These findings suggest progressive thickening and fibrosis of the SSCT in CTS etiology. Additionally, our high frequency motion protocol successfully discriminated between symptom severity using CTS symptomatics with relatively low severity, indicating SSCT assessments may be useful in the early detection of CTS.

Keywords: carpal tunnel syndrome, ultrasound, subsynovial connective tissue, carpal tunnel syndrome questionnaire, hand diagram

4.2 Introduction

Carpal tunnel syndrome (CTS) is the most frequently reported peripheral neuropathy. It is characterized by pain, paresthesia or weakness in regions innervated by the median nerve. The diagnosis of CTS can include a combination of physical examination, patient history for signs and symptoms, and electrodiagnostic tests (nerve conduction studies or needle electromyography). Clinicians frequently use electrodiagnostic tests for objective assessment of the pathophysiology by measuring motor and sensory nerve conduction velocities to determine neurological impairment (reduced velocity indicates damage) (Rempel et al. 1998). However, nerve conduction velocities can be affected by testing parameters such as electrode size, inter-electrode distance, amplifier gain, and tissue temperature (Jordan et al. 2002). Additionally, diagnoses involve comparing conduction velocities to normative values that are not well standardized (Rempel et al. 1998). These factors may account for the variable sensitivity in electrodiagnostic tests, leading to false negatives in the range of 49% to 84%, and suggests the need for additional tests to aid in the diagnosis of CTS (Jordan et al. 2002). With false negatives, an accurate and comprehensive clinical history becomes even more important.

While there is no single best way to assess CTS symptom characteristics, the Boston Carpal Tunnel Questionnaire (BCTQ) and Katz hand diagram are established techniques. The BCTQ is a self-administered survey that provides information on the severity of symptoms and functional status (Levine et al. 1993). It has excellent reproducibility, responsiveness, and internal consistency (Levine et al. 1993). The Katz

hand diagram is also useful as it allows patients to visually document the location of symptoms, specifically those that are relevant to the median nerve innervations, with high reproducibility, sensitivity and specificity (Katz & Stirrat, 1990). These tests are pragmatic for clinical practice as they are non-invasive and easily-administered. However, questionnaires alone are inadequate to diagnose CTS since self-reported symptoms can be subjective and do not provide detail on the etiology of the nerve or surrounding tissue (Jablecki et al. 1993).

Alternatively, ultrasound can be used to examine structures in the carpal tunnel including the median nerve and surrounding tissue. Recent advances in ultrasound resolution have also led to new findings including fibrosis and thickening of the surrounding tissue called the subsynovial connective tissue (SSCT) that have become a common pathological finding in CTS patients (van Doesburg et al. 2012a; Ettema et al. 2006). The SSCT is composed of layers of collagen bundles that are interconnected by perpendicular fibres, which mediate motion between the flexor tendons and median nerve. Pathological changes can impair the gliding function of the SSCT resulting in reduced SSCT excursions. Ultrasound-based measurements of SSCT excursions were used in a recent study to predict the most affected hand in CTS patients, resulting in high accuracy rates of 87% (Korstanje et al. 2012). The diagnostic application of evaluating SSCT motion is novel and demonstrates great potential for future research.

The precise etiology of SSCT fibrosis and thickening remains unclear; however, many studies indicate that excessive shear forces between the SSCT and adjacent structures (tendon and nerve) stretch the SSCT fibrils beyond their elastic limits and

break the interconnections resulting in "shear injury" (Vanhees et al. 2012; Ettema et al. 2008). This shear injury can occur with finger motions that cause large differential motion between the tendon and SSCT and/or nerve and SSCT. Epidemiological studies are consistent in showing a link between hand and finger motion, especially with high repetition and long duration, and CTS (Moore et al. 1990; Silverstein et al. 1987). We hypothesize that SSCT injury accumulates with the etiological progression of CTS severity such that fibrosis and thickness increases; however, this has yet to be investigated.

Ultrasound has the ability to detect small morphological and functional changes in the SSCT. This study used ultrasound to evaluate SSCT thickness and compare SSCT mechanics in CTS symptomatics and controls using a high frequency, repetitive finger task. Thickness and relative motion were used to infer pathological changes associated with thickening and fibrosis of the SSCT. We explored the relationship between SSCT pathology and severity of CTS using the BCTQ and Katz hand diagram. A better understanding of the progression of SSCT fibrosis and thickening can advance our knowledge of the etiology of CTS with implications in improving its diagnosis.

4.3 Methods

4.3.1 Participants

Eleven healthy participants (9 women and 2 men) with a mean age (± standard deviation) of 26.2 ± 3.1 years and eleven CTS symptomatic participants (9 women and 2 men) with a mean age of 41.5 ± 13.1 years volunteered for this study. Each participant

was screened for musculoskeletal disorders of the hand and wrist using an exclusion questionnaire for previous wrist surgery, radial malunion, colles fracture, bifid median nerve, degenerative joint disease, arthritis of the wrist/hand, gout, hemodialysis, sarcoidosis, amyloidosis, hypothyroidism, and diabetes mellitus. Informed consent was obtained prior to participation. The study was approved by the Hamilton Health Sciences and McMaster Health Sciences Research Ethics Board.

All participants completed the Boston Carpal Tunnel Questionnaire (BCTQ) and Katz hand diagram to assess CTS severity. The BCTQ consists of a symptom severity and a functional status evaluation (Levine et al. 1993). Symptom severity is assessed using multiple choice questions related to classic CTS symptoms (pain, paraesthesia, numbness, weakness, and nocturnal symptoms) on a 5-point scale (0-4 points). Functional status assessed the self-reported level of difficulty in performing daily tasks (writing, buttoning, gripping, opening, bathing, dressing) using the same scoring. The Katz hand diagram documents the distribution of symptoms (pain, tingling, numbness, decreased sensation) on the hand and forearm scored from 0 to 3 based on the location and type of symptoms relevant to median nerve compression (Katz and Stirrat, 1990). Participants were categorized into the CTS symptomatic and control groups based on scores from the BCTQ and Katz hand diagram. CTS symptomatics had a positive score on at least one of the severity questionnaires (BCTQ symptom severity, BCTQ functional status, and Katz hand diagram), while the control group scored 0 on all questionnaires indicating no clinical symptoms (Table 4.1). For all of our severity questionnaires, higher scores indicated greater severity of disease.

Table 4.1 Population characteristics and severity questionnaire scores (Katz hand diagram, BCTQ symptom severity, BCTQ functional status) for the CTS symptomatic and control groups with means (ranges). BCTQ indicates the Boston Carpal Tunnel Questionnaire.

	Control (N=11)	CTS symptomatic (N=11)
Age (yr)	26 (23-32)	42 (19-55)
Gender	2 Males, 9 Females	2 Males, 9 Females
Katz diagram (0-3 points)	0	1.2 (0-3)
BCTQ symptom severity (0-4 points)	0	1.9 (1-3.6)
BCTQ functional status (0-4 points)	0	1.3 (0-2.9)

4.3.2 Motion Protocol

Participants performed repeated flexion-extension cycles of the long finger (Figure 4.1) (Tat et al. 2013). Participants were seated with the forearm immobilized in supination to position the ultrasound probe on the palmar surface of the wrist. The hand was supported by padding, to maintain the wrist in a neutral posture while grasping a polyvinyl chloride tube (3.5 cm diameter). To isolate motion of the long finger, the tube was sectioned in the middle to fix all other fingers in a mid-flexed posture. The tube and padding provided physical end ranges to the finger motion and represented full finger flexion. Participants performed the finger motion continuously at a rate of 1 Hz for 10 s (10 flexion and 10 extension movements) in 3 trials. The frequency of finger movement fit the definition for highly repetitive work (Silverstein et al. 1987). A metronome indicated the start of each cycle and the transition between flexion and extension movements. Maximum flexion was defined as the pulp of the distal phalanx contacting the tube, while maximum extension was defined as the finger nail touching the table surface. Maximum flexion occurred at approximately 90º of flexion at both the MCP and PIP joints, representing a tendon excursion of 20-30 mm based on a geometric model (An et al. 1983).

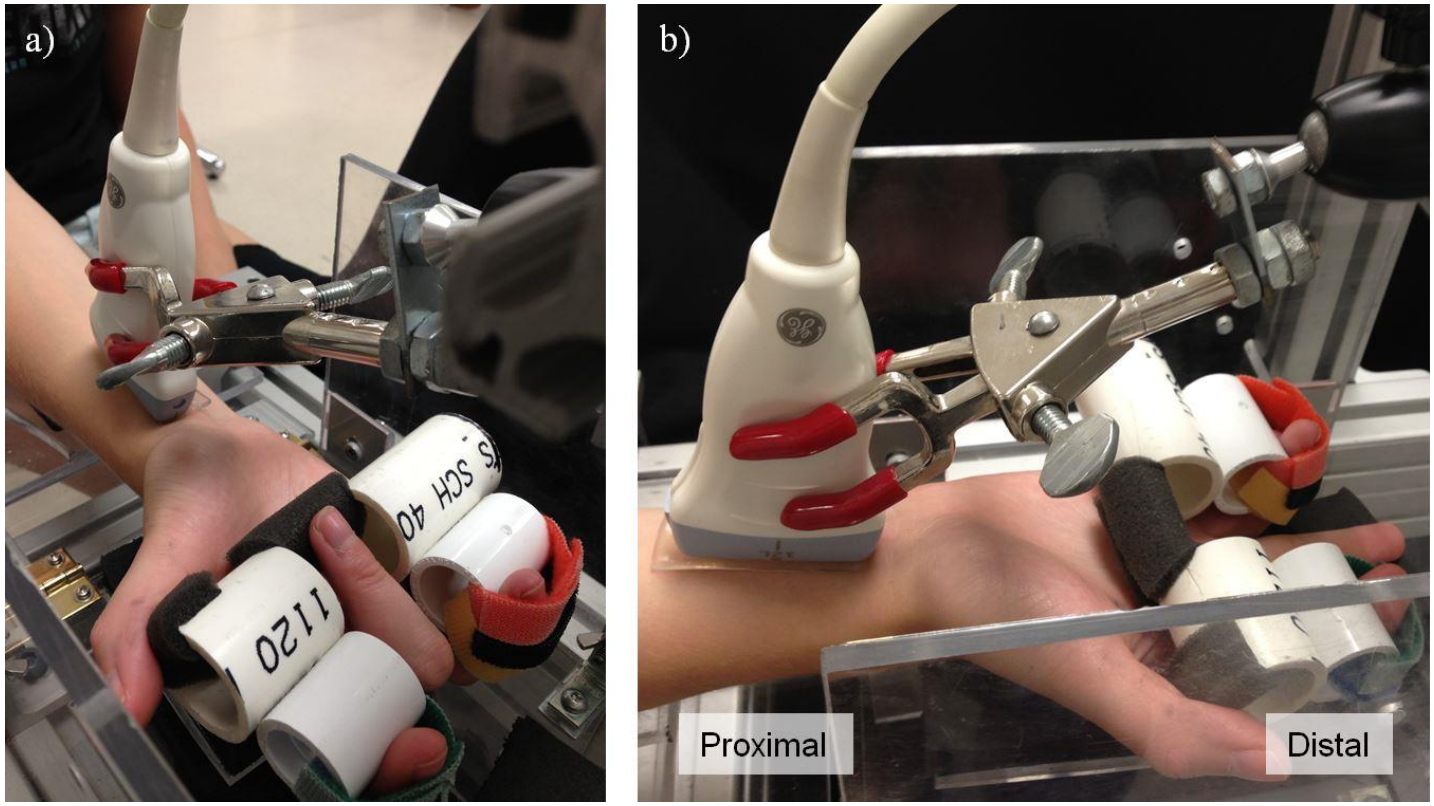

Figure 4.1 Testing apparatus. Movement end range for finger (a) flexion and (b) extension of the middle finger alone.

4.3.3 Ultrasound Assessment

A Vivid q BT10 (GE Healthcare, Milwaukee, WI, USA) console and a linear array transducer (12LRS) operating at a central frequency of 12 MHz were used to image the carpal tunnel in each participant. The SSCT associated with the middle flexor digitorum superficialis tendon was assessed. The transducer was positioned at the proximal wrist crease such that it was longitudinal and in line with the tendon. Participants were asked to perform active finger flexion and extensions to identify the tendon.

High resolution grayscale images were collected while the finger was in extension and uploaded to ImageJ software (National Institutes of Health, Bethesda, MD) to perform SSCT thickness measurements. Tendon thickness was measured perpendicular to the tendon fibre direction, and SSCT thickness was measured similarly adjacent to the tendon (Figure 4.2). We inferred SSCT fibrosis as altered tendon-SSCT gliding function, as fibrosis can only be determined through biopsy and histological examination. We used differential motion between the tendon-SSCT to represent the state of the SSCT interconnections (Ettema et al. 2008). Greater differential motion represented increased damage to the SSCT interconnections and greater fibrosis (Ettema et al. 2008). A dynamic assessment with colour Doppler ultrasound was used to measure differential motion between the tendon and SSCT. The colour Doppler technique has previously been validated for tendon excursion measurements in the carpal tunnel (Tat et al. 2014a; Oh et al. 2007). We used sonographic settings similar to Tat et al. (2014a) including a depth of 3.0 cm, 11.0 cm/s scale, frame rate of 29.5 frames/s, and a 20^{o} beam steer angle

that was augmented with a custom gel wedge (Aquaflex Gel Pad, Cone Instruments, Solon, OH).

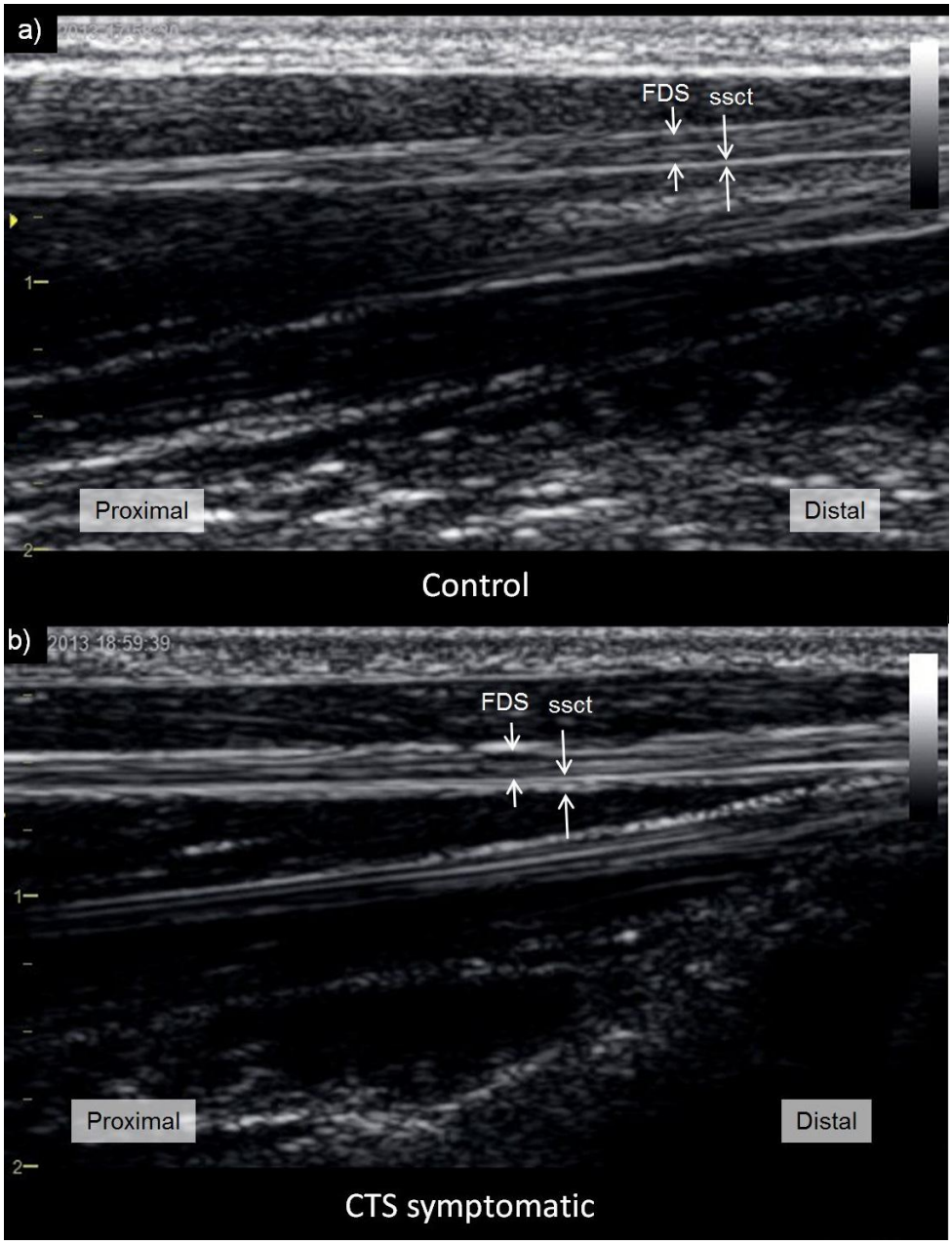

Figure 4.2 Thickness measurement. 2D grayscale echogram of the carpal tunnel at the proximal wrist crease for (a) a healthy control and (b) a CTS symptomatic patient. A pair of arrows indicates the FDS tendon (fibrillar striations) and the SSCT (hypoechoic band) structures. The thickness was measured as the distance between these arrows, oriented perpendicular to the fibre direction.

4.3.4 Data Analysis

Tendon excursions during the dynamic finger motion were captured with ultrasound colour maps. These colour maps overlaid the grayscale depiction of the tendon and SSCT and provided velocity profiles through the collected video. Dedicated analysis software (EchoPAC, GE Healthcare, Milwaukee, WI, USA) was used to extract tissue velocities in our offline analyses (Tat et al. 2014a). All sonographic measurements were performed by the same examiner, who was blinded to whether the participant was a patient or control. Three circular markers (0.5 mm diameter) were placed longitudinally along the long finger tendon (Figure 4.3). The markers represented a left, middle and right position on the colour map. We applied multiple markers to attenuate the effects of local imaging artifacts in our kinematic profiles. Three additional markers were placed adjacent to each tendon marker to represent the adjacent SSCT. The mean velocity profiles were low pass filtered at 4.0 Hz and corrected for the angle of insonation. Velocity was then integrated to obtain tissue displacement.

Ultrasound assessments included SSCT thickness and SSCT mechanics. SSCT thickness was represented as a thickness ratio (SSCT thickness / tendon thickness) to account for anthropometric differences between participants (van Doesburg et al. 2012a). Relative motion between the tendon and SSCT for flexion excursions were calculated using the shear strain index, SSI = (tendon displacement – SSCT displacement) / tendon displacement × 100% (Yoshii et al. 2008). The mean shear strain index for the 3 motion trials was calculated for each participant.

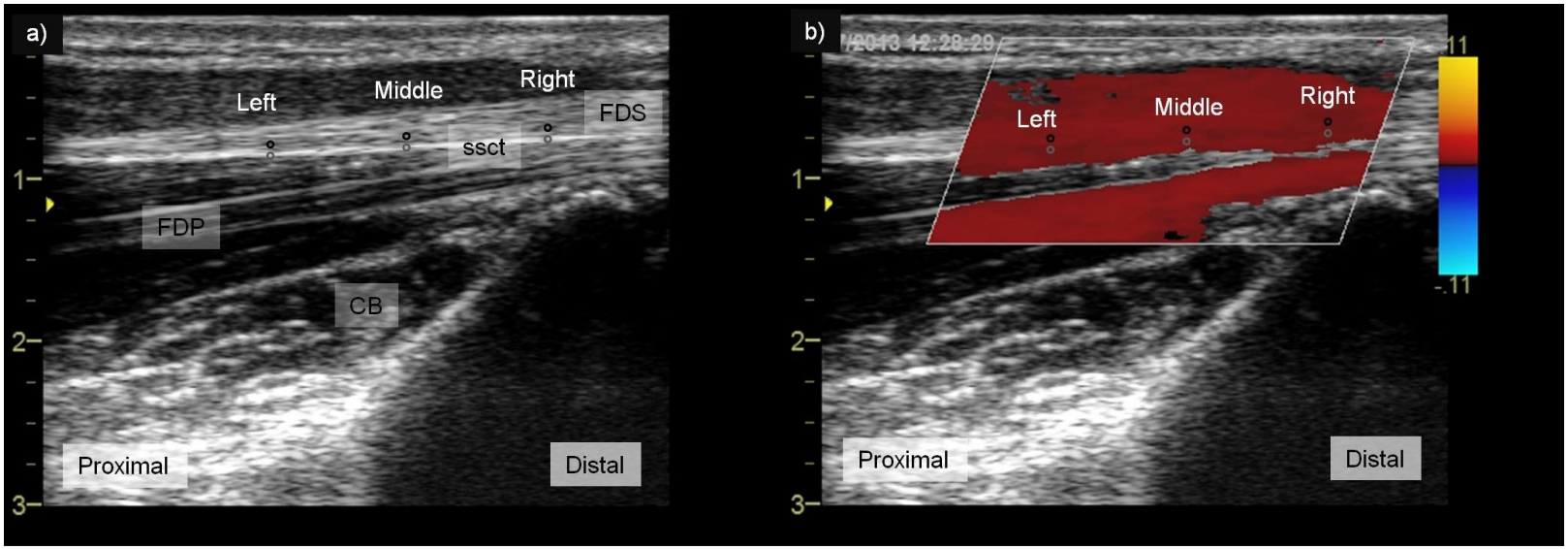
a)
Left
Middle
Right
FDS
ssct
FDP
CB
Proximal
Distal
b)
Left
Middle
Right
Proximal
Distal

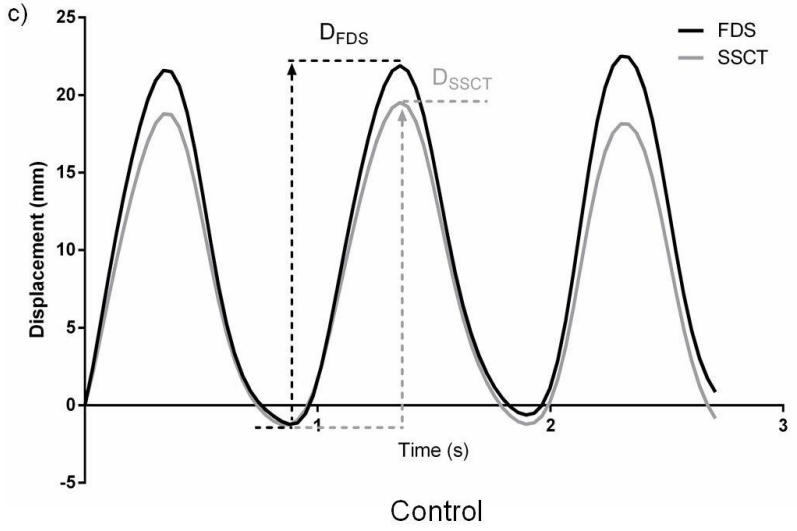
c)
D_{FDS}
D_{SSCT}
FDS
SSCT
Displacement (mm)
Time (s)
Control

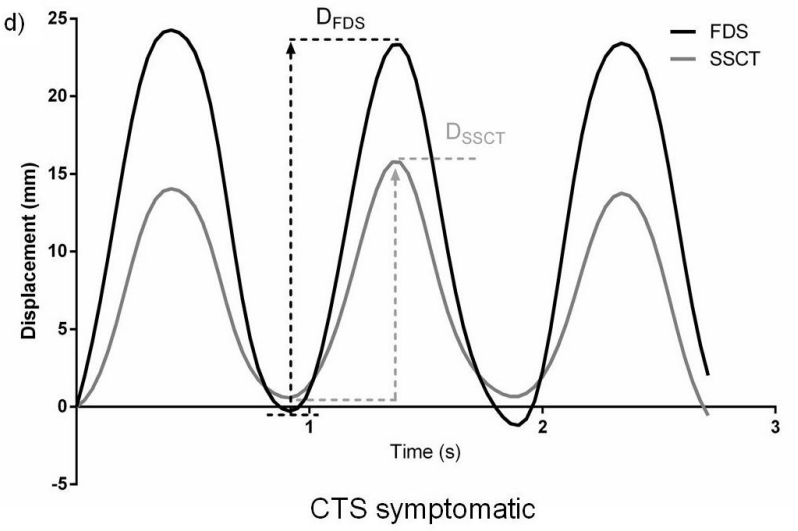
d)
D_{FDS}
D_{SSCT}
FDS
SSCT
Displacement (mm)
Time (s)
CTS symptomatic

Figure 4.3 Tendon-SSCT motion. A colour Doppler assessment measured relative motion between the tendon and SSCT for each participant. The (a) grayscale echograms identified the long finger tendon as a band of hypoechoic, fibrillar, striations that was bordered by a thin, hyperechoic SSCT layer (FDS, flexor digitorum superficialis tendon; SSCT, subsynovial connective tissue; FDP, flexor digitorum profundus tendon; CB, carpal bone). The grayscale echograms guided the placement of 6 markers over the tissue of interest and overlaying (b) colour maps. Pairs of markers were positioned at a left, middle, and right region of interest within the color maps, with each pair representing the tendon (black marker) and adjacent SSCT (gray marker) tissue velocities. The tissue velocities were integrated to obtain displacement profiles. Three cycles of flexion (positive deflection) and extension (negative deflection) are shown for (c) a control and (d) CTS symptomatic. The dashed arrows indicate the total tendon displacement (D_{FDS}) and associated SSCT displacement (D_{SSCT}) that was measured for a typical flexion excursion.

4.3.5 Statistical Analysis

An independent sampled t-test compared the ultrasound measurements (absolute and relative thickness, absolute and relative displacement) between the CTS symptomatic and control groups. A two-tailed Pearson correlation coefficient was used to assess the relationship between all clinical severity questionnaires and ultrasound measurements. Significance was set at a p-value <0.05 and all values were presented as means (standard deviations).

4.4 Results

The results of the ultrasound measures comparing the CTS symptomatics and controls are shown in Table 4.2. There was no difference between groups in the thickness of the FDS tendon ($p=0.38$) or FDS displacement during the dynamic task ($p=0.99$). However, we found significant group differences in the SSCT, which showed greater absolute thickness ($p<0.05$) and reduced displacement ($p<0.05$) in CTS symptomatics. The group differences in the SSCT measurements led to greater differences in the relative measures for CTS symptomatics compared to controls with 38.5% greater thickness ratios ($p<0.05$) and 39.2% larger shear strain indices (SSI) in symptomatics ($p<0.05$).

The Pearson correlation coefficients between the severity of clinical signs and symptoms and ultrasound measurements are presented in Table 4.3. The relative SSCT measurements for thickness and displacement were significantly associated with the symptom severity scores (Figure 4.4). The thickness ratio was positively associated with the BCTQ symptom severity and functional status scores, accounting for 27.4% and

18.9% of variance in the respective symptom scores ($p<0.05$). For SSCT mechanics, the SSI was also positively associated with severity scores from the Katz hand diagram and BCTQ symptom severity ($p<0.05$). SSI accounted for 19.3% of variance in the Katz hand diagram scores and 31.4% in the BCTQ symptom severity scores.

Table 4.2 Summary of ultrasound measurements (thickness and displacement) for the CTS symptomatic and control groups with means (ranges). * denotes a significant difference between the two groups based on t-tests ($p<0.05$). FDS represents the flexor digitorum superficialis tendon and SSCT is the subsynovial connective tissue.

Assessment	Group		
	Control (N=11)	CTS symptomatic (N=11)	p-value
Thickness			
FDS (mm)	1.4 (0.74-1.8)	1.2 (0.74-1.7)	0.38
SSCT (mm)	0.34 (0.22-0.45)	0.41 (0.25-0.56)	0.032*
Ratio	0.26 (0.19-0.33)	0.36 (0.24-.54)	0.006*
Displacement			
FDS (mm)	21.2 (15.9-25.9)	21.2 (17.1-25.1)	0.99
SSCT (mm)	16.7 (9.9-21.8)	14.8 (10.7-19.3)	0.18
Shear strain index (%)	21.7 (12.9-37.6)	30.2 (15.4-41.6)	0.016*

Table 4.3 Pearson correlation coefficients between severity questionnaires and all ultrasound measurements (N=22). * denotes significance at $p<0.05$. BCTQ is the Boston Carpal Tunnel Questionnaire, FDS is flexor digitorum superficialis tendon, SSCT is the subsynovial connective tissue, and SSI represents the shear strain index.

Clinical signs and symptoms		Thickness			Displacement		
		FDS	SSCT	Ratio	FDS	SSCT	SSI
Katz hand diagram	Correlation	-0.033	0.33	0.24	-0.15	0.16	0.44
	p-value	0.89	0.13	0.29	0.52	0.44	0.041*
BCTQ symptom severity	Correlation	-0.12	0.53	0.52	-0.005	0.33	0.56
	p-value	0.59	0.01*	0.01*	0.98	0.14	0.007*
BCTQ functional status	Correlation	-0.058	0.54	0.44	0.074	0.28	0.38
	p-value	0.79	0.01*	0.04*	0.74	0.2	0.083

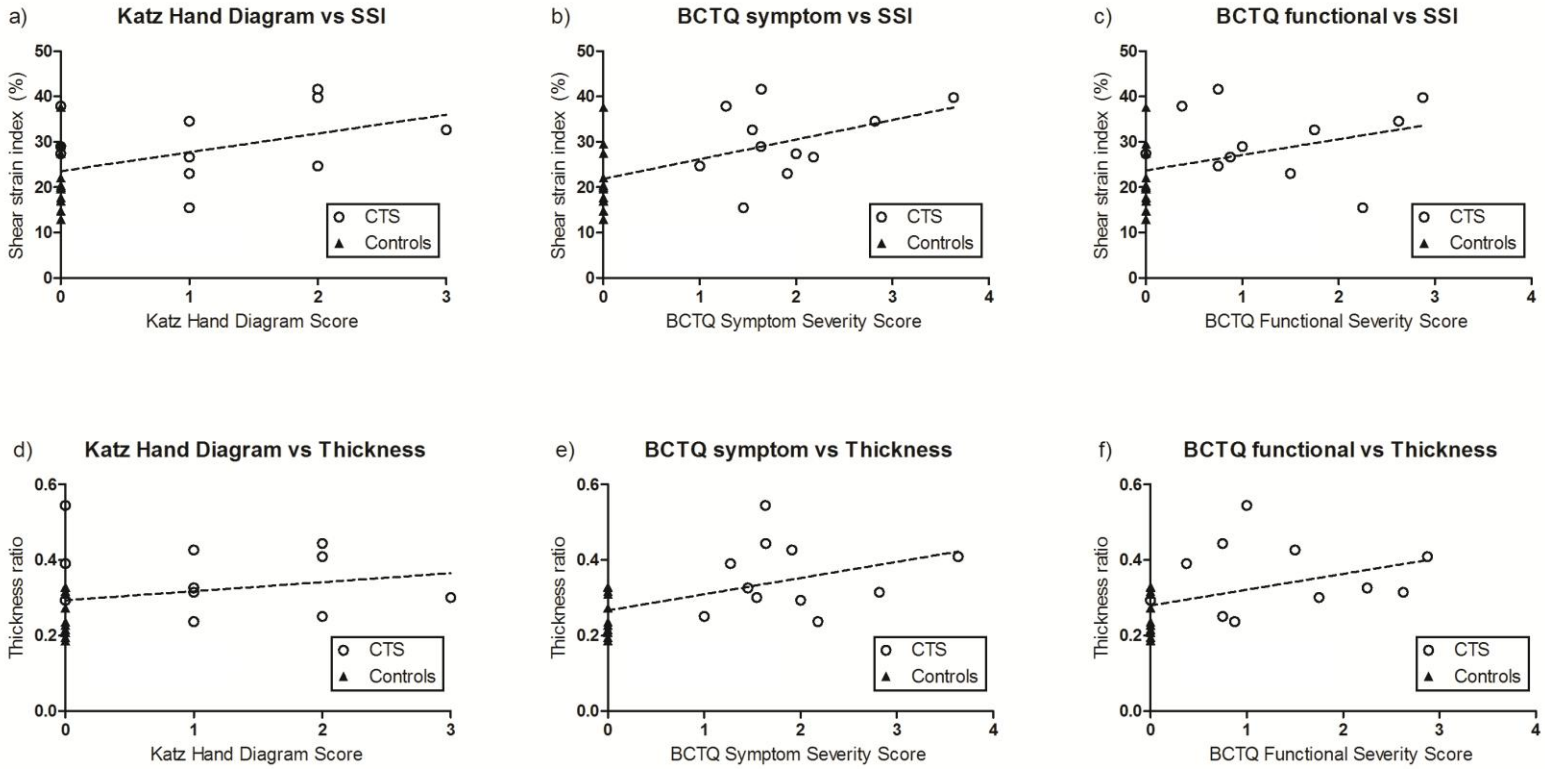

Figure 4.4 The relationships between symptom severity questionnaires (Katz hand diagram, Boston Carpal Tunnel Questionnaire symptom and functional scores) and ultrasound assessments. (a – c) Scatter plots for symptom severity scores versus shear strain index (SSI) are shown with lines of best fit. (d – f) Scatter plots for symptom severity scores versus thickness ratio with lines of best fit. Pearson correlations with significance of $p<0.05$ were achieved for scatter plots a,b,e,f.

4.5 Discussion

This study evaluated the relationship between CTS symptom severity and ultrasound measures of the SSCT. Ultrasound derived measures successfully distinguished healthy controls and CTS symptomatics using SSCT thickness and SSCT relative motion. These findings suggest pathological changes to the SSCT, including thickening and fibrosis, were present in our symptomatic group. Moreover, SSCT thickness and relative motion appear to progress with symptom severity. We found that controls exhibited the smallest thickness ratio and shear strain index, while symptomatic participants had larger relative thicknesses and shear strain indices, more so with more severe cases. This study provides a link between severity of CTS symptoms and SSCT morphology and mechanics that underscores the clinical relevance of the SSCT structure. Since we detected differences with ultrasound using a symptomatic group having low symptom severity, this suggests ultrasound may be useful for the early screening of CTS and could potentially assist electrodiagnostic tests in diagnosing false negatives. Nerve conduction velocities evaluate the function of large myelinated nerve fibres, which may not yet be affected in early stages (Koyuncuoglu et al. 1998). Approximately 16% to 51% of CTS patients are clinically suspected of having CTS, but have normal electrodiagnostic tests (Jordan et al. 2002), and thus alludes to a population where the precision of ultrasound assessments in the detection of small changes may be an advantage.

The role of SSCT pathology in CTS symptoms is likely related to elevated carpal tunnel pressure. We found greater absolute and relative thickness in the SSCT for our

CTS symptomatic group, which may in turn increase the volume of contents in the carpal tunnel. Our CTS symptomatics also had increased relative tendon-SSCT displacement, suggesting disrupted gliding of the SSCT that is consistent with pathological fibrosis. There is evidence that fibrotic SSCT have reduced permeability that can alter fluid balance in the carpal tunnel (Osamura et al. 2007a). These factors may all contribute to elevated carpal tunnel pressure. Increased carpal tunnel pressure is well documented in CTS patients and implicated in the development of neurological symptoms (Keir and Rempel, 2005).

Shear injury is the predominate theory in the pathomechanics of the SSCT. It involves excessive differential motion between the SSCT and adjacent structures (tendon and nerve) leading to greater viscoelastic shear strain (Tat et al. 2014b). CTS patients have consistently shown increased differential motion between the tendon-SSCT compared to healthy individuals (van Doesburg et al. 2012b) and we have demonstrated a dose-response increase with questionnaire based CTS severity. Osamura et al. (2007b) showed that injury to the SSCT can occur with finger movements in physiological range. For healthy individuals, damage and repair of the SSCT is likely in equilibrium allowing for the maintenance of healthy SSCT function. However, sustained exposure to occupational risk factors may inflict repetitive strain and not allow for adequate healing, thereby disturbing equilibrium (Moore et al. 1991; Silverstein et al. 1987). For example, highly repetitive hand motions performed for only 30 minutes was sufficient to significantly increase differential motion between the tendon and SSCT (Tat et al. 2013). In the workplace, tasks are performed for longer durations that can further increase

differential motion and may lead to a cascade of events including acute SSCT injury, disruption of SSCT gliding, and further increases in viscoelastic shear strain. Prolonged exposure could therefore result in a cycle of SSCT degradation. The relationship documenting increases in differential motion with symptom severity indicate shear damage likely accumulates with the progression of CTS disease.

Ultrasound shear was used as a surrogate measure of SSCT health because it measures the viscoelastic resistance associated with flexor tendon shear (stretch of SSCT layers and fibrils) (Tat et al. 2014b). Increased relative displacement represented a disruption in SSCT gliding that likely reflects damage to fibril connections in the SSCT. Our motion protocol was selected based on the work of Tat et al. (2014b) who showed that high velocity tendon excursions caused more delay in the SSCT motion relative to the tendon. We used a high rate of isolated finger motion to achieve high tendon velocities in flexion (mean peak velocity 7.8 ± 1.4 cm/s) and extension (mean peak velocity 7.6 ± 1.2 cm/s) in order to achieve higher differential motion. These parameters highlighted the viscoelastic effect and allowed differentiation in SSCT function between groups.

There are a few limitations to the study. Our CTS population was not clinically diagnosed and therefore may limit our findings as they relate to the clinical setting. However, we chose symptoms questionnaires because it allowed us to categorize our subjects on a functional scale to permit a comparison between progression of symptoms and SSCT etiology. More research is needed to validate and test the sensitivity, specificity, and predictive value of SSCT measurements, which was beyond the scope of

this study. Our relationship between symptoms severity and ultrasound measurements were driven by differences between our population groups; but, this was necessary to show that ultrasound could distinguish symptoms severity including those with no symptoms. The relationship between severity and ultrasound measured parameters did not reach significance in CTS patients alone (Pearson *r* values between -0.26 to 0.38), likely due to our CTS symptomatic population having low severity scores (Katz, 1.2 ± 0.9; BCTQ symptom, 1.9 ± 0.7; BCTQ function, 1.3 ± 0.9). Nonetheless, we noted positive trends (Figure 4), especially with the BCTQ symptom severity and SSI relationship (r=0.38, p=0.25), that may improve with a greater distribution of severity in our CTS patients (more severe cases). Lastly, there were age differences between our CTS symptomatics and control group that may have influenced our findings. The etiology for CTS is likely multi-factorial such that intrinsic factors (age, genetic, physiology) and physical exposure (occupational risk factors) probably share a role in the development of injury. Thus, we speculate that, under certain circumstances like chronic exposure to repetitive hand tasks, shear damage accumulates over time and in some individuals begins to initiate this cycle of tissue degradation that can lead to pathological changes.

4.6 Conclusions

The main finding of our study is the positive association between CTS severity and SSCT characteristics including thickness and fibrosis. The clinical utility of SSCT assessments with ultrasound is substantiated by its ability to evaluate the severity of CTS.

These changes likely occur throughout the development of CTS and indicate the value of ultrasound in the early screening of CTS.

4.7 Acknowledgements

This study was supported by funding from a Natural Sciences and Engineering Research Council Discovery Grant (# 217382-09).

4.8 References

An, K.N., Ueba, Y., Chao, W., Cooney, W.P., & Linscheid, R.L., 1983. Tendon excursion and moment arm of index finger muscles. *Journal of Biomechanics*, 16 (6), 419-425.

Ettema, A.M., Amadio, P.C., Zhao, C., Wold, L. E., O'Byrne, M.M., Moran, S.L., An, K.A., 2006. Changes in the functional structure of the tenosynovium in idiopathic carpal tunnel syndrome: A scanning electron microscope study. *Plastic and Reconstructive Surgery*, 118 (6), 1413-1422.

Ettema, A.M., An, K.N., Zhao, C., O'Byrne, M.M., & Amadio, P.C., 2008. Flexor tendon and synovial gliding during simultaneous and single digit flexion in idiopathic carpal tunnel syndrome. *Journal of Biomechanics*, 41 (2), 292-298.

Jablecki, C.K., Andary, M.T., So. Y.T., Wilkins, D.E., & Williams, F.H., 1993. Literature review of nerve conduction studies and electromyography for the evaluation of patients with carpal tunnel syndrome. AAEM Quality Assurance Committee. *Muscle & Nerve*, 16 (12), 1392-1414.

Jordan., R., Carter, T., & Cummins, C., 2002. A systematic review of the utility of electrodiagnostic testing in carpal tunnel syndrome. *British Journal of General Practice*, 52 (481), 670-673.

Katz J.N., & Stirrat, C.R., 1990. A self-administered hand diagram for the diagnosis of carpal tunnel syndrome. *The Journal of Hand Surgery*, 15 (2), 360-363.

Keir, P.J., & Rempel, D.M., 2005. Pathomechanics of peripheral nerve loading evidence in carpal tunnel syndrome. *Journal of Hand Therapy*, 18 (2), 259-269.

Kortanje J.W.H., Boer, M.S.D., Blok, J.H., Amadio, P.C., Hovius, S.E.R., Stam, H.J., & Selles, R.W., 2012. Ultrasonographic assessment of longitudinal median nerve and hand flexor tendon dynamics in carpal tunnel syndrome. *Muscle & Nerve*, 45 (5), 721-729.

Koyuncuoglu, H.R., Kutluhan, S, Yesildag, A., Oyar, O., Guler, K., & Ozden, A., 2005. The value of ultrasonographic measurement in carpal tunnel syndrome in patients with negative electrodiagnostic tests. *European Journal of Radiology*, 56 (3), 365-369.

Levine, D.W., Simmons, B.P., Koris, M.J., Daltory, L.H., Hohl, G.G., Fossel, A.H., & Katz, J.N., 1993. A self-administered questionnaire for the assessment of severity of symptoms and functional status in carpal tunnel syndrome. *The Journal of Bone and Joint Surgery*, 75 (11), 1585-1592.

Moore, A., Wells, R., & Ranney, D., 1991. Quantifying exposure in occupational manual tasks with cumulative trauma disorder potential. *Ergonomics*, 34 (12), 1433-1453.

Oh, S., Belohlavek, M., Zhao, C., Osamura, N., Zobitz, M.E., & An, K., 2007. Detection of differential gliding characteristics of the flexor digitorum superficialis tendon and subsynovial connective tissue using color Doppler sonographic imaging. *Journal of Ultrasound Medicine*, 26 (2), 149-155.

Osamura, N., Zhao, C., Zobitz, M.E., An, K.N., & Amadio, P.C., 2007a. Permeability of the subsynovial connective tissue in the human carpal tunnel: a cadaver study. *Clinical Biomechanics*, 22 (5), 524-528.

Osamura, N., Zhao, C., Zobitz, M.E., An, K.N., & Amadio, P.C., 2007b. Evaluation of the material properties of the in carpal tunnel syndrome. *Clinical Biomechanics*, 22 (9), 999-1003.

Rempel, D., Evanoff, B., Amadio, P. C., de Krom, M., Franklin, G., Franzblau, A., & Pransky, G. (1998). Consensus criteria for the classification of carpal tunnel syndrome in epidemiologic studies. *American Journal of Public Health*, 88 (10), 1447-1451.

Silverstein, B.A., Fine, L.J., & Armstrong, T.J., 1987. Occupational factors and the carpal tunnel syndrome. *American Journal of Industrial Medicine*, 11 (3), 343-358.

Tat, J., Kociolek, A.M., & Keir, P.J. 2013. Repetitive differential motion increases shear strain between the flexor tendon and subsynovial connective tissue. *Journal of Orthopaedic Research*, 31 (10), 1533-1539.

Tat, J., Kociolek, A.M., & Keir, P.J.. 2014a. Validation of colour Doppler ultrasonography for evaluating relative displacement between flexor tendon and subsynovial connective tissue. Accepted to the *Journal of Ultrasound in Medicine* on July 22, 2014.

Tat, J., Kociolek, A.M., & Keir, P.J. (July, 2014b). Tendon shear is only partially represent by tendon shear. In proceedings of the 7th World Congresss of Biomechanics, Boston, MA.

van Doesburg, M.H.W., van der Molen, A.M., Henderson, J., Cha,S.S., An, K.N., Amadio, P.C., 2012a. Sonographic measurements of subsynovial connective tissue

thickness in patients with carpal tunnel syndrome. *Journal of Ultrasound in Medicine*, 31 (1), 31-36.

van Doesburg, M.H.M., Yoshii, Y., Henderson, J., Villarraga, H.R., Moran, S.L., & Amadio, P.C., 2012b. Speckle-tracking sonographic assessment of longitudinal motion of the flexor tendon and subsynovial tissue in carpal tunnel syndrome. *Journal of Ultrasound in Medicine*, 31 (7), 1091-1098.

Vanhees, M., Morizaki, Y., Thoreson, A.R., Larson, D., Zhao, C., An, K.A., & Amadio, P.C., 2012. The effect of displacement on the mechanical properties of human cadaver subsynovial connective tissue. *Journal of Orthopaedic Research*, 30 (11), 1732-1737.

Yoshii, Y., Zhao, C., Zhao, K.D., Zobitz, M.E., An, K.N., & Amadio, P.C., 2008. The effect of wrist position on the relative motion of tendon, nerve, and subsynovial connective tissue within the carpal tunnel in a human cadaver model. *Journal of Orthopaedic Research*, 26 (8), 1153-1158.

CHAPTER 5 THESIS SUMMARY AND DISCUSSION

5.1 Thesis Summary

This thesis established a potential role for the use of ultrasound in the clinical assessment of carpal tunnel syndrome by showing that ultrasound measured relative tendon displacement captures viscoelastic stretch in the tenosynovium. In Chapter 2, we found colour Doppler measured tendon displacement with high accuracy and established a robust tool for measuring relative motion in the carpal tunnel. Our comprehensive analysis of tendon-SSCT motion through a physiological range provided novel insight into the gliding mechanism of the tenosynovium, showing different loading (stretch) and unloading (relaxation) movement patterns. Chapter 3 compared colour Doppler measurements of relative tendon displacement to a mechanical assessment of tendon shear *in vitro*. We found relative displacement reflected the viscoelastic component (stretch of the tenosynovium) but not the surface frictional work. This suggests ultrasound shear is different from flexor tendon shear and, therefore, may not fully represent the risk of occupational carpal tunnel syndrome. However, viscoelastic resistance in tendon shear is implicated in pathological fibrosis and thickening of the tenosynovium, a clinical finding in CTS patients. Chapter 4 served as a follow up to demonstrate the clinical implications of ultrasound assessments. We found ultrasound could be useful to assess pathological changes in the tenosynovium that could be useful in the diagnosis and determined that pathological changes progressed with CTS symptom severity.

5.2 Main Contributions

5.2.1 Evaluating Motion in the Carpal Tunnel with Colour Doppler Ultrasound

Chapter 2 provided a comprehensive evaluation of colour Doppler ultrasonography in the evaluation of flexor tendon displacement in the carpal tunnel. This was the first study to validate tendon displacement for colour Doppler. We found that colour Doppler underestimated tendon displacement with different experimental tendon velocities. However, the error associated with tendon velocity was systematic and, therefore, may be adjusted to improve *in vivo* estimates of tendon displacement. These findings were important for establishing a method for quantifying relative motion in the carpal tunnel.

Angle dependency is a limitation commonly documented with Doppler ultrasound. The orientation of carpal tunnel anatomy produces less than optimal insonation angles (approximately 60 degrees) and researchers often identify this to be a potential source of error. As a result, Doppler techniques are not typically used in relative tendon motion. However, we demonstrated that good image acquisition practice can effectively limit error associated with angle dependency. We used a 20^{o} beam steer angle, gel wedge and optimized the probe position to maintain appropriate angles of insonation. We improved upon colour Doppler velocity errors reported by Oh et al. (2007) and achieved measurement error similar to an *in vitro* validation study of speckle tracking (providing angle independent measurements) (Korstanje et al. 2010). At the same slow velocities (50 mm/s) and tendon excursion range (15 mm) tested by Korstanje

et al. (2010), we recorded absolute and relative measurement error that was less than 0.008 mm and 0.58% respectively.

Prior to this study, colour Doppler validation studies used the colour Doppler function to localize tendon position and pulse-wave Doppler to quantify tendon velocities (Soeters et al. 2004; Holland et al. 1999; Buyruk et al. 1998; Cigali et al. 1996). However, there are important differences between colour Doppler and pulse-wave Doppler. The methods use different Doppler shift computations; pulse-wave Doppler employs a fast Fourier transformation technique, while colour Doppler uses autocorrelation (Kukulski et al. 2003). These differences in shift computation can affect tissue velocity calculations and discrepancies in peak velocity have been reported between the methods (Kukulski et al. 2003). Additionally, pulse-wave Doppler lacks the ability to measure relative motion between the tendon and tenosynovium. It uses a single large sample volume that does not permit the simultaneous measurement of adjacent tissue or small structures such as the tenosynovium. Colour Doppler can assess the tendon and tenosynovium at the same time using sample volumes (0.5 mm) that are the approximate thickness of the tenosynovium in healthy participants (CTS patients have enlarged tenosynovium) (van Doesburg et al. 2012). Therefore, colour Doppler ultrasound is useful for the assessment of relative motion in the carpal tunnel.

Colour Doppler ultrasound was recently validated for tracking tendon velocities (Oh et al. 2007). In that study, the colour Doppler function measured tendon velocity while a cadaveric tendon was moved by a motor in the proximal direction for simulated flexion. Relative error was represented as a ratio of peak colour Doppler tendon velocity

compared to the prescribed motor velocity. Though colour Doppler demonstrated high accuracy in the range of 2.5 cm/s to 10 cm/s tendon velocities, only peak tendon velocities were evaluated and this may not reflect accuracy for tissue displacement. We addressed this gap by assessing the absolute measurement error (mm) for colour Doppler tendon displacements at multiple intervals of motor excursion.

5.2.2 Subysnovial Connective Tissue Mechanics

Chapter 2 validated colour Doppler for the assessment of tendon displacement that allowed us to examine important aspects of the carpal tunnel system. We were interested in the gliding mechanism of the tenosynovium. While we did not directly measure motion in individual layers of the tenosynovium, this was beyond the scope of our study (requires more sophisticated imaging techniques), and we evaluated the relative displacement profile between the tendon and SSCT to infer loading patterns between the tendon and SSCT.

The viscoelastic nature of the SSCT is strain-rate dependent as evident by our velocity-dependent changes in absolute and relative SSCT motion. We found smaller SSCT displacements with fast (150 mm/s) versus slow (50 mm/s) tendon velocities. The viscous properties are largely due to the gel-like interfibrillar matrix (protegolycans) that surround the collagen fibrils and layers of the SSCT (Guimberteau et al. 2010). There is evidence showing the removal of interfibrillar matrix in connective tissue decreases time-dependent behaviour such as relaxation, hysteresis, and stiffness (Minnis et al. 1973). Therefore, faster tendon velocities would recruit and move successive SSCT layers at a slower rate due to increased viscous resistance imposed by the interfibrillar matrix.

The stretch in the interconnecting collagen fibrils between SSCT layers is evidence of the elastic element. We found a nonlinear increase in relative displacement between the tendon and tenosynovium in simulated flexion that suggest fibrils were stretched. Interestingly, our nonlinear differential motion curve mimics the stress-strain curve well documented in mechanical testing of connective tissue (Dunn et al. 1983; Comninou et al. 1976; Viidik, 1972). In these studies, the stress-strain curve consists of a starting toe-region caused by straightening and stretching of randomly oriented, crimped collagen fibers referred to as realignment. After the initial elongation, collagen fibres become taut and tissue stress begins increasing more rapidly thereby producing a curvilinear shape. For SSCT motion, realignment occurs at the onset (fibril directions are randomly oriented requiring realignment), producing a similar initial delay. Thereafter, the curvilinear shape is likely due to the progressive fibril strain occurring between successive layers. As the tendon moves further in the flexion direction, fibrils become progressively stretched, with layers closest to the tendon experiencing the most stretch, which could produce a nonlinear increase in viscoelastic resistance (Figure 5.1). In ultrasound, we observed this effect with decreased SSCT motion relative to the tendon at greater tendon excursions. This phenomenon was further supported by our direct measurement of tendon frictional work, which also increased at a nonlinear rate (Figure 5.2). Therefore the SSCT exhibited nonlinear elastic properties that increased shear force with increasing strain during tendon excursion.

The evaluation of relative displacement throughout tendon excursion also suggested different tenosynovium gliding patterns in flexion versus extension movement

directions. In our testing paradigm, flexion excursions (proximal tendon motion) resulted in tendon "loading" which stretched the SSCT, while extension excursions involved "unloading" the tendon to relax the SSCT (Figure 5.1). In flexion excursions, we attributed the nonlinearity to the sequential and progressive strain of the interconnecting fibrils that was consistent with nonlinear increases in both ultrasound and frictional work. We would expect a similar curvilinear shape if the fibrils were unloaded in a sequential manner. Rather, we found a linear return for both ultrasound and frictional work (Figure 5.2), suggesting the entire SSCT system slackened together, such that layers of the SSCT moved by uniform relaxation of fibrils. Motion facilitated by passive fibril relaxation may account for slower SSCT excursions during tendon unloading (extension motion).

We examined the progression of relative tissue displacement on a point-by-point basis to better understand the way structures in the carpal tunnel move as a system. We demonstrated the viscoelastic nature of the SSCT and the unique gliding mechanism involved in tendon loading and unloading. An understanding of the relative displacement between the tendon-SSCT during tendon excursion is important for elucidating the role of hand and wrist motions in shear injury.

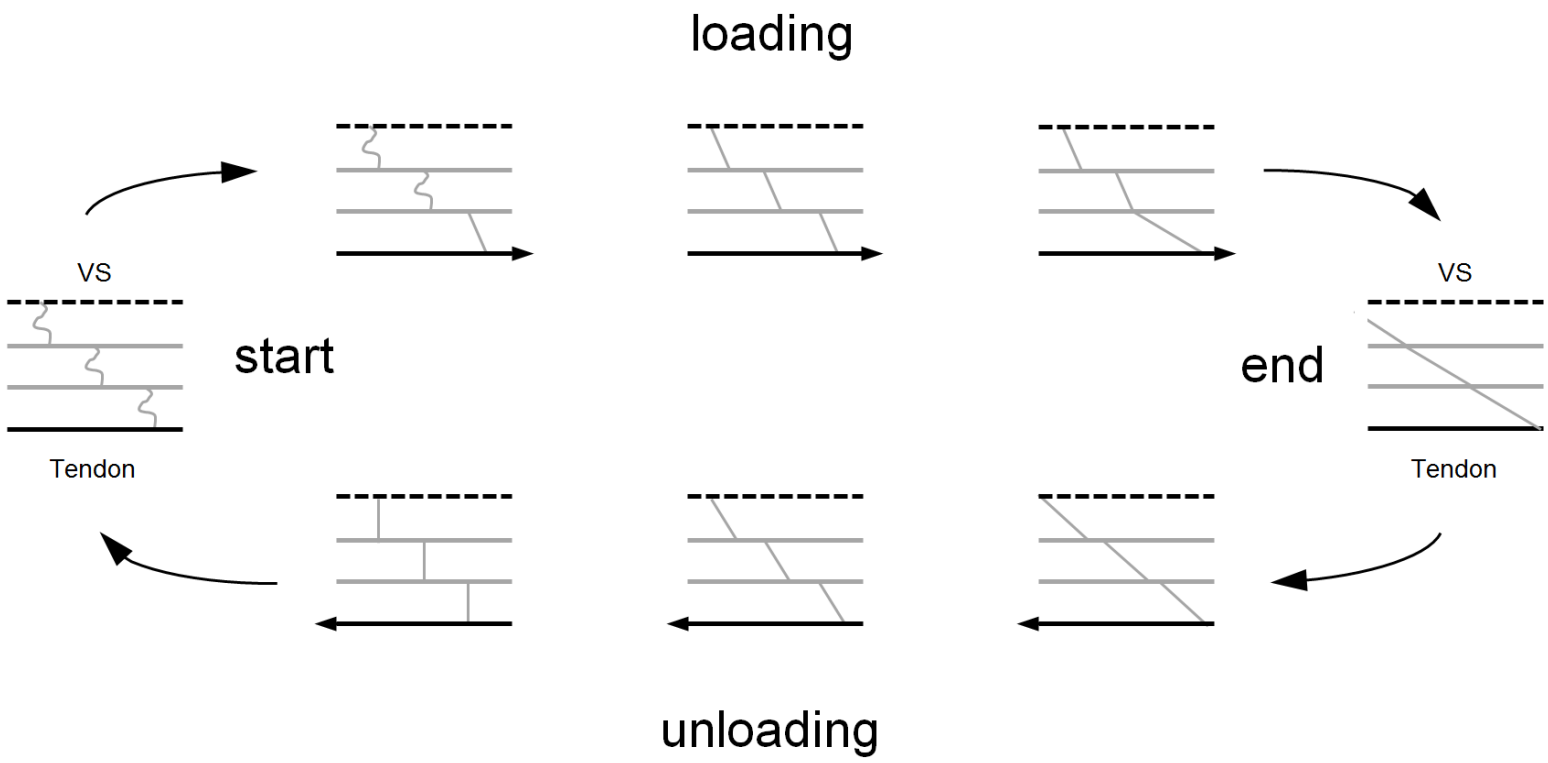

Figure 5.1 The gliding mechanism of the SSCT. The SSCT (grey lines) extends from the tendon to the visceral synovium (VS). Motion of the SSCT layers (horizontal grey lines) are mediated by interconnecting collagen fibrils (vertical grey lines), which are simplified to demonstrate the sliding mechanisms. Tendon loading (flexion, indicated by right arrow) is facilitated by sequential recruitment of SSCT layers, while unloading (extension, indicated by left arrow) occurs uniformly. The "start" position is represented by loose and relaxed collagen fibrils. With tendon loading, successive layers are recruited by sequentially stretching fibrils, with fibrils closest to the tendon experiencing the greatest strain. The "end" position represents the end of tendon loading and the maximum stretch of fibrils occurring with the given tendon excursion. During tendon unloading, fibrils relax together, moving the SSCT layers at a uniform rate.

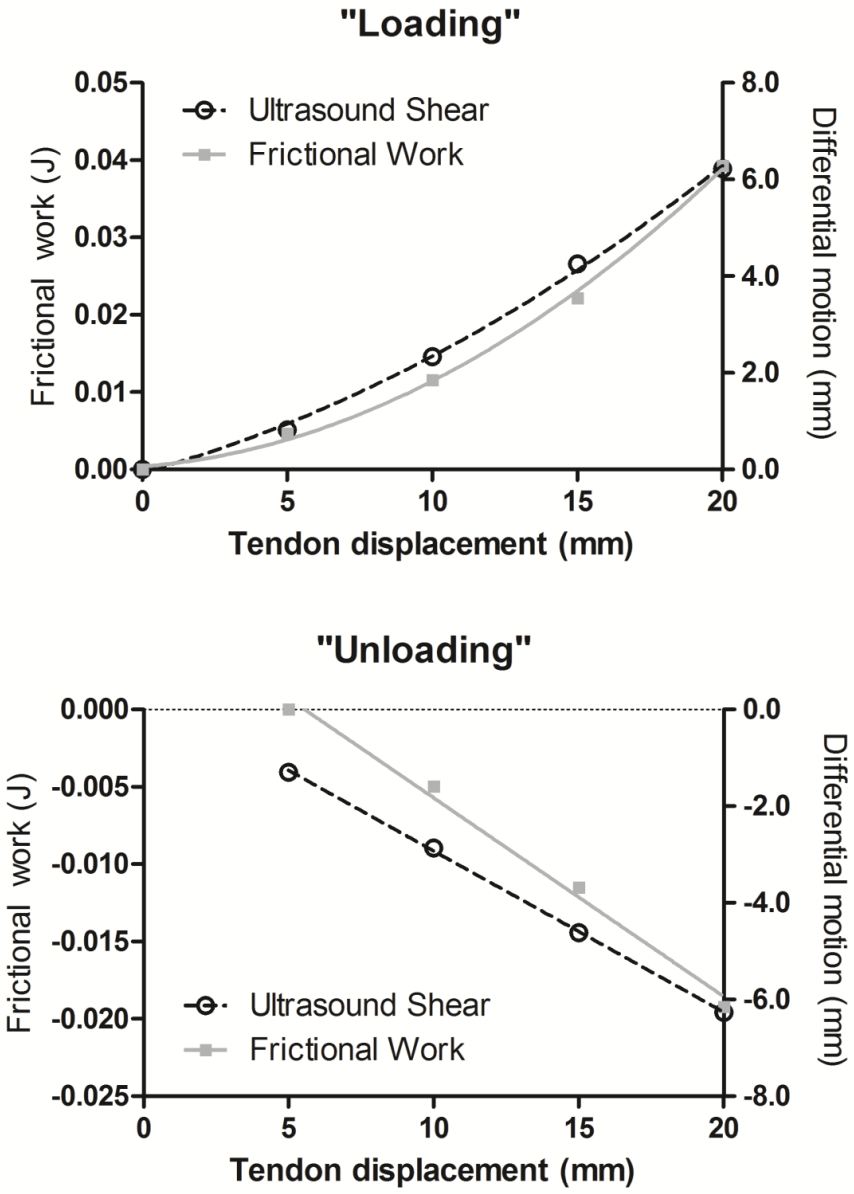

Figure 5.2 Average tendon shear profile (N=8) for one condition (neutral posture, 20 N, 150 mm/s). Tendon shear was represented using frictional work (left y-axis) and ultrasound (right y-axis). (*Above*) SSCT "loading" occurs by moving the tendon in the flexion direction, producing curvilinear increases in both shear measurements. *(Below)* The SSCT is "unloaded" with extension direction excursions. The uniform relaxation of SSCT fibrils and layers was captured as a linear return in both shear variables.

5.2.3 Implications for Ultrasound

Excessive tendon shear is implicated in the pathomechanics of the tenosynovium. Ultrasound has frequently been used to represent tendon "shear" with relative displacement between the tendon and tenosynovium; however, these findings have not been substantiated. Chapter 3 compared tendon shear measured by ultrasound (relative displacement) versus a direct mechanical assessment of tendon forces to calculate tendon frictional work.

This thesis used different wrist postures (neutral, 30^{o} flexion), velocities (50, 100 150 mm/s), and forces (10, 20 30 N) in cadavers to evaluate tendon shear. We found a posture × force interaction in frictional work that did not coincide with an interaction effect in ultrasound shear. The posture × force interaction in frictional work was consistent with biomechanical models of the wrist, indicating increased contact stress of the tendon against the transverse carpal ligament in a flexed wrist and high tendon force (Armstrong and Chaffin, 1979); while the ultrasound measured parameters had main effects for posture and force. Therefore, we concluded that ultrasound and mechanical tendon shear captured different phenomena. Ultrasound appears to miss the surface frictional contributions from neighbouring anatomical structures in the carpal tunnel, but rather reflects only the viscoelastic component of tendon shear (associated with stretch of the tenosynovium). We further examined the viscoelastic component by using different tendon velocities, which assumed viscoelastic stretch was velocity-dependent and surface friction was velocity-independent. Thus, our independent and additive velocity responses for both ultrasound ($p<0.05$, effect size = 0.862) and frictional work ($p<0.05$, effect size =

0.937) likely reflected the same viscoelastic effect. These results have important implications for the future testing paradigm of ultrasound tendon shear studies.

Relative displacement between the tendon and SSCT (measured by ultrasonography) is mediated by traditional carpal tunnel syndrome risk factors including duration, posture, force and repetition (Tat et al. 2013; Yoshii et al. 2011; Yoshii et al. 2009; Yoshii et al. 2008). As a result, there was the potential that ultrasound could be useful in the ergonomic assessment of injury in the workplace by evaluating flexor tendon shear. However, this thesis verifies that ultrasound evaluations of differential movement and mechanical tendon shear measures different phenomena. Epidemiology studies for carpal tunnel syndrome have shown strong relationships with awkward wrist postures, high force and high repetition (Bernard, 1997; Schoenmarklin et al. 1994; Chiang et al. 1993; Silverstein et al. 1987). These studies highlight the inter-play between the occupational risk factors, which was consistent with our frictional work results. For example, Schoenmarklin et al. (1994) found that awkward postures alone were minimally related to injury, however coupling deviated wrist postures with high forces were significant predictors of workplace carpal tunnel syndrome. We found no multiplicative response by coupling posture and force in our ultrasound measure, but instead found them to be independent. Contact stress on the tendon, especially in a flexed wrist posture, likely plays an important role in the pathomechanics of CTS. Therefore, by missing the surface friction element of tendon shear, ultrasound likely captures an incomplete relationship between occupational risk factors and risk of carpal tunnel syndrome.

Pathological fibrosis and thickening of the tenosynovium is almost universally found in carpal tunnel syndrome patients (van Doesburg et al. 2012; Ettema et al. 2006; Jinrok et al. 2004). Since we showed that ultrasound can provide a non-invasive assessment of viscoelastic resistance during tendon motion, this suggests ultrasound evaluations will have important applications in the clinical setting. In particular, ultrasound assessments will be valuable in our understanding of local mechanisms of tissue injury and the pathophysiology. In Chapter 4, we explored the clinical utility of ultrasound *in vivo* by assessing functional and morphological changes in the tendon sheath of carpal tunnel syndrome symptomatics.

We found that participants with CTS symptoms (based on self-report questionnaires) had significantly increased SSCT thickness and relative tendon-SSCT motion compared to healthy individuals. These findings suggest pathological thickening and fibrosis were present in our symptomatics and indicate ultrasound may be useful in diagnosing CTS. The severity of CTS symptoms also correlated with the level of impairment in gliding of the tenosynovium, such that more severe cases experienced greater loading to the tenosynovium for the same finger motion. This is in line with previous pathomechanics theory indicating pathological fibrosis involves a vicious cycle of tissue degradation, in which fibrosis predisposes to even more fibrosis (Ettema et al. 2006).

We are the first to demonstrate a positive association in CTS severity with either SSCT morphology or SSCT mechanics ($p<0.05$). Previous studies used electrodiagnostic testing to compare SSCT thickness and mechanics without success (van Doesburg et al.

2012; Korstanje et al. 2012). This may have been due to using nerve conduction velocities to categorize CTS severity, which are a function of large myelinated nerve fibres that may not yet be affected in early stages of CTS (Koyuncuoglu et al. 1998). Also, in these studies, subjects performed a functional finger motion (full fist hand motion) that was uncontrolled for speed or range of motion. Our study differs by using clinical questionnaires to categorize CTS symptomatics, which provides a symptom severity score on a functional scale (Boston Carpal Tunnel Questionnaire and Katz hand diagram) that may better compare to small pathophysiological changes detected by ultrasound. For our motion protocol, we controlled for range of motion and velocity using a polyvinyl chloride tube and metronome respectively. A high frequency independent finger task allowed us to best highlight the state of connections in the tenosynovium. Our study successfully differentiated symptom severity using a CTS symptomatic population with relatively low severity, which suggests it may be useful in the early diagnosis of CTS.

The thesis concludes that ultrasound is best suited for the clinical setting. Specifically, ultrasound will be useful in the clinical assessment of the tenosynovium, including the early detection of carpal tunnel syndrome disease and understanding local mechanisms of injury such as shear strain injury in the tenosynovium. Evaluating characteristics of the tenosynovium is important to the pathomechanics of fibrosis and thickening of the tenosynovium and may help to elucidate the etiology of CTS.

5.3 Future directions

In Chapter 2 we demonstrated the validity of colour Doppler ultrasound in the measurement of tendon displacement and highlighted its utility in future studies to quantify relative motion for shear injury. The initial goal of this study was to perform a direct comparison between colour Doppler and speckle tracking by validating both techniques with tendon displacement *in vitro*. However, during cadaveric testing, we found the number of conditions to not be feasible and elected to use colour Doppler over speckle tracking since it was more robust (with speckle tracking insufficient speckle patterns makes tracking impractical) (See Pilot work in Appendix D). More conditions would increase movement cycles and deteriorate the fidelity of the cadaver model by disrupting SSCT connections and further dehydrate the specimen (changing viscous properties). We found speckle tracking had difficulty tracking the tenosynovium, indicating it may be inadequate to assess the complete carpal tunnel system. Alternatively, colour Doppler was highly useful in our relative measurement of displacement in the tendon and tenosynovium.

We had difficulty representing the anatomical fidelity of the wrist at different wrist postures. The flexor tendons were detached on both sides of the carpal tunnel such that the entire carpal tunnel complex could interact erroneously with our apparatus. Therefore, to represent *in vivo* conditions in wrist flexion, we needed to move the flexor tendons proximally to simulate proximal tendon displacement occurring with muscle contractions. We displaced the flexor tendons 10 mm in the proximal direction compared to the tendon position in a neutral wrist posture (Armstrong and Chaffin, 1978). This

procedure was vitally important to characterize the viscoelastic properties of the SSCT. While we did not test wrist extension (again due to large number of testing conditions), we suggest a similar procedure that would move the flexor tendons distally to represent the stretch that would occur in flexor muscles *in vivo*. As a result, we would anticipate a stretch of the SSCT fibrils in the opposite direction, so that fibrils will need to unload before being stretched in the proximal (flexion) direction. Wrist extension should have the smallest viscoelastic resistance (frictional work and relative displacement) compared to either neutral or flexed wrist postures, however, this contrasts previous ultrasound tendon studies showing the smallest relative displacement in neutral postures (Yoshii et al. 2009). Therefore the effect of wrist posture deserves further investigation.

While we simplified the relationship between the tendon and SSCT for our testing paradigm (assessing kinematics for two adjacent regions), in reality the SSCT is a complex system of collagen fibres that loosely connects all structures in the carpal tunnel. Movement of the flexor tendons transmits forces via SSCT connections to other flexor tendons and the median nerve (Ettema et al. 2008; Yoshii et al. 2008). Studying the relationship between the SSCT, tendons, and median nerve will be an important next step considering compression of the median nerve is primary in the pathophysiology of CTS.

Compression of the median nerve can lead to ischemia, altered nerve function, and neurological symptoms. Carpal tunnel pressure has been used to indirectly evaluate median nerve ischemia with a 30 mmHg threshold (Lundborg et al. 1982). Recently, ultrasound has provided a direct measure of median nerve blood flow (Wilson et al. 2014; Wilder-Smith, 2012). In Chapter 4, we tested a number of novel diagnostic ultrasound

techniques on our CTS symptomatic population including an assessment of the tenosynovium (morphology and function) and measuring blood flow to the median nerve (Wilson et al. 2014). Interestingly, we found relationships between pathological changes in the tenosynovium and median nerve blood flow. We theorize that fibrosis and thickening of the tenosynovium can increase carpal tunnel pressure leading to ischemia in the median nerve and CTS symptoms. The tenosynovium is an integral component of the carpal tunnel system that can affect the median nerve and future studies should examine the interplay between these structures.

The thesis demonstrated the clinical relevance of ultrasound in the assessment of the tenosynovium. Ultrasound was established as a tool to measure viscoelastic resistance associated with stretching the tenosynovium during tendon excursion that will be useful in the clinical setting, including the diagnosis of CTS and understanding the pathomechanics leading to tenosynovium pathology. However, the role of shear injury in the epidemiology of CTS is not well understood and future studies are needed to fully appreciate the importance of shear injury in carpal tunnel syndrome.

REFERENCES

1. An, K.N., 2007. Tendon excursion and gliding: Clinical impacts from humble concepts. *Journal of biomechanics,* 40 (4), 713-718.
2. An, K.N., Ueba, Y., Chao, W., Cooney, W.P., & Linscheid, R.L., 1983. Tendon excursion and moment arm of index finger muscles. *Journal of Biomechanics,* 16 (6), 419-425.
3. Armstrong, T.J., & Chaffin, D.B., 1978. An investigation of the relationship between displacements of the finger and wrist joints and the extrinsic finger flexor tendons. *Journal of Biomechanics,* 11 (3), 119-128.
4. Barr, A.E., Barbe, M.F., & Clark, B.D., 2004. Work-related musculoskeletal disorders of the hand and wrist: Epidemiology, pathophysiology, and sensorimotor changes. *Journal of Orthopaedic and Sports Physical Therapy*, 34 (10), 610-27.
5. Bernard, B.P., 1997. *Musculoskeletal disorders and workplace factors: A critical review of epidemiologic evidence for work-related musculoskeletal disorders of the neck, upper extremity, and low back (Publication # 97-141).* Cincinnati, OH: National Institute for Occupational Safety and Health (Department of Health and Human Services).
6. Brand, P. W., & Hollister, A. (1993). Clinical mechanics of the hand, Mosby Year Book.

7. Buyruk, H.M., Holland, W.P.J., Snijders, C.J., Laméris, J.S., Hoorn, E., Stoeckart, R., & Stam, H.J., 1998. Tendon excursion measurements with color Doppler imaging. *Journal of Hand Surgery*, 23 (3), 350-353.
8. Chiang, H.C., Ko, Y.C., Chen, S.S., & Yu, H.S., 1993. Prevalence of shoulder and upper-limb disorders among workers in the fish-processing industry. *Scandinavian Journal of Work and Environmental Health*, 19 (2), 126-131.
9. Cigali, B.S., Buyruk, H.M., Snijders, C.J., Laméris, J.S., Holland, W.P.J., Mesut, R., & Stam, H.J., 1996. Measurement of tendon excursion velocity with colour doppler imaging: A preliminary study on flexor pollicis longus muscle. *European Journal of Radiology*, 23(3), 217-221.
10. Comninou, M., & Yannas, I.V., 1976. Dependence of stress-strain curve nonlinearity of connective tissue on geometry of collagen fibers. *Journal of Biomechanics*, 9 (7), 427-433.
11. Dennerlein, J.T., 2005. Finger flexor tendon forces are a complex function of finger joint motions and fingertip forces. *Journal of Hand Therapy*, 18 (2), 120-127.
12. Dilley, A., Greening, J., Lynn, B., Leary, R., & Morris, V. (2001). The use of cross-correlation analysis between high-frequency ultrasound images to measure longitudinal median nerve movement. *Ultrasound in Medicine & Biology*, 27(9), 1211-1218.

13. Dunn, M.G., & Silver, F.H., 1983. Viscoelastic behaviour of human connective tissue: Relative contribution of viscous and elastic components. *Connective Tissue Research*, 12 (1), 59-70.
14. Ettema, A.M., Amadio, P.C., Zhao, C., Wold, L. E., O'Byrne, M.M., Moran, S.L., An, K.A., 2006. Changes in the functional structure of the tenosynovium in idiopathic carpal tunnel syndrome: A scanning electron microscope study. *Plastic and Reconstructive Surgery*, 118 (6), 1413-1422.
15. Ettema, A.M., An, K.N., Zhao, C., O'Byrne, M.M., & Amadio, P.C., 2008. Flexor tendon and synovial gliding during simultaneous and single digit flexion in idiopathic carpal tunnel syndrome. *Journal of Biomechanics*, 41 (2), 292-298.
16. Feuerstein, M., Burrell, L.M., Miller, V.I., Lincoln, A., Huang, G.D., & Berger, R., 1999. Clinical management of carpal tunnel syndrome: a 12-year review of outcomes. *American Journal of Industrial Medicine*, 35 (3), 232-245.
17. Goldstein, S.A., Armstrong, T.J., Chaffin, D.B., & Matthews, L.S., 1987. Analysis of cumulative strain in tendons and tendon sheaths. *Journal of Biomechanics*, 20 (1), 1-6.
18. Filius, A., Thoreson A.R., Yang, T.H., Vanhees, M., An, K.A., Zhao, C., & Amadio, P.C., 2014. The effect of low- and high-velocity tendon excursion on mechanical properties of human cadaver subsynovial connective tissue. *Journal of Orthopaedic Research*, 32 (1), 123-128.

19. Guimberteau, J.C., Delage, J.P., McGrouther, D.A., & Wong, J.K.F., 2010. The microvacuolar system: how connective tissue sliding works. *The Journal of Hand Surgery*, 35 (8), 614-622.
20. Hagberg, M., Morgenstern, H., & Kelsh, M., 1992. Impact of occupations and job tasks on the prevalence of carpal tunnel syndrome. *Scandinavian Journal of Work and Environmental Health*, 18 (6), 337-345.
21. Hendersen, J., Thoreson, A., Yoshii, Y., Zhao, K.D., Amadio, P.C., An, K.A., 2011. Finite element model of the subsynovial connective tissue deformation due to tendon excursion in the human carpal tunnel. *Journal of Biomechanics*, 44 (1), 150-155.
22. Holland, W.P.J., Buyruk, H.M., Hoorn, E., & Stam, H.J., 1999. Tendon displacement assessment by pulsed Doppler tissue imaging: Validation with a reciprocating string test target. *Ultrasound in Medicine & Biology*, 25 (8), 1229-1239.
23. Jablecki, C.K., Andary, M.T., So. Y.T., Wilkins, D.E., & Williams, F.H., 1993. Literature review of nerve conduction studies and electromyography for the evaluation of patients with carpal tunnel syndrome. AAEM Quality Assurance Committee. *Muscle & Nerve*, 16 (12), 1392-1414.
24. Jordan., R., Carter, T., & Cummins, C., 2002. A systematic review of the utility of electrodiagnostic testing in carpal tunnel syndrome. *British Journal of General Practice*, 52 (481), 670-673.

25. Jinrok, O., Zhao, C., Amadio, P.C., An, K.N., Zobitz, M.E., Wold, L.E., 2004. Vascular pathological changes in the flexor tenosynovium (subsynovial connective tissue) in idiopathic carpal tunnel syndrome. *Journal of Orthopaedic Research*, 22 (6), 1310-1315.
26. Katz J.N., & Stirrat, C.R., 1990. A self-administered hand diagram for the diagnosis of carpal tunnel syndrome. *The Journal of Hand Surgery*, 15 (2), 360-363.
27. Keir, P.J., & Rempel, D.M., 2005. Pathomechanics of peripheral nerve loading evidence in carpal tunnel syndrome. *Journal of Hand Therapy*, 18 (2), 259-269.
28. Kociolek, A.M. Tat, J., & Keir, P.J. (July, 2014). Finger flexor tendon frictional work increases with tendon velocity and force. In proceedings of the 7th World Congress of Biomechanics, Boston, MA.
29. Korstanje, J.W.H., Boer, M.S.D., Blok, J.H., Amadio, P.C., Hovius, S.E.R, Stam, H.J., & Selles, R.W., 2012. Ultrasonographic assessment of longitudinal median nerve and hand flexor tendon dynamics in carpal tunnel syndrome. *Muscle & Nerve*, 45 (5), 721-729.
30. Korstanje, J.W.H., Selles, R.W., Stam, H.J., Hovius, S.E.R., Bosch, J.G., 2010. Development and validation of ultrasound speckle tracking to quantify tendon displacement. *Journal of Biomechanics*, 43 (7), 1373-1379.
31. Koyuncuoglu, H.R., Kutluhan, S, Yesildag, A., Oyar, O., Guler, K., & Ozden, A., 2005. The value of ultrasonographic measurement in carpal tunnel syndrome in

patients with negative electrodiagnostic tests. *European Journal of Radiology*, 56 (3), 365-369.

32. Kukulski, T., Voigt, J.U., Wilkenshoff, U.M., Strotmann, J.M., Wranne, B., Halte, L., & Sutherland, G.R., 2003. A comparison of regional myocardial velocity information derived by pulsed and color Doppler techniques: an in vitro and in vivo study. *Echocardiography: A Journal of Cardiovascular Ultrasound and Allied techniques,* 17 (7), 639-651.
33. Koyuncuoglu, H.R., Kutluhan, S, Yesildag, A., Oyar, O., Guler, K., & Ozden, A., 2005. The value of ultrasonographic measurement in carpal tunnel syndrome in patients with negative electrodiagnostic tests. *European Journal of Radiology*, 56 (3), 365-369.
34. Liu, E.Y., Steinman, A.H., Cobbold, R.S., & Johnston, K.W., 2005. Human factors as a source of error in peak Doppler velocity measurement. *Journal of Vascular Surgery*, 42 (5), 972-979.
35. Manktelow, R.T., Binhammer, P., Tomat, L.R., Bril, V., & Szalai, J.P., 2004. Carpal tunnel syndrome: Cross-sectional and outcome study in Ontario workers. *Journal of Hand Surgery*, 29A (2), 307-317.
36. Minnis, R.J., & Sodem, P.D., 1973. The role of fibrous components and ground substance in the mechanical properties of biological tissues: A preliminary investigation. *Journal of Biomechanics*. 6 (2), 153-165.

37. Moore, A., Wells, R., & Ranney, D., 1991. Quantifying exposure in occupational manual tasks with cumulative trauma disorder potential. *Ergonomics*, 34 (12), 1433-1453.
38. Oh, S., Belohlavek, M., Zhao, C., Osamura, N., Zobitz, M.E., & An, K., 2007. Detection of differential gliding characteristics of the flexor digitorum superficialis tendon and subsynovial connective tissue using color Doppler sonographic imaging. *Journal of Ultrasound Medicine*, 26 (2), 149-155.
39. Osamura, N., Zhao, C., Zobitz, M.E., An, K.N., & Amadio, P.C., 2007a. Permeability of the subsynovial connective tissue in the human carpal tunnel: a cadaver study. *Clinical Biomechanics*, 22 (5), 524-528.
40. Osamura, N., Zhao, C., Zobitz, M.E., An, K.N., & Amadio, P.C., 2007b. Evaluation of the material properties of the in carpal tunnel syndrome. *Clinical Biomechanics*, 22 (9), 999-1003.
41. Peacock, A. M., Matsunaga, S., Renshaw, D., Hannah, J., & Murray, A. 2000. Reference block updating when tracking with block matching algorithm. *Electronics Letters*, 36 (4), 309-310.
42. Rempel, D., Evanoff, B., Amadio, P. C., de Krom, M., Franklin, G., Franzblau, A., & Pransky, G. (1998). Consensus criteria for the classification of carpal tunnel syndrome in epidemiologic studies. *American Journal of Public Health*, 88 (10), 1447-1451.

43. Schoenmarklin, R.W., Marras, W.S., & Leurgans. S.E. 1994. Industrial wrist motions and incidence of hand/wrist cumulative trauma disorders. *Ergonomics*, 37 (9), 1449-1459.

44. Schoenmarklin, R.W. & Marras, W.S. 1990. A dynamic biomechanical model of the wrist joint. *Proceedings of the Human Factors and Ergonomics Society*, 34, 805-809.

45. Schuind, F., Garcia-Elias, M., Cooney III, W.P., An, K.N. 1992. Flexor tendon forces: in vivo measurements. *Journal of Hand Surgery*, 17 (2), 291- 298.

46. Silverstein, B.A., Fine, L.J., & Armstrong, T.J., 1987. Occupational factors and the carpal tunnel syndrome. *American Journal of Industrial Medicine*, 11 (3), 343-358.

47. Soeters, J.N.M., Roebroeck M.E., Holland, W.P.J., Hovius, S.E.R, & Stam, H.J. 2004. Non-invasive measurement of tendon excursion with a colour Doppler imaging system: a reliability study in healthy subjects. *Scandinavian Journal of Plastic and Reconstructive Surgery and Hand Surgery*, 38 (6), 356-360.

48. Tanaka, S., & McGlothlin, J.D., 1993. A conceptual quantitative model for prevention of work-related carpal tunnel syndrome (CTS). *International Journal of Industrial Ergonomics*, 11 (3), 181-193.

49. Tanaka, S., Petersen, M., & Cameron, L. Prevelance and risk factors of tendinitis and related disorders of the distal upper extremity among US workers. *American Journal of Industrial Medicine*, 39 (3), 328-335.

50. Tat, J., Kociolek, A.M., & Keir, P.J. 2013. Repetitive differential motion increases shear strain between the flexor tendon and subsynovial connective tissue. *Journal of Orthopaedic Research*, 31 (10), 1533-1539.

51. Tat, J., Au,, J., Keir, P.J., & MacDonald, M.J., 2014. Assessment of longitudinal shear strain in the common carotid artery wall with speckle tracking increases with spinal cord injury. In preparation for the *Journal of Clinical Physiology and functional imaging*.

52. Uchiyama, S., Coert, J.H., Berglund, L., Amadio, P.C., & An, K.N., 1995. Method for the measurement of friction between tendon and pulley. *Journal of Orthopaedic Research*, 13 (1), 83-89.

53. van Doesburg, M.H.W., van der Molen, A.M., Henderson, J., Cha,S.S., An, K.N., Amadio, P.C., 2012a. Sonographic measurements of subsynovial connective tissue thickness in patients with carpal tunnel syndrome. *Journal of Ultrasound in Medicine*, 31 (1), 31-36.

54. van Doesburg, M.H.M., Yoshii, Y., Henderson, J., Villarraga, H.R., Moran, S.L., & Amadio, P.C., 2012b. Speckle-tracking sonographic assessment of longitudinal motion of the flexor tendon and subsynovial tissue in carpal tunnel syndrome. *Journal of Ultrasound in Medicine*, 31 (7), 1091-1098.

55. Vanhees, M., Morizaki, Y., Thoreson, A.R., Larson, D., Zhao, C., An, K.A., & Amadio, P.C., 2012. The effect of displacement on the mechanical properties of human cadaver subsynovial connective tissue. *Journal of Orthopaedic Research*, 30 (11), 1732-1737.

56. Viddik, A., 1972. Simultaneous mechanical and light microscopic studies of collagen fibrils. *Z Anat Entwicklungsgesch*, 136 (2), 204-212.

57. Wilson, K.E., & Keir, P.J., 2014. Effect of wrist posture and finger tip force on median nerve blood flow velocity. Master's Thesis, McMaster University, Hamilton, Canada.

58. Wren, T.A., Tishya, S.A., Beaupré, G.S., & Carter, D.R., 2001. Mechanical properties of the Achilles tendon. *Clinical Biomechanics*, 16 (3), 245-251.

59. Yeung, F., Levinson, S.F., Parker, K.J., 1998. Multilevel and motion model-based ultrasonic speckle tracking algorithms. *Ultrasound in Medicine and Biology*, 24 (3), 427-441.

60. Yoshii, Y., Zhao, C., Zhao, K.D., Zobitz, M.E., An, K.N., & Amadio, P.C., 2008. The effect of wrist position on the relative motion of tendon, nerve, and subsynovial connective tissue within the carpal tunnel in a human cadaver model. *Journal of Orthopaedic Research*, 26 (8), 1153-1158.

61. Yoshii, Y., Zhao, C., Henderson, J., Zhao, K.D., An, K.N., & Amadio, P.C., 2009. Shear strain and motion of the subsynovial connective tissue and median nerve during single digit motion. *Journal of Hand Surgery*, 34 (1), 65-79.

62. Yoshii, Y., Zhao, C., Henderson, J., Zhao, K.D., An, K.N., & Amadio, P.C., 2011. Velocity dependent changes in the relative motion of the subsynovial connective tissue in the human carpal tunnel. *Journal of Orthopaedic Research*, 29 (1), 62-66.

63. Zahnd, G., Orkisz, M., Sérusclat, A., Moulin, P., & Vray, D., 2013. Evaluation of a Kalman-based block matching method to assess the bi-dimensional motion of

the carotid artery wall in B-mode ultrasound sequences. *Medical Image Analysis*, 17 (5), 573-585.

64. Zakaria, D., Robertson, J., Koval, J., MacDermid, J., & Hartford, K., 2004. Rates of claims for cumulative trauma disorder of the upper extremity in Ontario workers during 1997. *Chronic Diseases in Canada*, 25 (1), 22-31.
65. Zhao, C., Ettema, A.M., Osamura, N., Berglund, L., An, K.N., & Amadio, P.C., 2006. Gliding characteristics between flexor tendons and surrounding tissue in the carpal tunnel: a biomechanical cadaver study. *Journal of Orthopaedic Research*, 25 (2), 185-190.

APPENDICES

APPENDIX A: **Characteristics for cadaver specimen (Chapter 2 and 3) and participants (Chapter 4).**

Table 1 Characteristics of donated cadaver specimens (Chapter 2 and 3).

Specimen	Age	Gender	Handedness	Weight (lbs)	Height (in)	Ethnicity
1	54	Male	Right	150	71	Caucasion
2	49	Male	Left	165	73	Caucasion
3	48	Male	Right	320	66	Caucasion
4	55	Female	Left	200	64	Caucasion
5	82	Male	Left	250	70	African American
6	75	Male	Left	180	73	Caucasion
7	57	Male	Left	220	72	Native American
8	33	Male	Right	270	73	African American
Mean (SD)	56.6 (15.5)			219.3 (57.7)	70.3 (3.5)	

Table 2 Participant characteristics with qualitative clinical CTS scores (Chapter 4).

Characteristic	Healthy participant (N=11)	CTS symptomatic (N=11)
Age	26.2 (3.1)	41.5 (13.1)
Gender	2 M, 9 F	2 M, 9 F
Right hand dominance	11	11
BCTQ symptom severity	0	1.9 (0.7)
BCTQ functional status	0	1.3 (0.9)
Katz hand diagram	0	1.2 (0.9)

Mean (± standard deviation)

APPENDIX B: **Ethics approval for Study 1 (Chapter 2 and 3).**

Hamilton Health Sciences

McMaster University

HHS/FHS REB #	DATE RECEIVED
REB Use Only	*STAMP HERE*

Guidelines for Studies Involving the Use of Human Tissue/Blood/Body Fluid

In accordance with Tri-Council Policy, research studies requiring collection or access to human tissue must be reviewed and approved by The Hamilton Health Sciences Human Tissue Committee, a sub-committee of the HHS/FHS Research Ethics Board.

1. An application for the study of human tissue for research purposes can arise for several reasons:
   a) as a retrospective study of tissue previously collected, i.e. archived or banked tissue
   b) as part of an ongoing clinical trial to gather relevant trial-specific information or as part of a prospective study that requires collection of the use of excess tissue./blood/body fluid from patients and directly related to the objectives of the research project.
   c) as a prospective study of tissue collected for a specific research study.
   d) as a collection of tissue/blood/body fluid for research purposes, internally or externally in case of limited sampling.

2. Prior to a submission of the application to HTC, the application form and research plan must first be submitted to site group members of the HTC: a representative of clinical site group/program leader and a site group pathologist. These members will evaluate the scientific value, availability of tissue, and utilization priority of the tissue for the submitted application. Signatures of these site group members are required to acknowledge that appropriate tissue is available at source for the proposed project and that there is demonstrable scientific merit for the proposed project.

3. The Principal Investigator must sign the application form; by signing the application form, the Principal Investigator agrees to comply with the HHS confidentiality policies, and to conduct the study in compliance with the TCPS, and relevant legislation and regulatory requirements; and acknowledges that the person who will be gaining direct access to the information (research coordinator, fellow student, research assistant, monitor) is acting as an agent or delegate of the Principal Investigator. The Principal Investigator accepts full responsibility for the protection of the information. The person carrying out the study also will be required to sign a statement of declaration regarding confidentiality.

4. To receive REB approval for tissue review, submit an electronic copy of your **complete** submission **AND one hard copy** of the completed application form and research proposal/protocol to the Research Ethics Board Office. **There is no submission deadline.** For inquiries please contact:
   Deborah Mazzetti, Ph: (905) 521-2100 x42013 E-Mail: mazzedeb@hhsc.ca

Hamilton Health Sciences

McMaster University

HHS/FHS REB #	DATE RECEIVED
REB Use Only	*STAMP HERE*

Application for the Use of Human Tissue/Blood/Body Fluid For Research Purposes

SECTION 1a	Study Title				
Study Title:	Measuring Flexor Tendon Motion and Gliding Resistance in a Cadaveric Model				
SECTION 1b	**Principal Investigator** *(Must be a HHS/FHS Staff Member)*				
Name:	Peter Keir	Title:	Associate Professor	Telephone:	Ext. 23543
Department:	Kinesiology			Fax:	905-523-6011
Email:	pjkeir@mcmaster.ca			Mailing Address:	IWC 212
SECTION 1c	**Co-Investigator(s)**				
Name(s):	1. Aaron Kociolek 2. Jimmy Tat	Title:	1. Ph.D. Student 2. M.Sc. Student	Telephone:	1. Ext. 20175 2. Ext. 20175
Department:	1. Kinesiology 2. Kinesiology			Fax:	1. 905-523-6011 2. 905-523-6011
Email:	1. kociolam 2. tatj2			Mailing Address:	1. IWC A107 2. IWC A107
SECTION 1d	**Person(s) who will access retrospective patient data if applicable:** *(Include as many persons as necessary)*				
Name(s):	1. 2. 3.	Title:	1. 2. 3.	Telephone:	1. 2. 3.
Division/ Department:	1. 2. 3.			Fax:	1. 2. 3.
Email:	1. 2. 3.			Mailing Address:	1. 2. 3.

SECTION 2	Study Details			
Time Frame:	**Proposed Start Date:**	01/11/2012 (DD/MM/YYYY)	**Approx. Duration of Study:**	12 months
How will this be funded? *(Check all that apply. Submit all grants and contracts to the Office of Grants and Contract Services for review and Signature).* ***Attach Budget.***	☒ Grant Specify funding source: NSERC	☐ Industry Sponsor:	☐ Internal Specify funding source:	☐ No Funding Required ☐ Applied or In Process ☐

Tissue Source Blocked resected specimens must ensure source supply.	☐ Archived Fixed Tissue If biopsy, obtain approval from Site Group. ☐ Frozen Tumour Bank → Specify Bank: ☐ Autopsy ☐ Fetal ☒ Fresh Tissue → Obtained from: ☐ Surgical Specimen ☐ Excess Blood Sample/Body Fluid ☒ Donated Sample
Consent Attached? (Include consent to be used with application - if applicable).	Yes ☐ No ☒ If no, provide rationale. Not applicable (bodies will be donated for research)
Site(s) where tissue will be retrieved and/or consent will be obtained **Note: permission is also required from SJHH if consent and/or tissue is to be obtained at that site**	MUMC ☐ JCC ☐ Henderson ☐ SJHH ☐ General ☐ Other (describe): Specimens will be obtained from a whole body donation organization (Research For Life, Phoenix, AZ - Further info provided in Section 3, Question 3)
Consent for 'Use of Human Tissue and Blood and Body Fluids for Future Research' will be used?	Yes ☐ No ☒
Does the study involve genetic research?	Yes ☐ No ☒ If yes, please provide details:
Division/Site Group:	☐ Breast ☐ CNS ☐ GI ☐ GU ☐ Gynaecology ☐ Head & Neck ☐ Lung ☐ MSK ☐ Soft Tissue ☐ Lymphoid Tissues ☐ Hematology ☐ Eye ☐ Endocrinology ☐ Cardiac ☒ Other(s) (specify): Kinesiology & Anatomy

SECTION 3	Research Proposal for the Study of Human Tissue
1. Primary objective and hypothesis of the study: **2. Scientific Methodology:** **3. Anticipated Results:**	INTRODUCTION Occupational risk factors of wrist and hand musculoskeletal disorders are well-documented, and include awkward postures, repetitive movements, and high forces. However, the exact relationships between these physical workplace factors and underlying pathomechanics of wrist and hand injuries remain uncertain. Current research shows that shear forces due to flexor tendon motion in the carpal tunnel are involved in the etiology of wrist and hand disorders such as flexor tendinopathies and carpal tunnel syndrome. OBJECTIVES The objectives of this study are to assess tendon motion and shear over a range of different tendon forces and velocities typical of hand tasks in the

workplace and to determine the effect of wrist posture on tendon gliding.

HYPOTHESES

It is hypothesized that gliding resistances will increase with flexor tendon force and velocity, especially when the wrist is flexed.

METHODS

Sixteen fresh frozen cadaver arms amputated proximal to the elbow will be tested. The cadavers will be thawed at room temperature for 12 to 15 hours prior to dissection. The flexor tendons will be identified proximal and distal to the transverse carpal ligament and seperated from their attachment sites.

Each cadaver will be fastened to a custom testing apparatus. Clamps will affix the forearm to the testing device while an external fixator will attach on both sides of the wrist complex to adjust flexion/extension angle. Next, 4 light-weight load cells will be coupled to the flexor tendons of the middle finger, including 2 sensors attached to the FDP and 2 sensors connected to the FDS (proximally and distally to the carpal tunnel). The 2 load cells on the proximal ends of the middle finger FDP and FDS tendons will be connected to a mechanical actuator. The proximal flexor tendons of the index, ring, and little fingers will also be attached to the motor. The 2 force sensors on the distal ends of the middle finger FDP and FDS tendons will be connected to constant force springs along with the other distal flexor tendons of the index, ring and little fingers (to generate tendon tension).

The mechanical actuator will displace the tendons proximally (against the constant force springs) to represent finger flexion. The motor will also be reversed to produce distal tendon excursions (simulating finger extension).

Proximal and distal tendon forces of the middle finger FDP and FDS will be recorded with 4 load cells as the cadavers are subjected to various test conditions. The mechanical actuator will displace the flexor tendons at velocities of 15, 20, and 25 cm/s, which coincide with previous ultrasound studies of carpal tunnel dynamics. Three tension levels will be tested using constant force springs rated at 10, 20, and 30 N. Tendon forces will also be measured in three different wrist angles, including 30° flexion, 0°, and 30° extension. A total of five middle finger flexion/extension cycles will be tested for each condition (per cadaver).

Flexor tendon motion may also be assessed using a portable ultrasound system equipped with a high-frequency linear array probe throughout the testing protocol to monitor tendon motion near the carpal tunnel. These measurements will also be useful for validating the use of ultrasound modalities to assess tendon motion and shear.

Gliding resistances of the middle finger FDP and FDS tendons will be

	calculated for each test condition. The differences between the proximal and distal tendon forces represent these gliding resistances (equations 1 and 2). Both mean and peak gliding resistances will be calculated in the flexion and extension phases of each movement simulation. (1) FDP Gliding Resistance = FDP Proximal - FDP Distal Tendon Force (2) FDS Gliding Resistance = FDS Proximal - FDS Distal Tendon Force EXPECTED RESULTS This study will improve our understanding of flexor tendon mechanics in the carpal tunnel and our knowledge of the development of flexor tendinopathies and carpal tunnel syndrome. Estimates of flexor tendon shear over a wide range of simulated conditions (3 tendon forces * 3 tendon velocities * 3 wrist postures) will lead to the development of an ergonomic prediction model. This model will be used to predict occupational injury risks and reduce work-related musculoskeletal disorders. Further knowledge of flexor tendon shear might also improve consequences to surgery and rehabilitation.
2. How will the tissue be collected? *(For prospective studies only)*	Not applicable (this is not a prospective study)
3. Where Does the Tissue comes from?	The specimens will be obtained from (and returned to) a well-established whole-body donation program based in southwestern USA (Research For Life). Contact Info: John Cover, Chief Operating Officer, CTBS Research For Life, LLC 2230 E Magnolia Phoenix, AZ., 85034 Phone: 480-940-1310 Cell: 480-253-7209 Fax: 480-705-0023 Email: jcover@research-for-life.org
4. Identify which individual has responsibility for the Tissue	Dr. Peter Keir
5. Indicate the approximate number of tissue samples	16 distal upper limbs amputated proximal to the elbow (8 cadavers)

that will be required for this study.	
6. How will the tissue be labelled? *(For prospective studies only)*	Not applicable (this is not a prospective study)
7. Will any identifying information be recorded?	Yes ☐ No ☒ If yes, please specify the identifying information and justify the necessity for its collection:
8. Will individual identifiers be removed once the relevant data is collected? *(For prospectively collected tissue only)*	Yes ☐ No ☒ If no, please justify: Not applicable (this is not a prospective study)
9. How will security and confidentiality of the data be ensured?	No personal descriptors or markers will be used
10. Is there any anticipated linkage of the data to be collected with clinical database?	No
11. Will the data be available or distributed to others?	Yes ☐ No ☒ If yes, specify how confidentiality will be protected:
12. Will the data being collected be used now or in the future for commercial purposes?	Yes ☐ No ☒ N/A ☐ If yes, please provide details:
13. Will the tissue be sent to another facility for study?	Yes ☐ No ☒ If yes, please name location and provide the REB approval letter of the institution:

THIS SECTION TO BE COMPLETED ONLY IF ACCESSING MEDICAL CHARTS

SECTION 4	**Request to Access Retrospective Data for Research Purposes** ☒ *Please indicate if this section is not applicable (N/A) to your study*		
1. Data to be extracted from *(check all that apply):*	☐ Clinical Records	☐ Cancer Registry	☐ Database (Specify):
2. List specific data requested: *(Attach data collection forms, if applicable)*			
3. Proposed number of research subjects (charts):	HHS:	Other sites:	
4. Proposed start date:	/ / (DD/MM/YYYY)	**Proposed termination date:**	/ / (DD/MM/YYYY)
5. Time period of requested data:	**Start Date:** / / (DD/MM/YYYY)	**End Date:**	/ / (DD/MM/YYYY)
6. Will this data be transferred external to HHS?	Yes ☐ No ☐ If yes, where?		
7. How will confidentiality be protected?			
8. Will this data be reported publicly? *(e.g. publication)*	Yes ☐ No ☐		
9. Have you already developed a list of specific patients?	Yes ☐ No ☐ If yes, please indicate how patients were identified:		
10. Is patient-identifying data required?	Yes ☐ No ☐ If yes, please justify:		
11. Please indicate the type of patient identifying data: *(check all that apply)* ☐ HHS Medical Record Number ☐ Patient Number ☐ Address ☐ Date of Birth ☐ Provincial Health Card Number (OHIN) ☐ Visit Number ☐ Telephone Number ☐ Family Members Names			
12. Will this data be linked to any other data?	Yes ☐ No ☐ If yes, please provide details:		

13. Will data be anonymised?	Yes ☐ No ☐ N/A ☐ If no, please justify:

Agreements

Confidentiality Agreement

I, the undersigned, agree to adhere to the **HHS/FHS policy on Information and Data Security** and understand that a breach of this policy will be just cause for termination of my employment and /or affiliation with this hospital. I agree that all health information, which I may have access to, is to be dealt with in keeping with the institutional policies and procedures with respect to confidentiality. If identifying information is collected, the information will be kept secure and identifiers removed at the completion of collection. I also accept full responsibility for protection of information that has been collected by a delegate on my behalf.

Principal Investigator Signature:	Print Name: Peter Keir	Date: _____ / _____ / _____ (DD/MM/YYYY)
Signature of Individual(s) Accessing Retrospective Data if applicable (if not PI):	Print Name:	Date (DD/MM/YYYY):

Department/Division/Site Group/Pathologist:

I have reviewed the proposal and agree that the proposed use of human tissue materials in the project represents appropriate use of the human tissues available for research.

Division / Site Group Clinical Representative Signature:	Print Name: Martin Gibala (Chair, Kinesiology)	Date: _____ / _____ / _____ (DD/MM/YYYY)
Signature Head of Department/Chief of Service Responsible for Tissue	Print Name: Bruce Wainman (Director, Anatomy)	Date: _____ / _____ / _____ (DD/MM/YYYY)

APPENDIX C: **Study 2 (Chapter 4) participant questionnaires including the Boston Carpal Tunnel Questionnaire and Katz Hand Diagram.**

Participant Questionnaire

PARTICIPANT IDENTIFICATION

Name: _____ ***Date:*** _____
Age: _____

HANDEDNESS

1) Are you are you right-handed or left-handed or ambidextrous (use both hands equally)?

right-handed □ ***left-handed*** □ ***ambidextrous*** □

HEALTH HISTORY

1) Have you ever had any of the following health conditions and/or treatment protocols performed on you currently and/or in the past? [*please check all that apply*]

□ Diabetes mellitus
□ Thyroid condition (e.g. hypothyroidism)
□ Gout
□ Amyloidosis
□ Sarcoidosis
□ Renal failure (or hemodialysis)
□ Degenerative joint disease
□ Arthritis of the wrist/hand
□ Corticosteroid injection
□ Cervical radiculopathy
□ Peripheral neuropathy
□ Radial malunion
□ Colles fracture
□Wrist/hand musculoskeletal disorder
□ Flexor tendonopathy
□ Carpal tunnel syndrome
□ Ultrasound/laser/soft tissue treatment
□ Wrist/hand surgery
□ Pain/tingling/numbness of the hand

2) Are you currently on any medications that affect blood flow? ***Yes*** □ ***No*** □

* If ***yes***, please list:

_____
_____
_____

WORK HISTORY

1) Occupation: _____

2) Hours at work per week: _____

3) Years at current job: _____

4) Typical tasks performed at work: _____
_____
_____
_____
_____
_____

5) Have you ever-experienced a wrist or hand injury? ***Yes*** □ ***No*** □

* If ***yes***, please elaborate (type of injury, onset of injury, what do you attribute it to, how long have you have had the injury, symptoms, treatment of injury, time off work): _____
_____
_____
_____
_____

I verify that I have answered the above questions to the best of my knowledge. I understand that no confidential health information will be released without my written consent.

_____	_____	_____
Name of Participant (Print)	Signature	Date

_____	_____	_____
Name of Research Investigator Obtaining Consent (Print)	Signature	Date

BOSTON CARPAL TUNNEL QUESTIONNAIRE

CTS QUESTIONNAIRE

The following questions refer to your symptoms for a typical twenty-four hour period during the past two weeks (circle one answer to each question).

SEVERITY SCALE: 0 = None or Never; 1 = Mild; 2 = Moderate; 3 = Severe; 4 = Very severe

SYMPTOM SEVERITY SCALE

QUESTION SEVERITY SCORE 0= NONE; 4=SEVERE	0	1	2	3	4
1. How severe is the hand or wrist pain that you have at night?	0	1	2	3	4
2. How often did hand or wrist pain wake you up during a typical night in the past two weeks (times/night)?	0	1	2-3	4-5	5+
3. Do you typically have pain in your hand or wrist during the daytime?	0	1	2	3	4
4. How often do you have hand or wrist pain during the daytime (times/day)?	0	1-2	3-5	5+	constant
5. How long, on average, does an episode of pain last during the daytime (minutes)?	0	<10	10-60	>60	constant
6. Do you have numbness (loss of sensation) in your hand?	0	1	2	3	4
7. Do you have weakness in your hand or wrist?	0	1	2	3	4
8. Do you have tingling sensations in your hand?	0	1	2	3	4
9. How severe is numbness (loss of sensation) or tingling at night?	0	1	2	3	4
10. How often did hand numbness or tingling wake you up during a typical night during the past two weeks?	0	1	2-3	4-5	5+
11. Do you have difficulty with the grasping and use of small objects such as keys or pens?	0	1	2	3	4

FUNCTIONAL STATUS SCALE

QUESTION SEVERITY SCORE 0= NONE; 4=SEVERE	0	1	2	3	4
1. Writing	0	1	2	3	4
2. Buttoning of clothes	0	1	2	3	4
3. Holding a book while reading	0	1	2	3	4
4. Gripping of a telephone handle	0	1	2	3	4
5. Opening of jars	0	1	2	3	4
6. Household chores	0	1	2	3	4
7. Caring of grocery bags	0	1	2	3	4
8. Bathing and Dressing	0	1	2	3	4

COMMENTS:

_____
_____
_____
_____

ID _____
DATE _____

M /F _____ **AGE**_____ **DOI** _____

Levine DW, Simmons HP, Koris MJ, Daltroy LH, Hohl GG, Fossel AH, Katz JN. A self-Administered questionnaire for the assessment of severity of symptoms and functional status in carpal tunnel syndrome. J Bone and Joint Surgery, 1993; 75-A:1585-1592.

KATZ HAND DIAGRAM

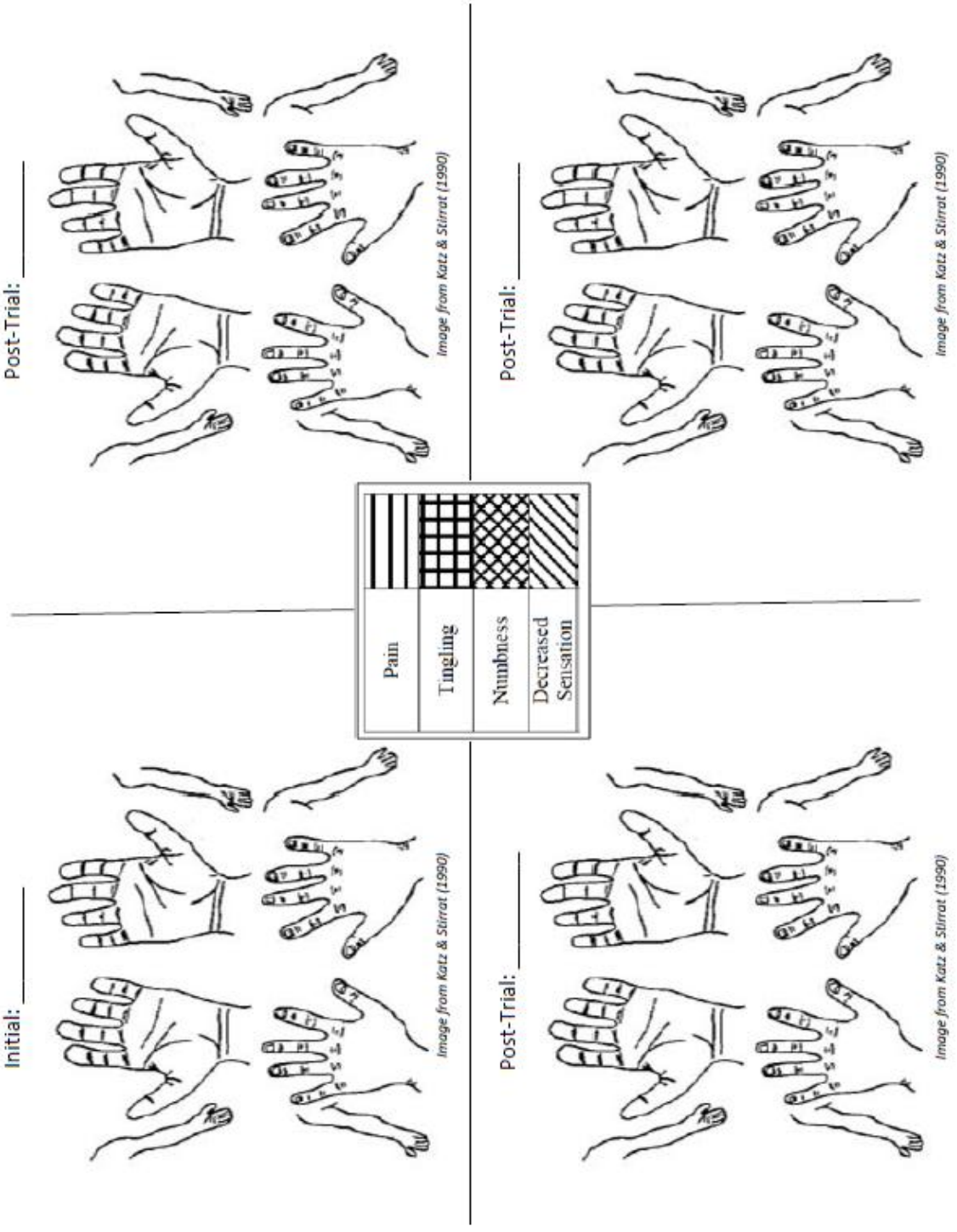

Table 1 Scoring criteria for hand diagrams

Rating	Description of area shaded on the hand[a]
Classic (3)	Tingling, numbness, burning or pain in at least 2 of the digits (thumb, index and long). Symptoms in palm and dorsum of hand excluded; small finger symptoms, wrist pain or radiation proximal to the wrist allowed. • *For index and long digits, must include shading between the distal tip and the proximal finger crease volarly, and include >1/2 of the middle phalanx &/or some of the distal phalanx. For thumb, must include shading in the distal phalanx volarly.* • *Digit may include shading dorsally from fingernail to the distal MP mark on the hand diagram.* • *If joint of digit (including MP) is the only area shaded and less than half of two adjacent phalanges, this may be considered arthritic complaints.*
Probable (2)	Same shading as for classic but allowed the shading to extend into the palm volarly unless it was confined to the ulnar aspect of the palm.
Possible (1)	Tingling, numbness, burning, or pain in at least one of the digits (thumb, index and long). • *May include the dorsum of the hand*
Unlikely (0)	No shading of the primary digits or shading restricted to the dorsum of the digits only.

[a] Modifications to rules in italics

APPENDIX D: **Pilot Work**

Speckle Tracking

Recent communications identify speckle tracking as a novel and promising technique for tendon tracking and extensive pilot work was performed to try and use it in my thesis. My independent study involved the development of our own in-house speckle tracking program, consisting of a block-matching scheme capable of tracking tissue heterogeneities (speckle patterns) through a sequence of high-resolution ultrasound images. During this work, we found major limitations with the speckle tracking method for tendon motion, that suggest the preference for speckle tracking over Doppler methods in tendon motion literature is not completely one-sided.

A fundamental assumption with speckle tracking is that it requires stability of pixel intensity patterns over time; such that translations in pixels represent tissue displacement. However, musculoskeletal tissue, such as the tendon, lack fixed patterns (unlike musculotendinous junctions or cardiovascular tissue) that make tracking difficult. Moreover, tendons are especially susceptible to motion artifacts, since tendons move at high velocities and over large displacements. Therefore, tendon speckle patterns are highly variable from frame to frame, even using high sampling rates. This produces pixel translations that are unrelated to tissue movement, called *decorrelation*, leading to measurement error and a very laborious analysis process. We experienced decorrelation in tracking the tendon and tenosynovium in the carpal tunnel (*in vitro* and *in vivo)* and found tendon displacements were underestimated. These findings are consistent with Yoshii et al. (2009) who also found speckle tracking to largely underestimate tendon

excursion, measuring about 10 mm of tendon motion for a finger motion expected to produce 20 mm based on a geometric model (An et al. 1983).

A common approach to limit decorrelation has been to increase the number of speckle patterns in the target block (tissue region of interest) by increasing the size of the block. However, this solution is less effective for tracking small tissue such as the tenosynovium. The thickness of the tenosynovium at the proximal wrist crease is approximately 0.46 mm (range of 0.23-0.7 mm) in healthy individuals (van Doesburg et al. 2013). To accurately track the tenosynovium the block must reside within the tissue of interest. This limits the block to a maximum height of only 6 pixels (based on ultrasound image resolution); which drastically reduces the number of pixels involved in tracking. The tenosynovium becomes an even greater challenge to track considering that its hyperechoic imaging characteristics provide very few speckle patterns to track (virtually homogenous and white). Thus, we found speckle tracking had difficulty measuring the tenosynovium and suggests it may not be useful for relative tendon-SSCT motion studies.

My pilot work revealed that speckle tracking techniques currently lack robust outcomes that cannot provide a reliable measure of tendon and SSCT motion. The high accuracy previously reported with speckle tracking used conservative *in vitro* experimental conditions (likely to limit decorrelation) including very slow tendon velocities (less than 16 mm/s) and small tendon excursion ranges (up to 15 mm) (Korstanje et al. 2010; Dilley et al. 2001). However, this insufficiently represents physiological conditions which can exceed 150 mm/s of tendon velocity (Tat et al. 2013) and reach up to 30 mm of excursion for a full finger motion consisting of complete

flexion of the PIP and MCP joints (Brand and Hollister, 1993). This may explain why *in vitro* accuracy rates have yet to be replicated *in vivo*. On the other hand, we had success applying our speckle tracking program to track tissue in the cardiovascular system (layers of the arterial wall) (Tat et al. 2014). Though layers of the arterial wall are approximately the same thickness as the tenosynovium (0.5 mm), we were able to achieve excellent tracking. We believe this was due to the image architecture of cardiovascular tissue which included a high degree of heterogeneous pixel intensity, high temporal continuity in pixel intensities and limited motion artifact (layers move less than 2 mm in longitudinal direction). A future direction for tendon tracking may need to employ an adaptive block-matching scheme (such as the kalman update strategy); as this would help to account for noise and variability of pixel patterns in the reference block for image sequences with motion artifacts (Zahnd et al. 2013; Peacock et al. 2000).

Duration as Shear Injury Risk Factor

The current thesis concept was inspired by work during my undergraduate thesis to investigate our tenosynovium phenomenon. My undergraduate study involved performing a repetitive finger task for 30 minutes and we found a dose-response increase in relative displacement between the tendon and tenosynovium. We hypothesized a mechanism of cumulative shear damage over time that could eventually progress to pathological changes in the tenosynovium. Considering the workplace involves higher loads, more awkward postures, and longer durations than we tested; exposure to demanding finger motions can potentially inflict and accumulate shear damage over the course of a worker's career. However, to better understand this mechanism, we needed to understand the meaning of ultrasound-based relative displacement and investigate if pathological changes progress in a CTS population.

In Chapter 3 we established the implications of relative tendon displacement. We demonstrated that relative displacement was associated with greater work done by the tendon on the surrounding tenosynovium. In particular, we found velocity-dependent changes had the greatest increase (more than force or posture) in relative motion that supports the role of high repetition (high velocity) finger motions in injury risk. Therefore, highly repetitive hand tasks, performed for extended durations, may increase loading to the tenosynovium and potentially predispose to shear damage.

Chapter 4 demonstrated that fibrosis and thickening of tenosynovium progressed along with symptom severity in CTS symptomatics that suggests cumulative shear damage. This was evidenced by a positive association with symptom severity and

relative tendon displacement. Also, this may indicate that pathological changes could play a role in CTS symptoms. Increased fibrosis and thickening of the tenosynovium could increase carpal tunnel pressure by changing the volume of carpal tunnel content and reducing permeability within the tenosynovium.

This thesis succeeded in advancing our understanding of the tenosynovium and its injury mechanism. Greater relative displacement between the tendon and tenosynovium can increase loading to the tenosynovium and result in shear injury. Evidence of shear damage coincided with severity of CTS symptoms in our symptomatic population, which suggests an accumulation of damage with the progression of disease. Finally, we added that the risk of shear injury appears independent and additive for traditional occupational risk factors including posture, force, and repetition (velocity).